

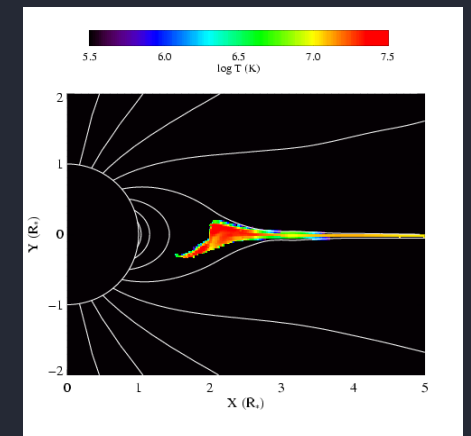
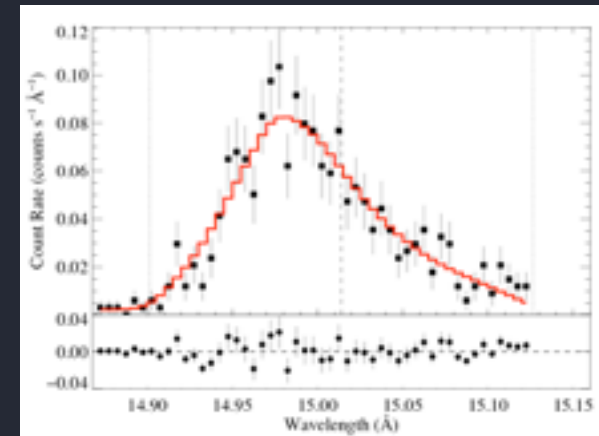
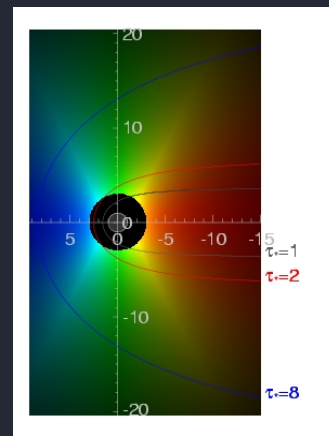
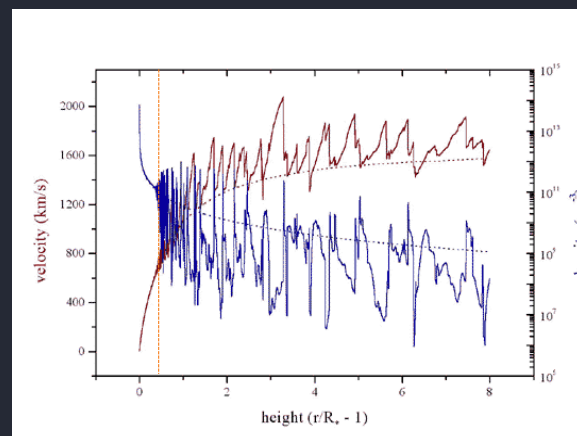
X-ray Emission from the Winds of Massive Stars

David Cohen
Department of Physics & Astronomy
Swarthmore College

Véronique Petit (Florida Tech), Maurice Leutenegger (GSFC), Stan Owocki & Dylan Kee (Delaware), Jon Sundqvist (Madrid),
Marc Gagné (West Chester), Asif ud-Doula (Penn St. Worthington-Scranton)

with

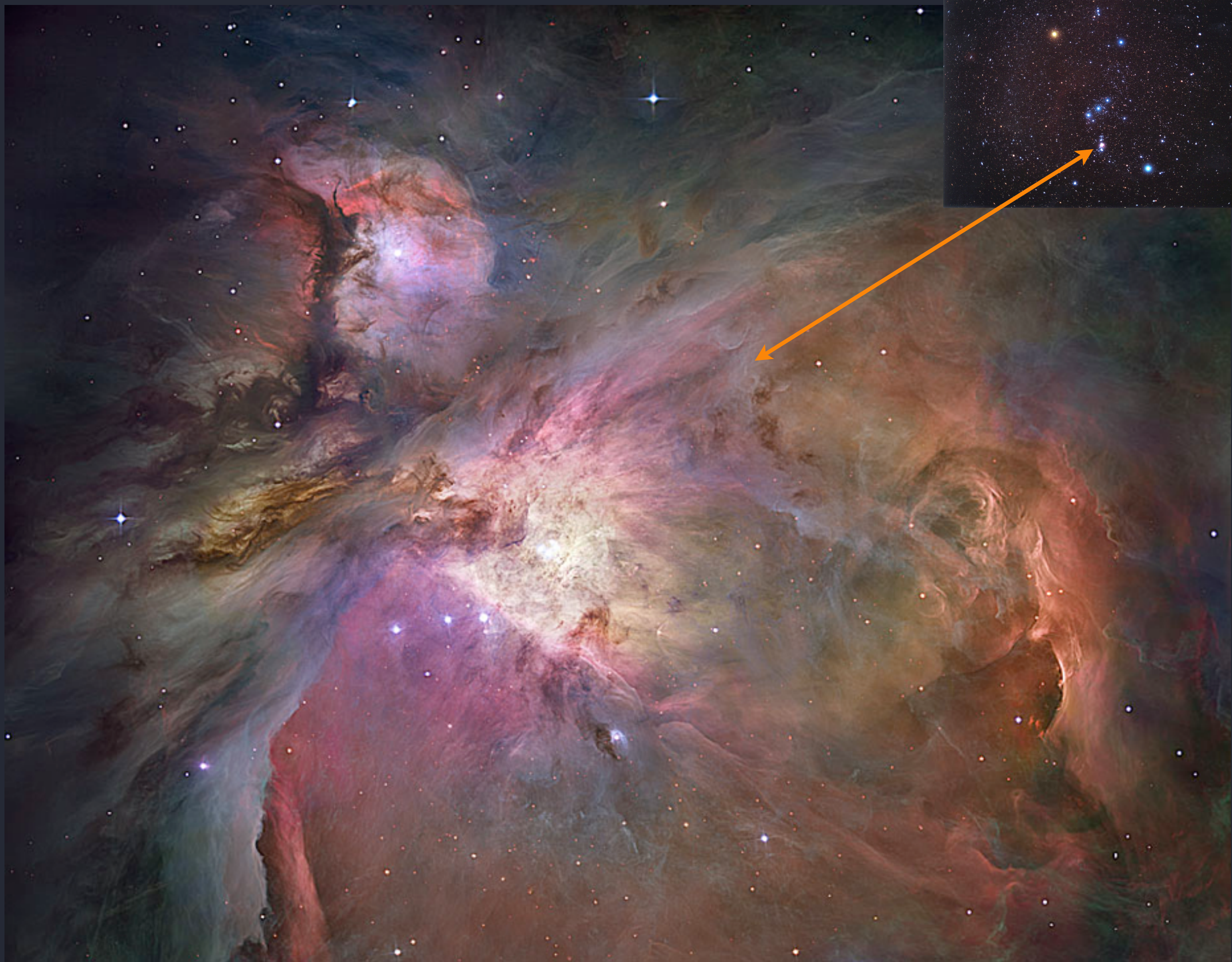
Emma Wollman (Caltech, Swarthmore '09), James MacArthur (Stanford, Swarthmore '11),
Jake Neely (Swarthmore '13), Zack Li (Swarthmore '16), Jackie Pezzato (Swarthmore '17)



massive stars are usually hot & therefore blue

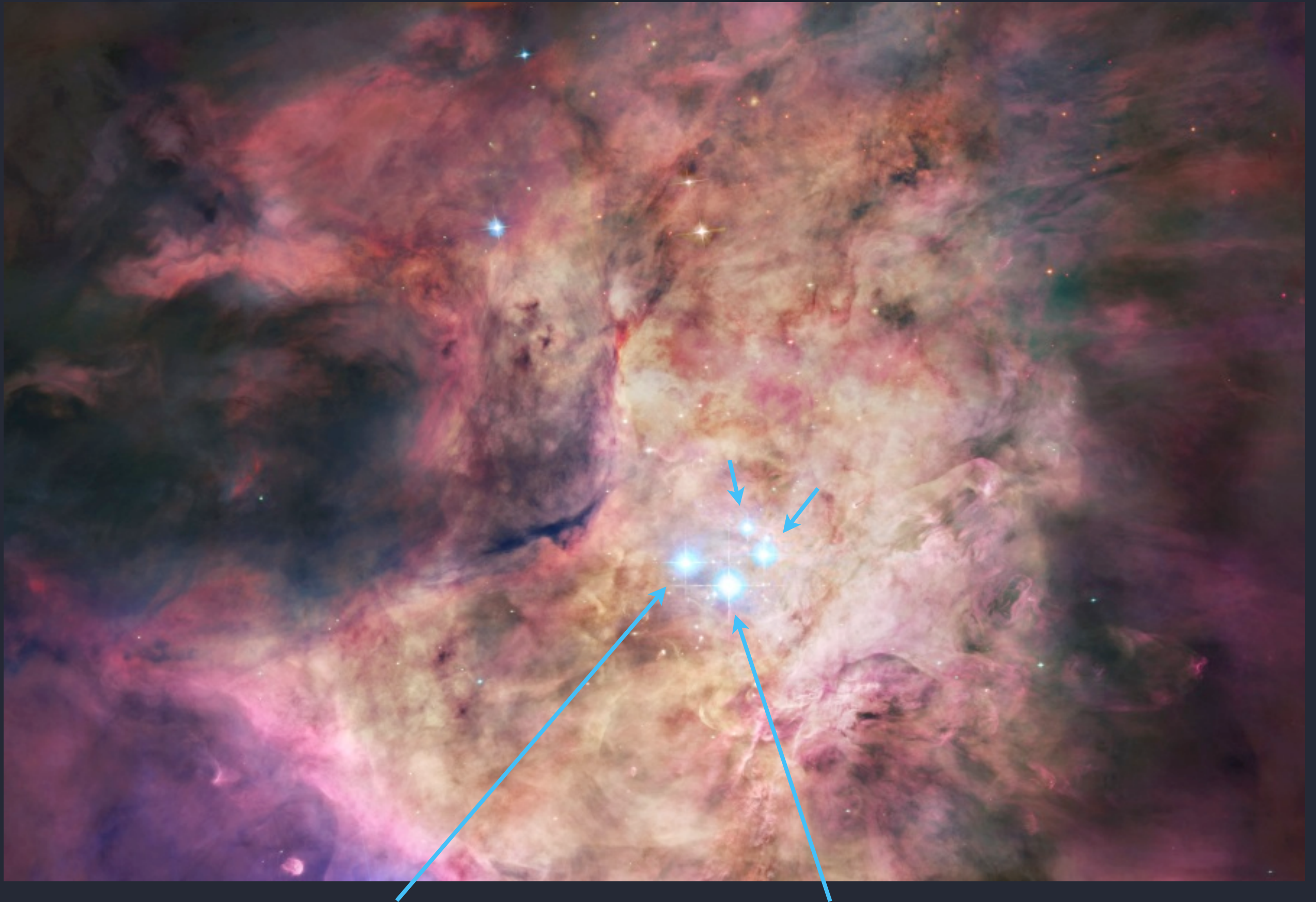


Orion



Orion Nebula, *Hubble Space Telescope*

“O-type star” is the hottest stellar spectral classification



θ^1 Ori C: only O star here

Basic properties of O stars

mass $\sim 50 M_{\text{sun}}$

luminosity $\sim 10^6 L_{\text{sun}}$

surface temperature $\sim 45,000 \text{ K}$



Basic properties of O stars

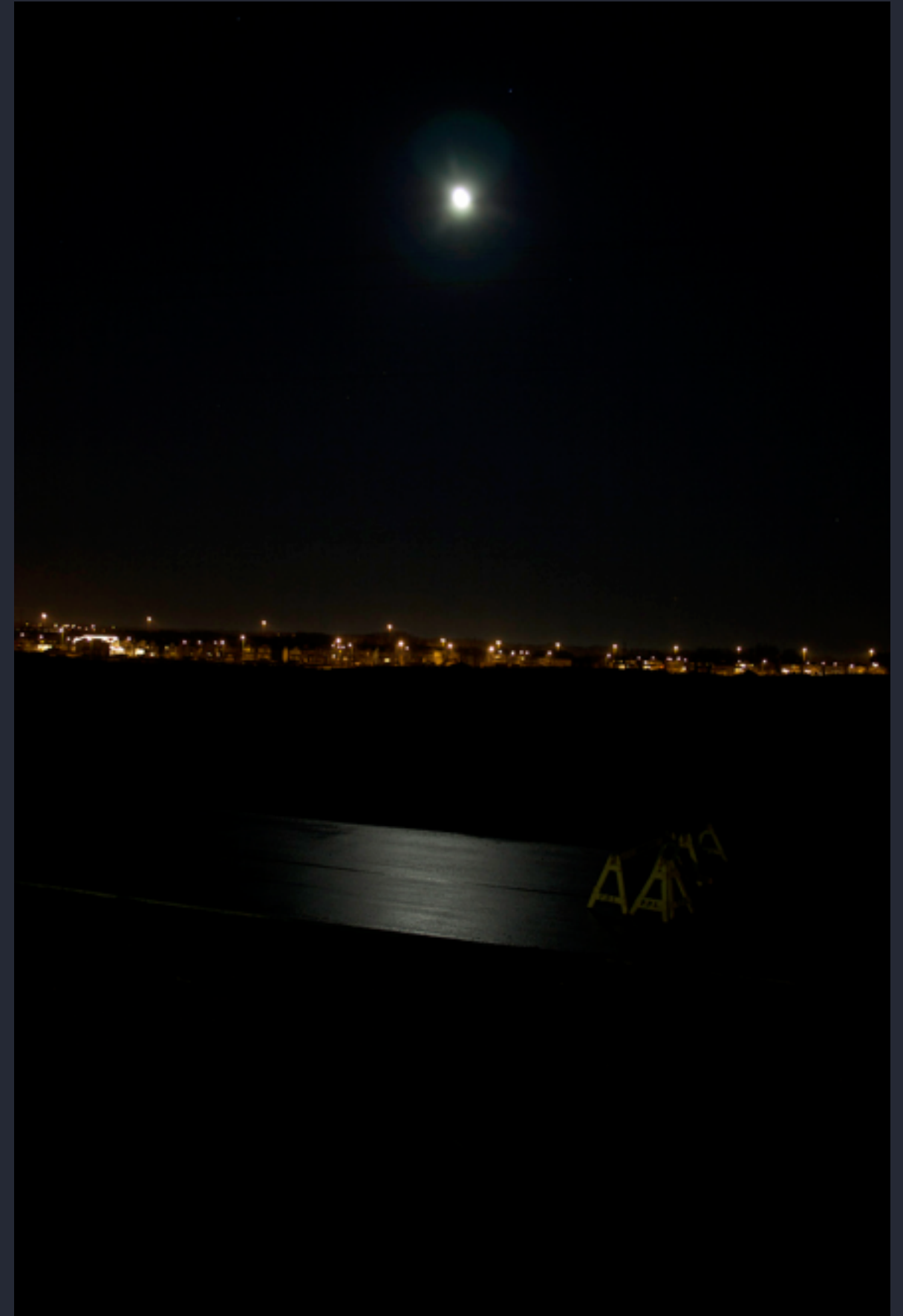
mass $\sim 50 M_{\text{sun}}$

luminosity $\sim 10^6 L_{\text{sun}}$

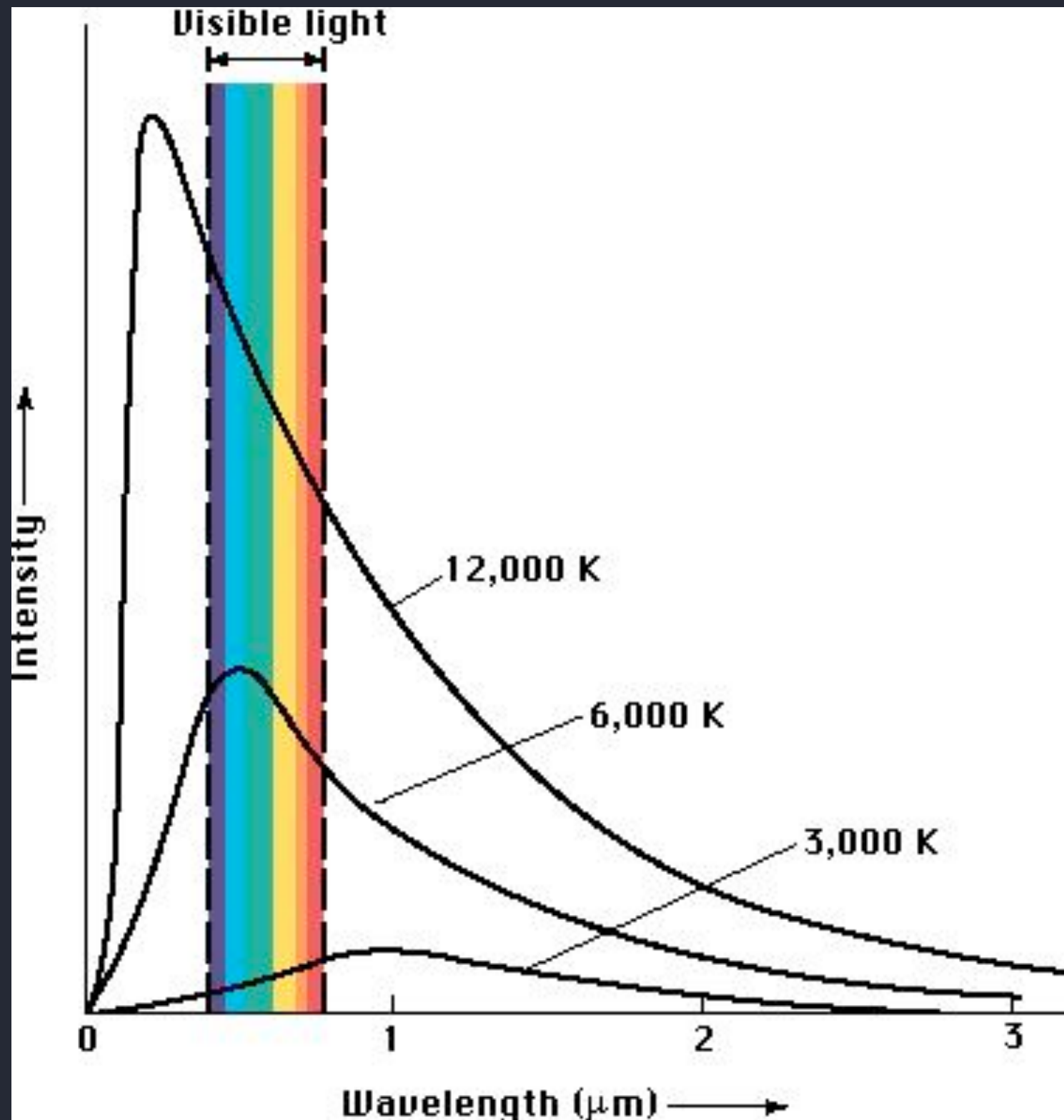
surface temperature $\sim 45,000 \text{ K}$



Sun and full Moon - factor of a million (10^6) in brightness



Blackbody spectra



above $T \sim 10,000 \text{ K}$
most of a star's
emission is in the UV

O stars are even more
extreme: $T > 30,000 \text{ K}$

even so, no X-ray
emission from the
photospheres (surfaces)
of even the hottest stars

Basic properties of O stars

mass $\sim 50 M_{\text{sun}}$

luminosity $\sim 10^6 L_{\text{sun}}$

surface temperature $\sim 45,000 \text{ K}$

*significant momentum in
the photospheric
radiation field*

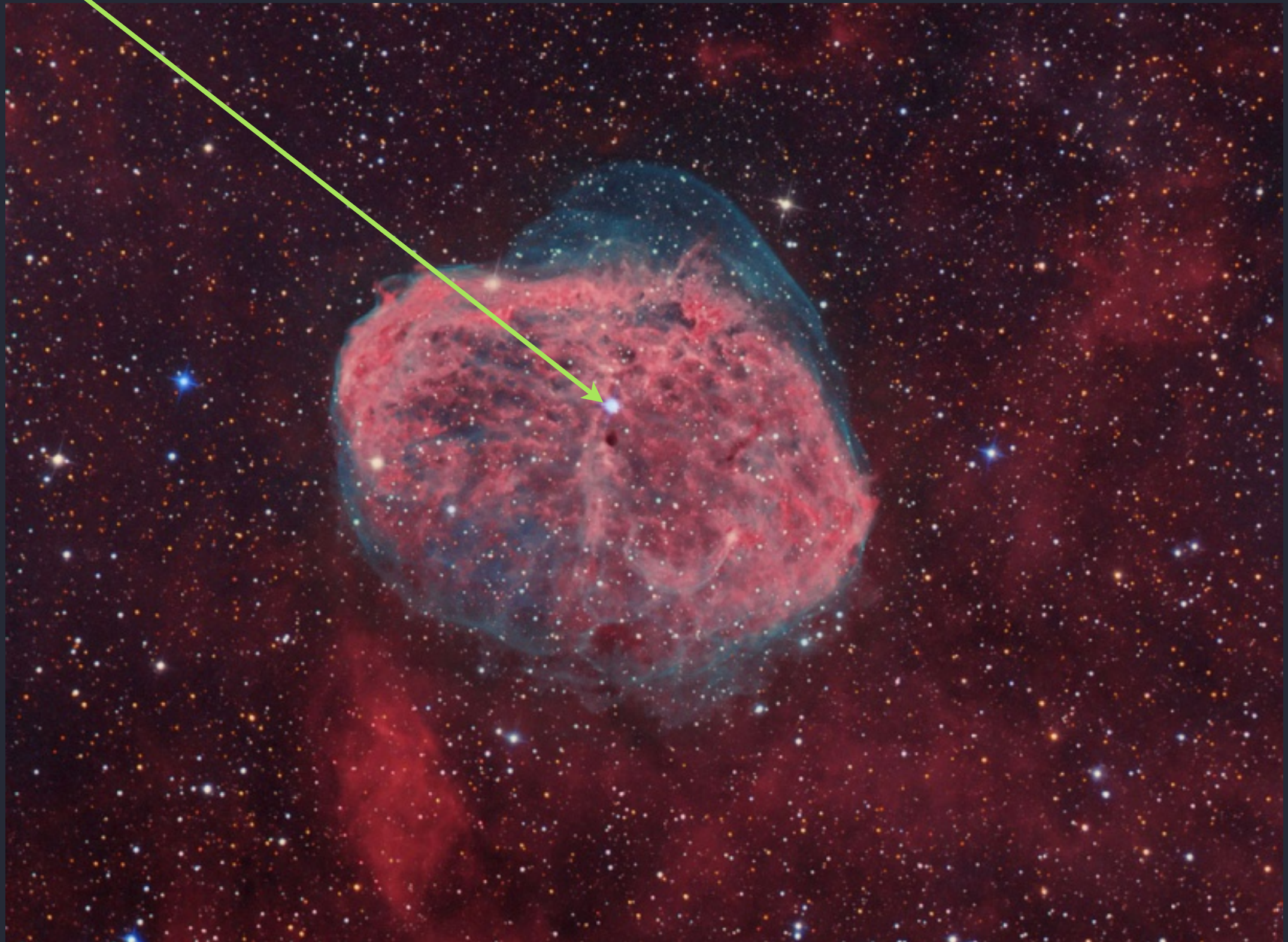


Strong, *radiation-driven* stellar winds are a characteristic of massive stars



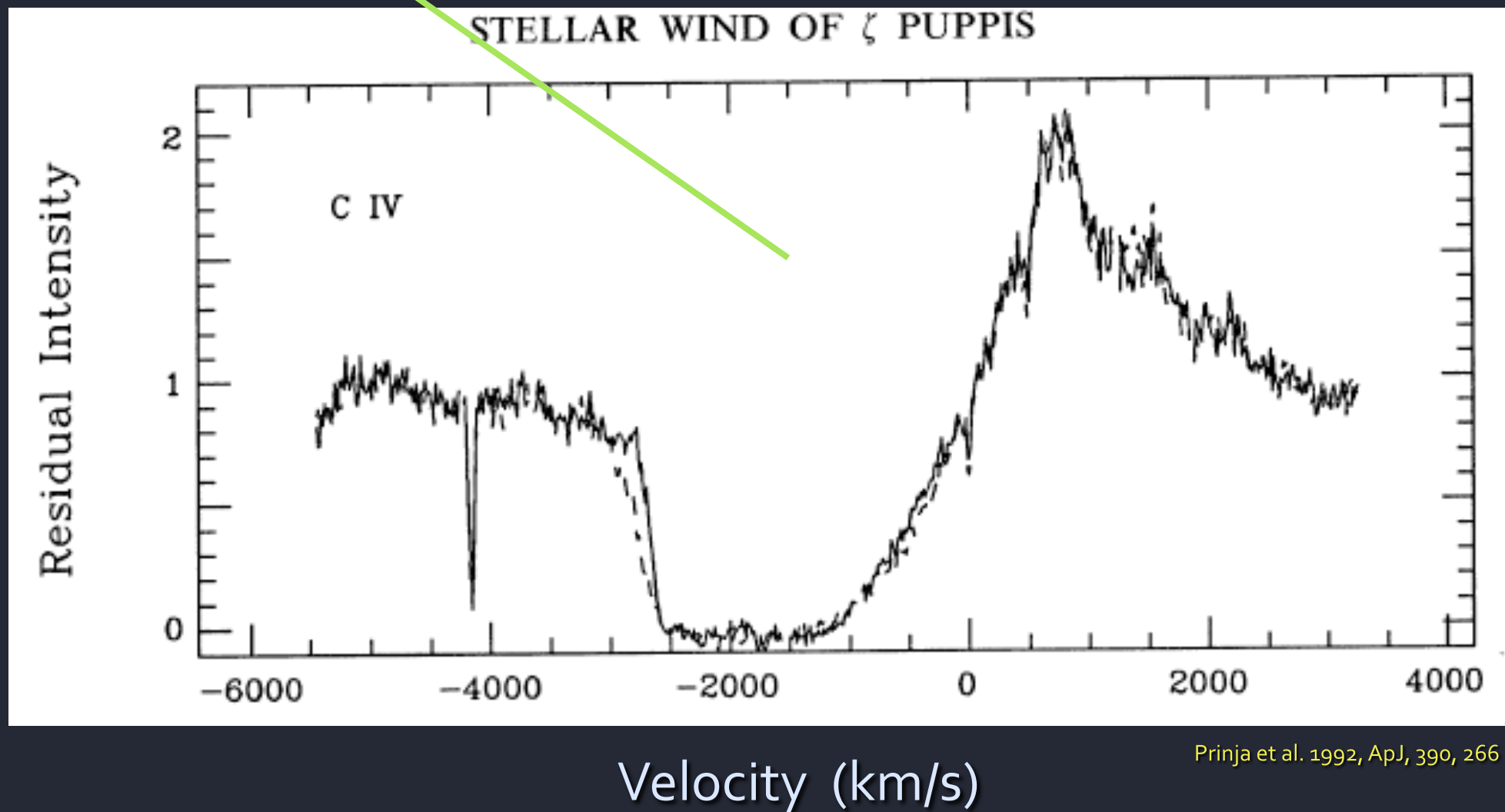
NGC 6888 Crescent Nebula - Tony Hallas

O star - source of wind bubble:
~1 arc second instrumental resolution;
star's angular size is 10^4 times smaller



NGC 6888 Crescent Nebula - Tony Hallas

small spatial scales can be studied using
spectroscopy

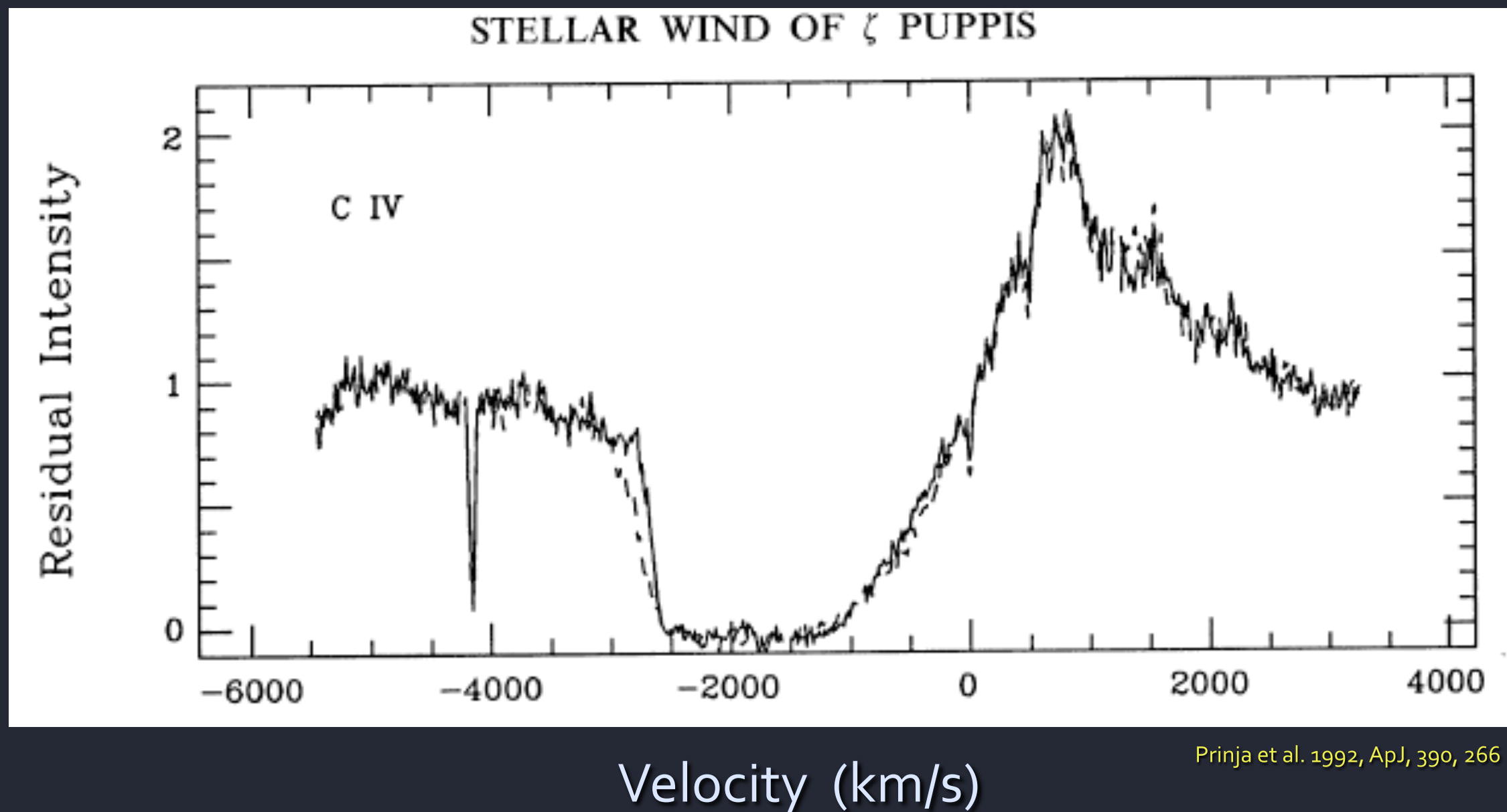


Prinja et al. 1992, ApJ, 390, 266

Ultraviolet spectrum showing wind feature from C^{+3}

ζ Pup (O4 supergiant): $\dot{M} \sim \text{few } 10^{-6} M_{\text{sun}}/\text{yr}$

UV spectrum: C IV 1548, 1551 Å



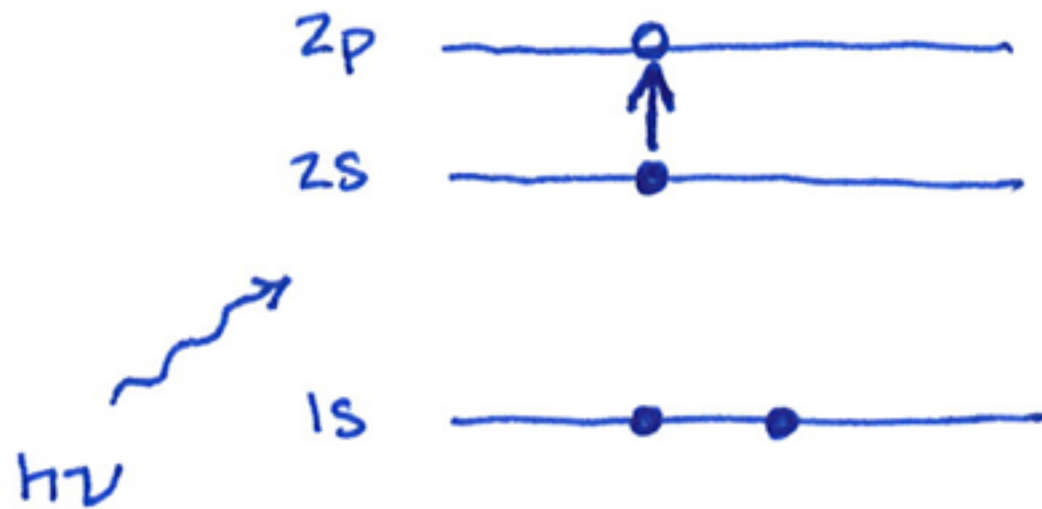
Spectral lines:

absorption line when translucent gas is between you and a hotter, opaque source of continuum photons

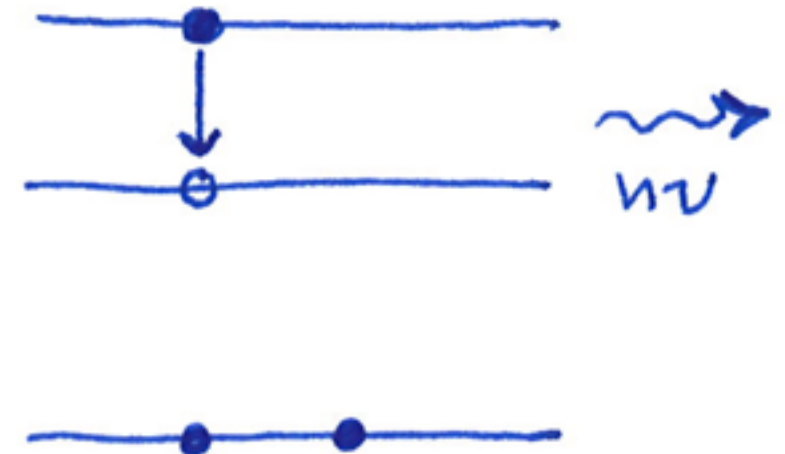
emission line when hot gas is seen against a cold background

absorption and emission: atomic energy level diagrams

C^{+3} is lithium-like

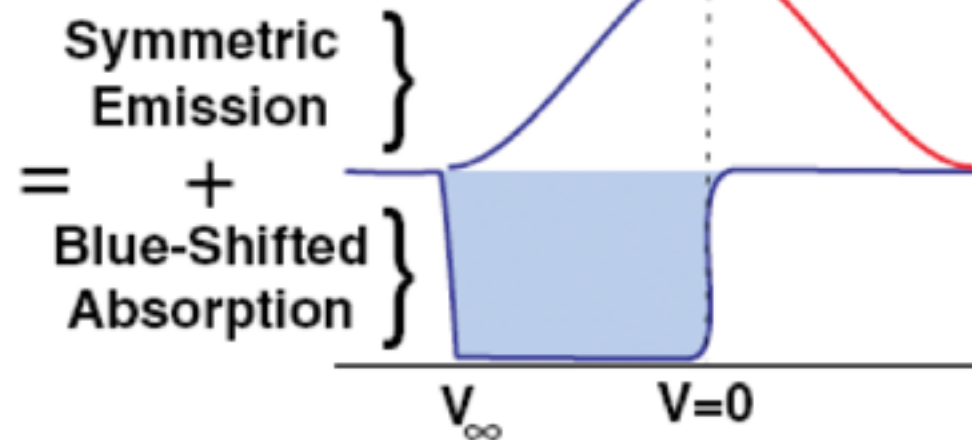
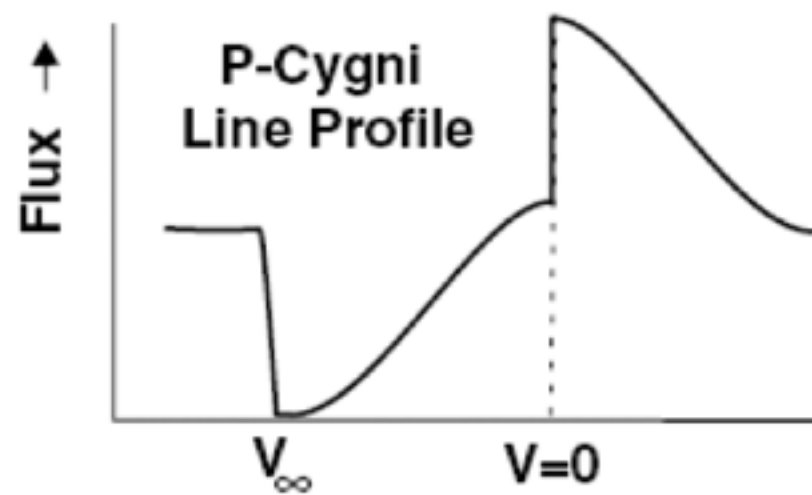
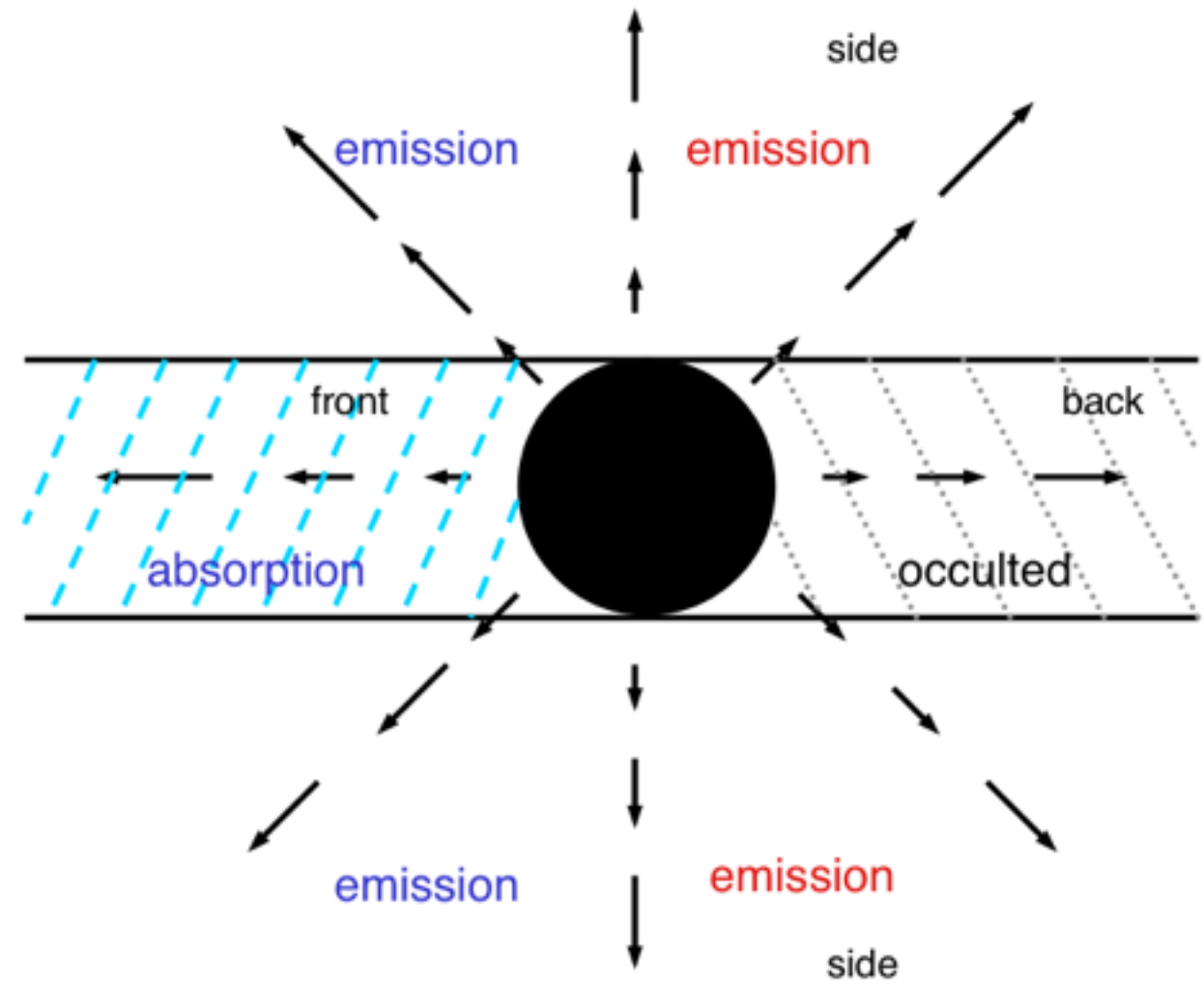


Absorption



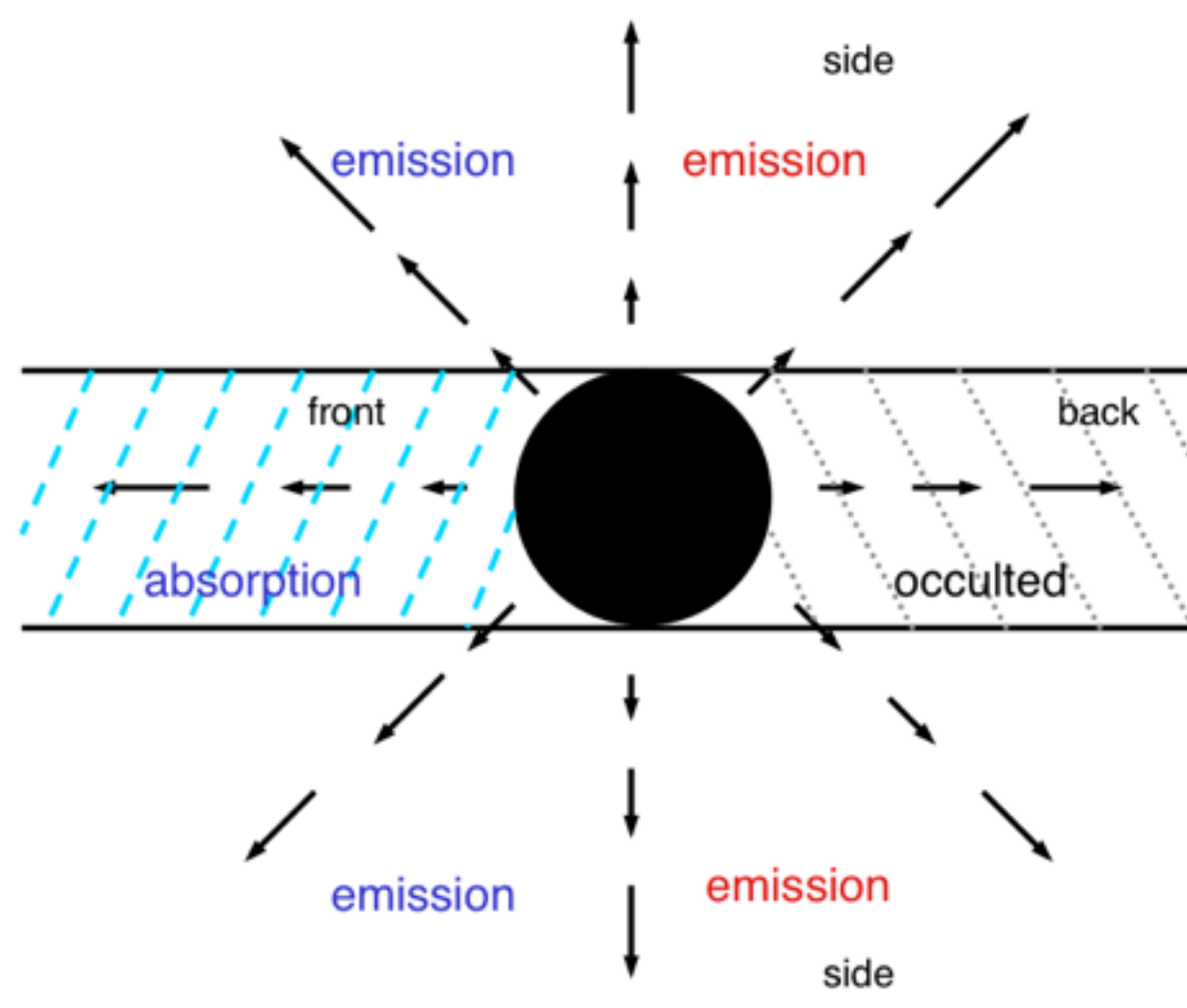
Emission

UV telescope

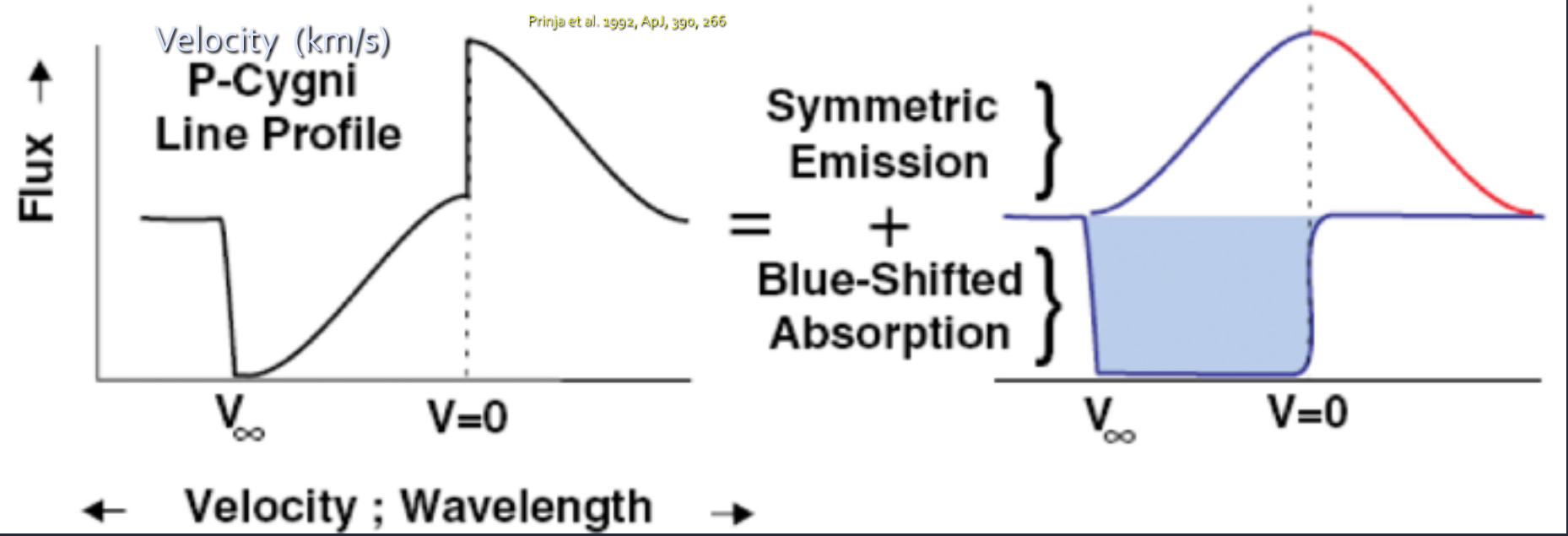
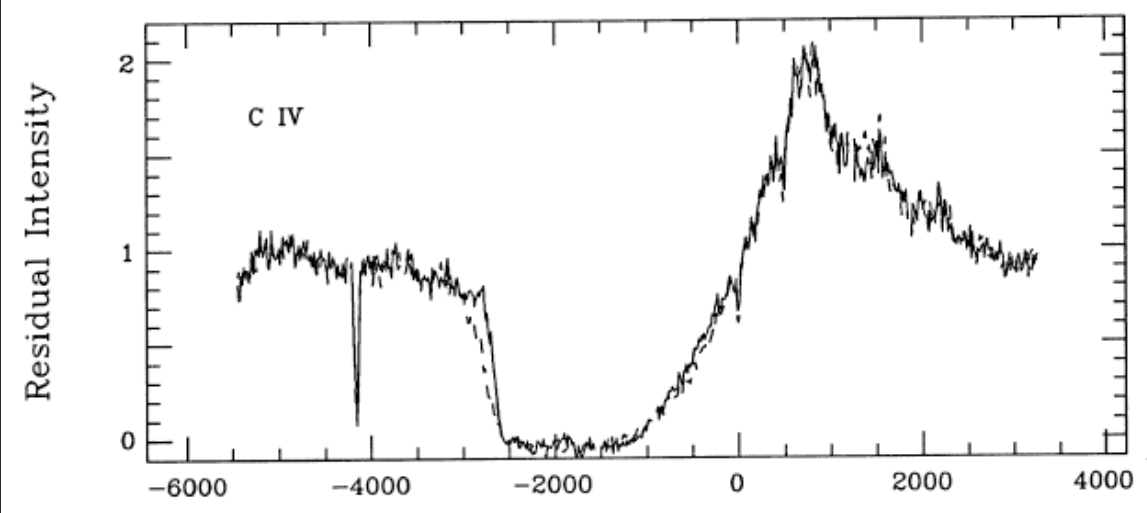


\leftarrow Velocity ; Wavelength \rightarrow

UV telescope



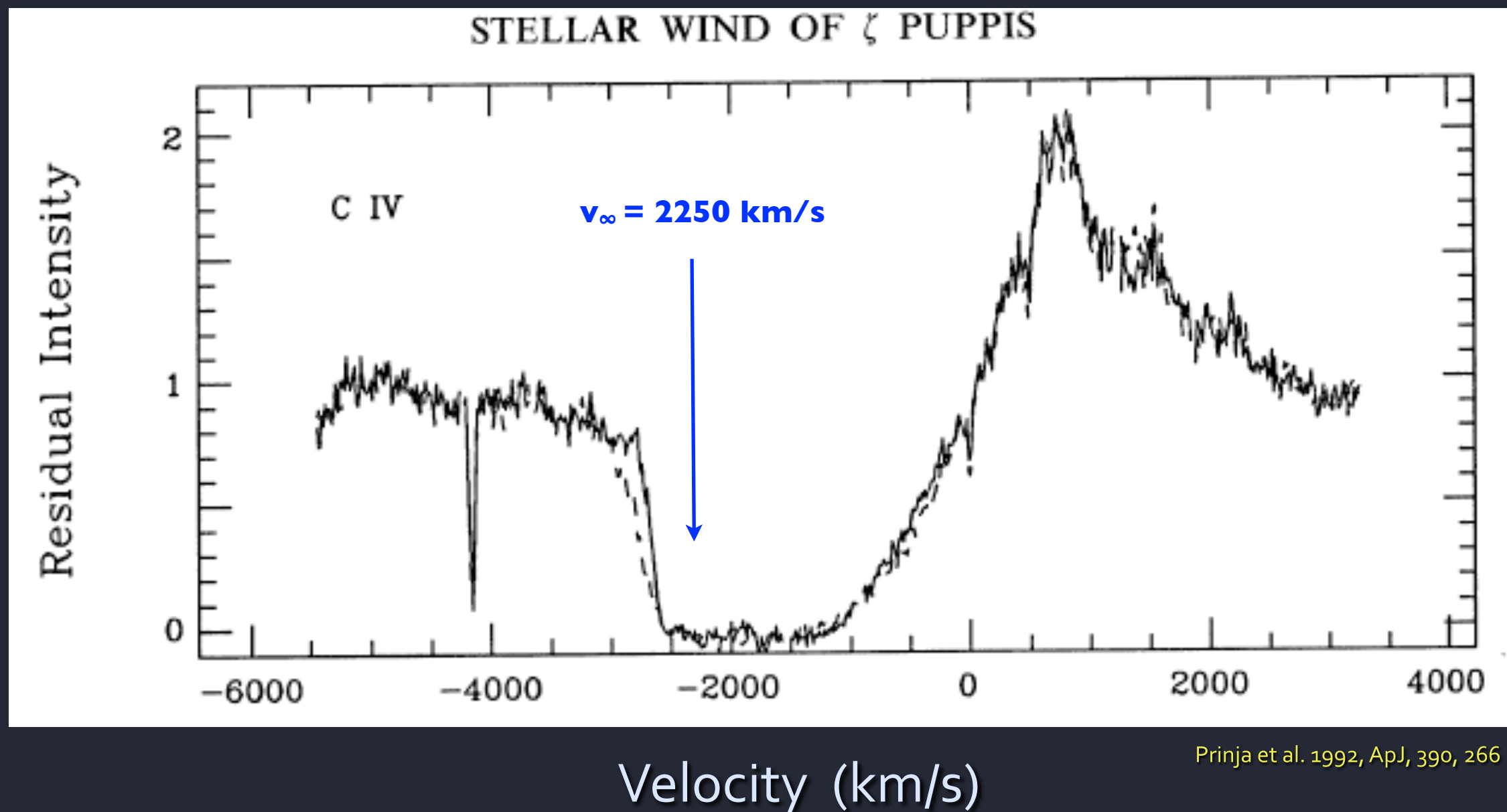
STELLAR WIND OF ζ PUPPIS



Ultraviolet spectrum showing wind feature from C^{+3}

ζ Pup (O4 supergiant): $\dot{M} \sim \text{few } 10^{-6} M_{\text{sun}}/\text{yr}$

UV spectrum: C IV 1548, 1551 Å



Radiation Force on an atom



$h\nu$ (energy)

$\frac{h\nu}{c}$ (momentum, p)

rate at which atom
absorbs momentum

$$\frac{dp}{dt} = F_{\text{rad}}$$

$$F_{\text{rad}} = \frac{L\sigma}{4\pi r^2 c}$$

luminosity, star's power output (watts)

absorption cross section of atom (m^2)

Radiation driving of massive star winds

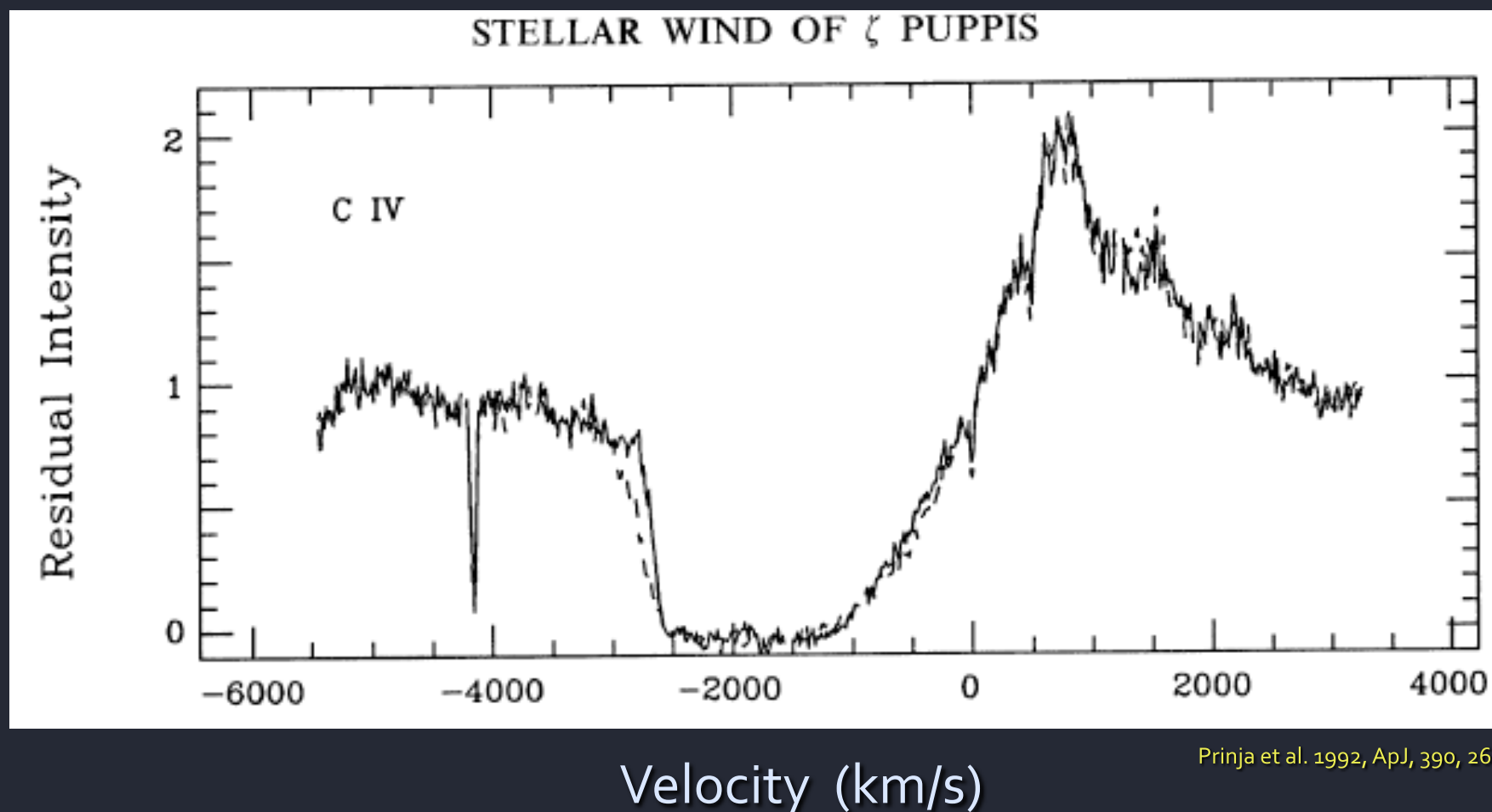
$$\dot{M} \sim 10^{-6} M_{\text{sun}}/\text{yr} \quad (10^8 \text{ times the Sun's value})$$

$$\text{kinetic power in the wind} = 1/2 \dot{M} v_{\infty}^2 \quad (\sim 10^{-3} L_{\text{bol}})$$

Radiation driving of massive star winds

$\dot{M} \sim 10^{-6} M_{\text{sun}}/\text{yr}$ (10^8 times the Sun's value)

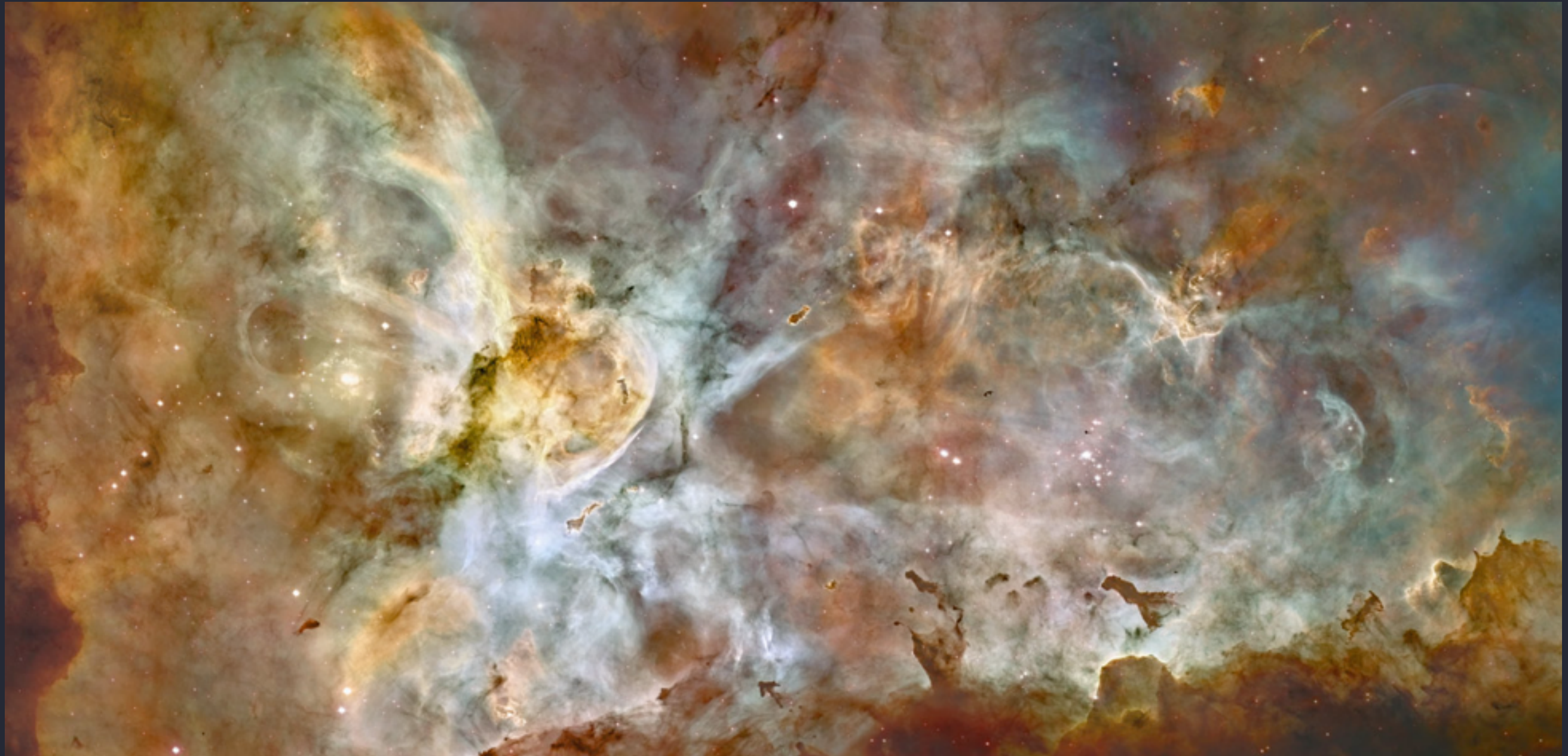
kinetic power in the wind = $1/2 \dot{M} v_{\infty}^2$ ($\sim 10^{-3} L_{\text{bol}}$)



Carina Nebula

massive, luminous stars drive the physics

winds, eruptive mass loss, and supernovae all contribute



Carina Nebula, *Hubble Space Telescope*

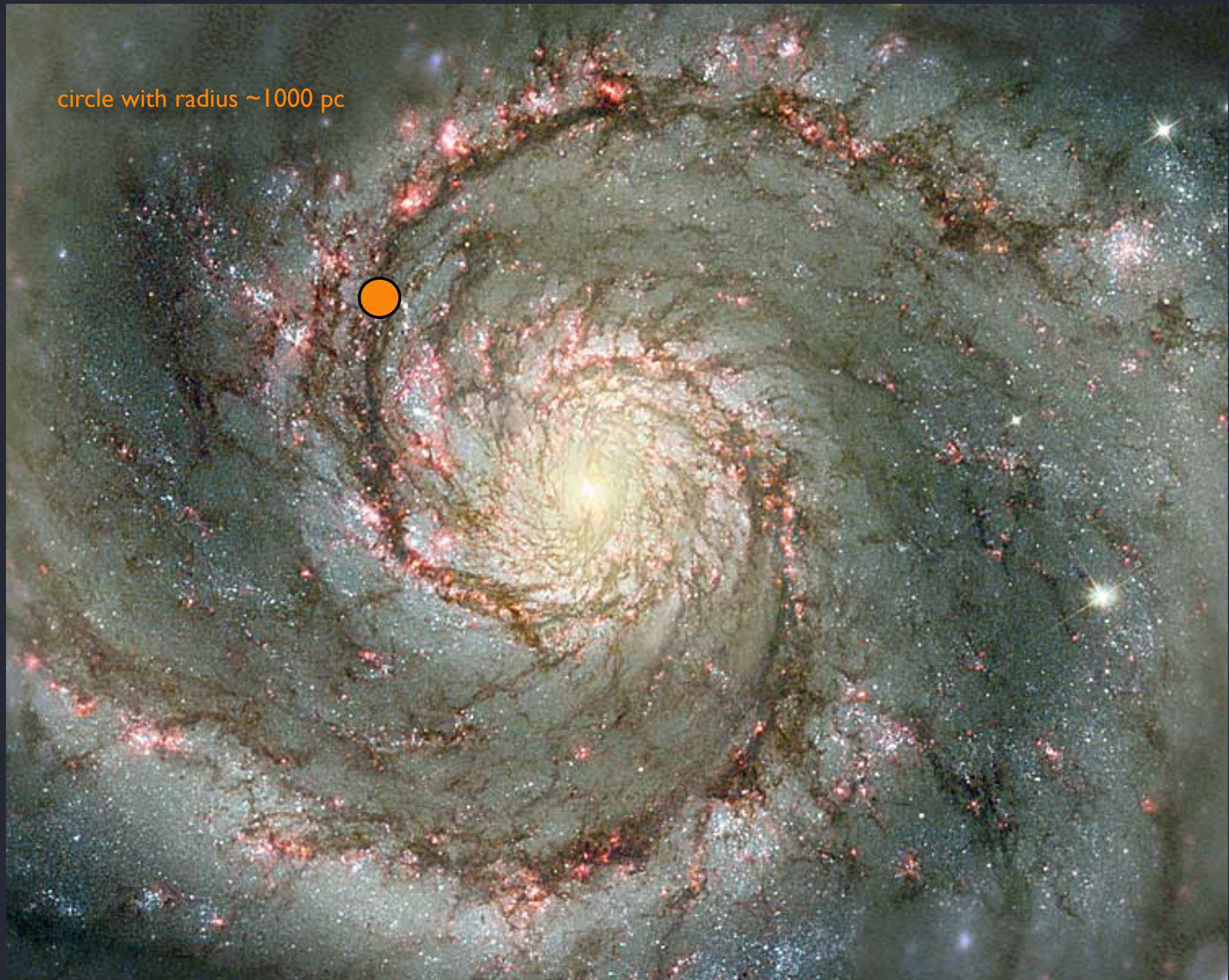
~1000 year-old core-collapse supernova remnant



Crab Nebula, WIYN

Scale

nearest massive stars are ~ 1000 parsecs* away



*1 parsec = 3.26 light years

Whirlpool Galaxy, Hubble Space Telescope

Massive stars as drivers of Galactic physics



Tarantula, *HST*

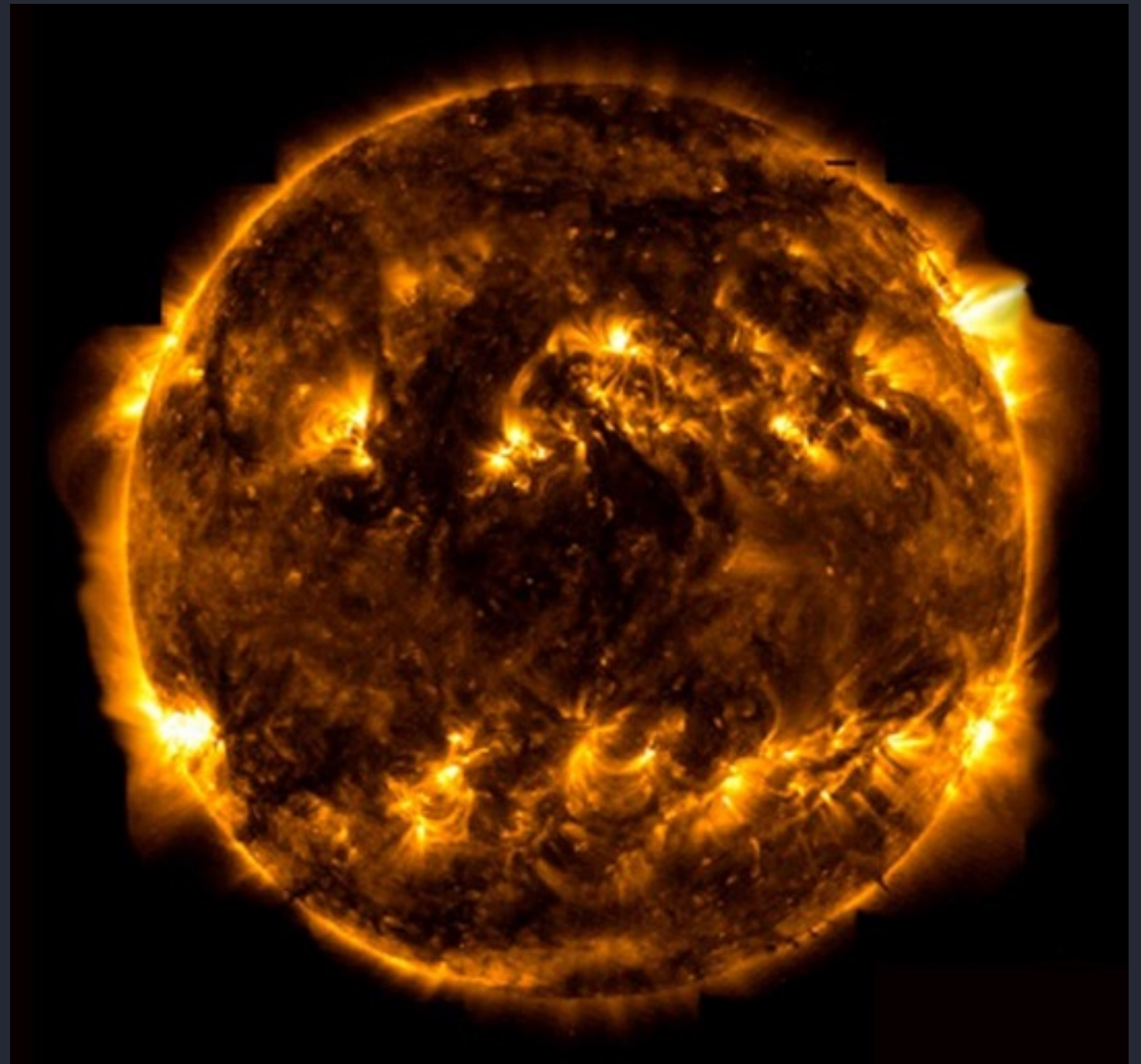
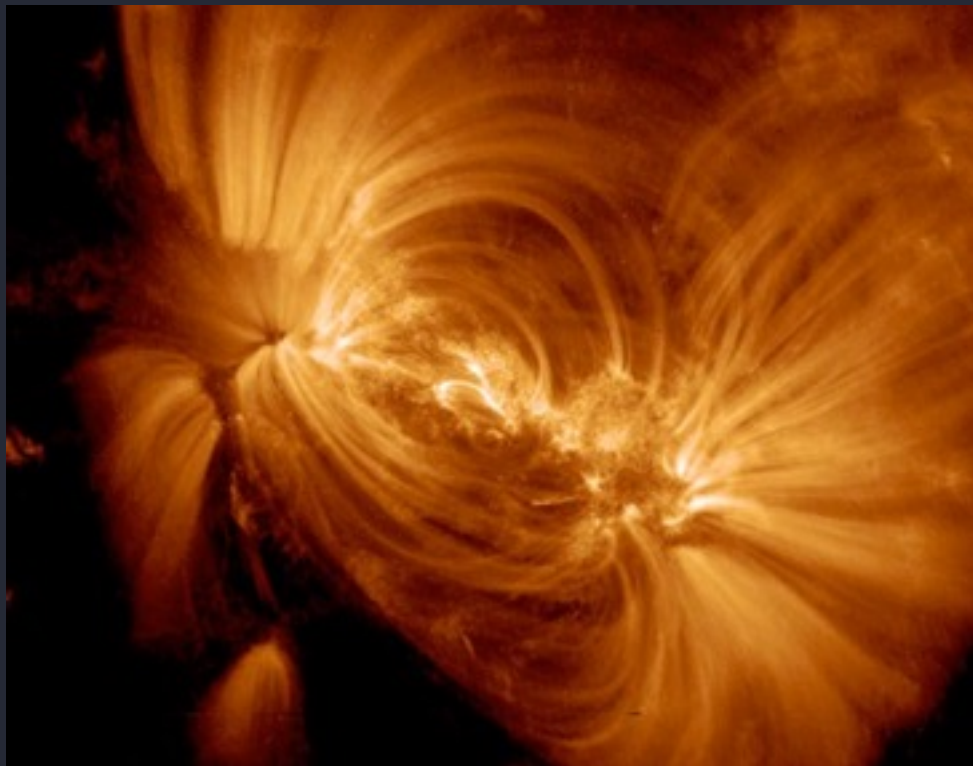
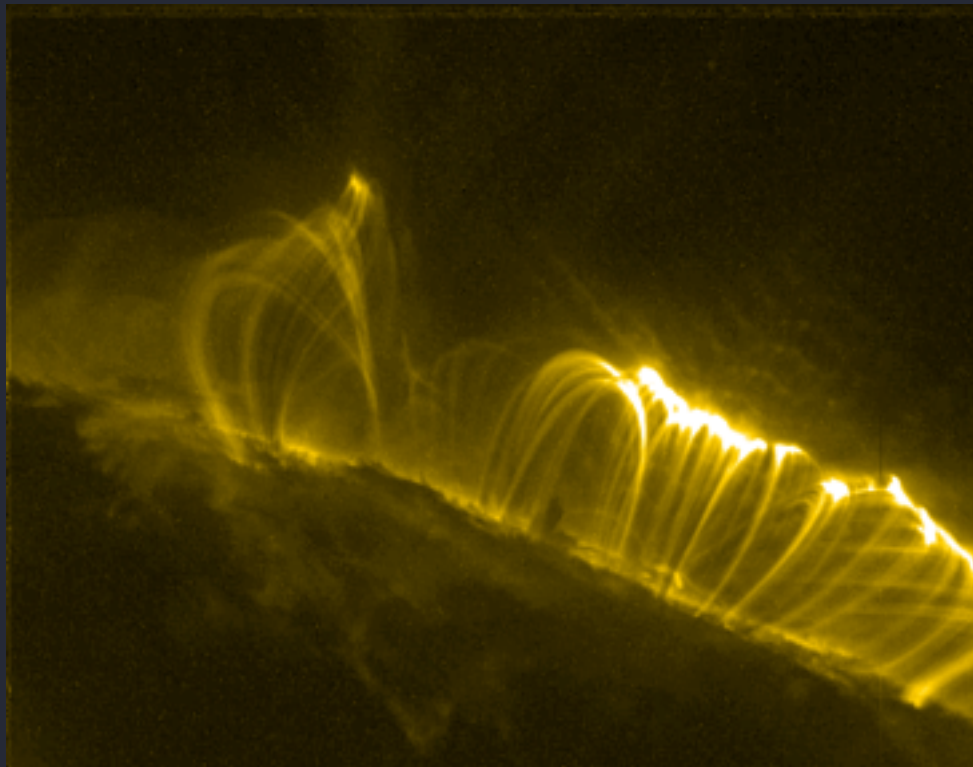
Key points so far:

Massive stars have strong winds

Spectroscopy allows us to study structures that we can't see in images

Next: Stellar X-ray emission

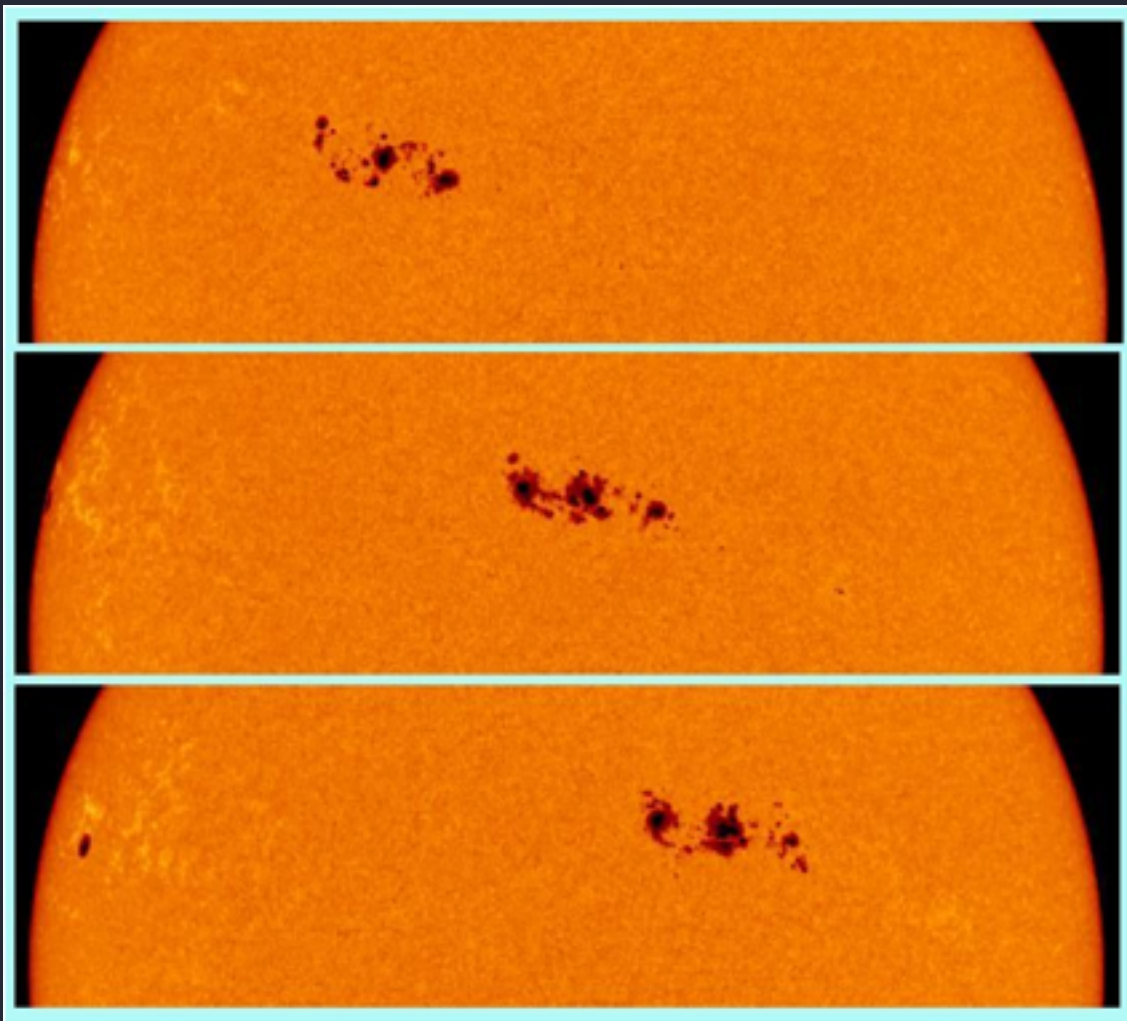
The Sun - and other cool, low-mass stars - emit X-rays



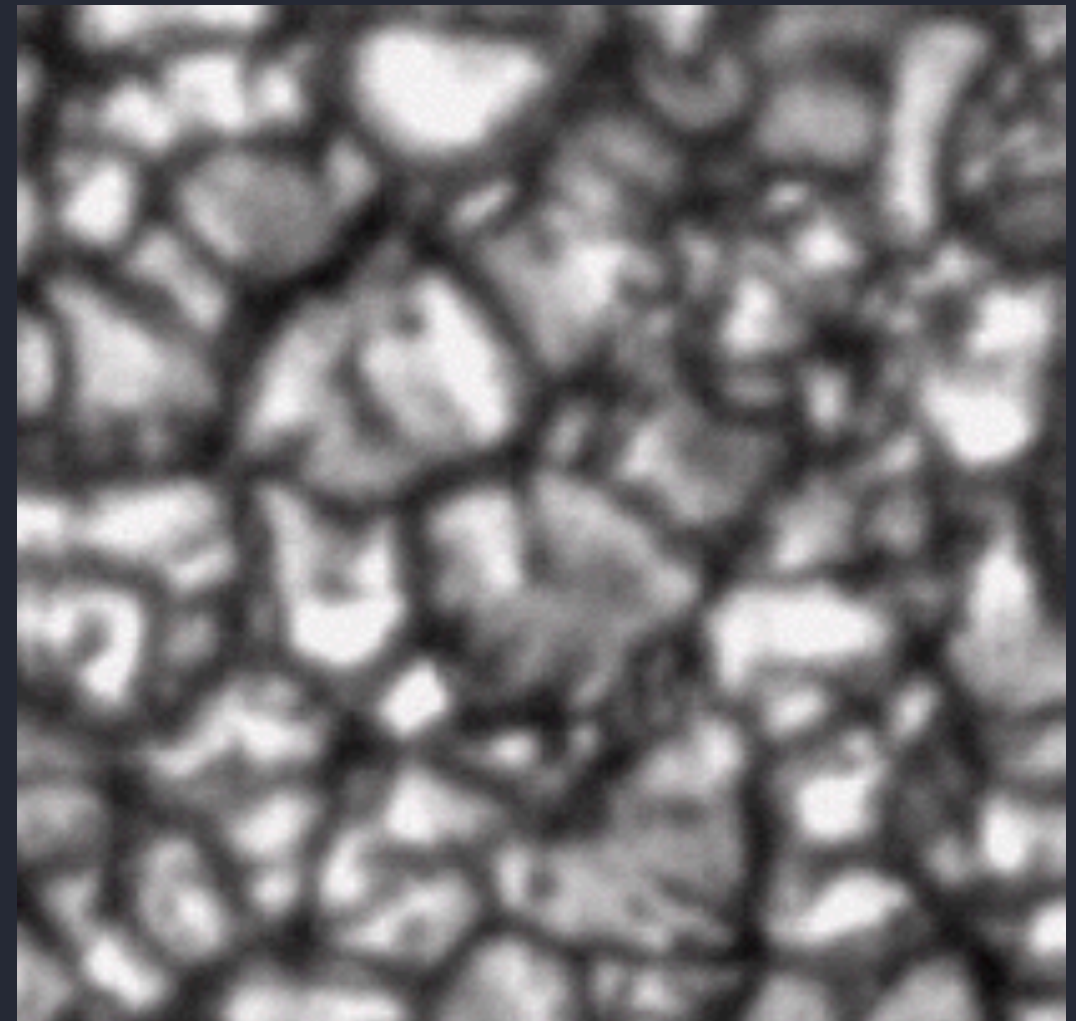
NASA:TRACE

The Sun's X-ray emission is associated with its magnetic dynamo (rotation + convection are key ingredients)

rotation



convection



cool stars

vs.

hot stars



starfish, *in situ*, at the Monterey, California Aquarium (photo: D. Cohen)

cool stars

vs.

hot stars

no convection, no dynamo, no
magnetic field, no corona, no
X-rays?



starfish, *in situ*, at the Monterey, California Aquarium (photo: D. Cohen)

discovery of massive star X-ray emission in 1970s

THE ASTROPHYSICAL JOURNAL, 234:L51-54, 1979 November 15
© 1979. The American Astronomical Society. All rights reserved. Printed in U.S.A.

DISCOVERY OF AN X-RAY STAR ASSOCIATION IN VI CYGNI (CYG OB2)

F. R. HARNDEN, JR., G. BRANDUARDI, M. ELVIS,¹ P. GORENSTEIN, J. GRINDLAY,
J. P. PYE,¹ R. ROSNER, K. TOPKA, AND G. S. VAIANA²

Harvard-Smithsonian Center for Astrophysics, Cambridge, Massachusetts

Received 1979 June 26; accepted 1979 July 26

ABSTRACT

A group of six X-ray sources located within $0^{\circ}.4$ of Cygnus X-3 has been discovered with the *Einstein* Observatory. These sources have been positively identified and five of them correspond to stars in the heavily obscured OB association VI Cygni. The optical counterparts include four of the most luminous O stars within the field of view and a B5 supergiant. These sources are found to have typical X-ray luminosities L_x (0.2–4.0 keV) $\sim 5 \times 10^{33}$ ergs s⁻¹, with temperatures $T \sim 10^{6.8}$ K and hydrogen column densities $N_H \sim 10^{22}$ cm⁻², and therefore comprise a new class of low-luminosity galactic X-ray sources associated with early-type stars.

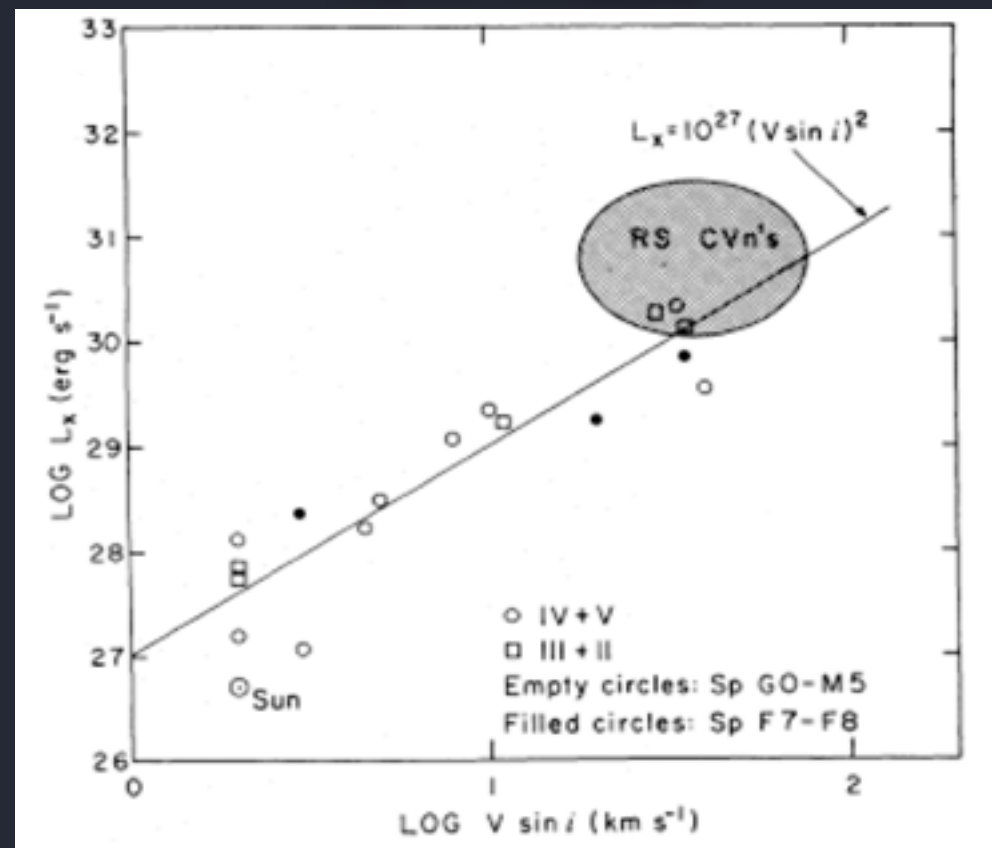
Massive stars have some *different* X-ray production mechanism



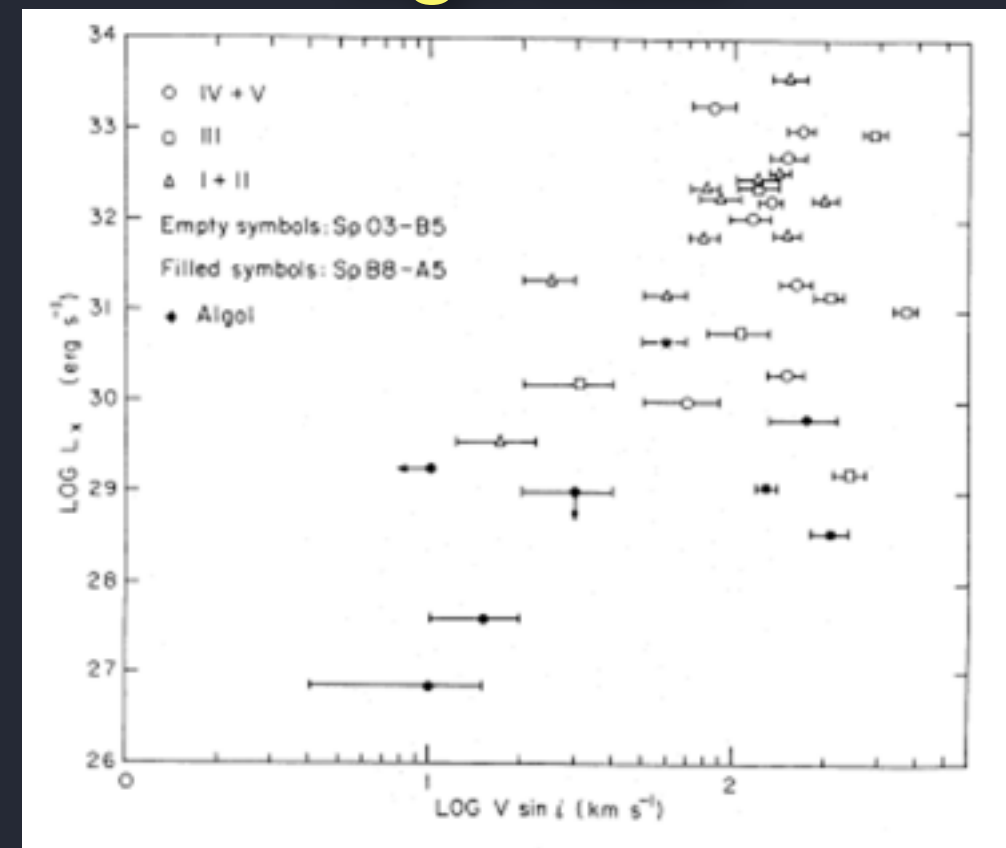
Maybe due to their powerful winds?

No observed correlation between rotation and X-ray luminosity

low mass



high mass



X-ray properties of bright OB-type stars detected in the ROSAT all-sky survey

T.W. Berghöfer^{1,2*}, J.H.M.M. Schmitt¹, R. Danner^{1,3}, and J.P. Cassinelli⁴

¹ Max-Planck-Institut für Extraterrestrische Physik, Giessenbachstr, 1, D-85740 Garching, Germany

² Center for EUV Astrophysics, 2150 Kittredge Street, University of California, Berkeley, CA 94720, USA

³ Division of Physics, Mathematics, and Astronomy, Caltech 105-24, Pasadena, CA 91125, USA

⁴ University of Wisconsin - Madison, Department of Astronomy, 475 North Charter Street, Madison, WI 53706-1582, USA

Received 17 July 1996 / Accepted 26 November 1996

Abstract. The ROSAT all-sky survey has been used to study the X-ray properties for all OB-type stars listed in the Yale Bright Star Catalogue. Here we present a detailed astrophysical discussion of our analysis of the X-ray properties of our complete sample of OB-type stars; a compilation of the X-ray data is provided in an accompanying paper (Berghöfer, Schmitt & Cassinelli 1996).

We demonstrate that the “canonical” relation between X-ray and total luminosity of $L_x/L_{\text{Bol}} \approx 10^{-7}$ valid for O-type stars extends among the early B-type stars down to a spectral type B1–B1.5; for stars of luminosity classes I and II the spectral type B1 defines a dividing line for early-type star X-ray emission.

1979, Pallavicini *et al.* 1981, Chlebowski *et al.* 1989, Sciortino *et al.* 1990). However, the scatter for values of individual stars, 2 orders of magnitude, around the mean value is quite large. The widely accepted model for the X-ray emission from O stars assumes that it is produced by shock-heated gas propagating in the strong winds of these stars. In a phenomenological model Lucy & White (1980) and Lucy (1982) postulate the existence of shocks in the radiation driven winds of hot stars which are formed as a consequence of a strong hydrodynamic instability (e.g., Lucy & Solomon 1980). Hydrodynamical calculations for hot star winds (e.g., Owocki, Castor & Rybicki 1988) provide strong support for such a model. The base corona source of X-

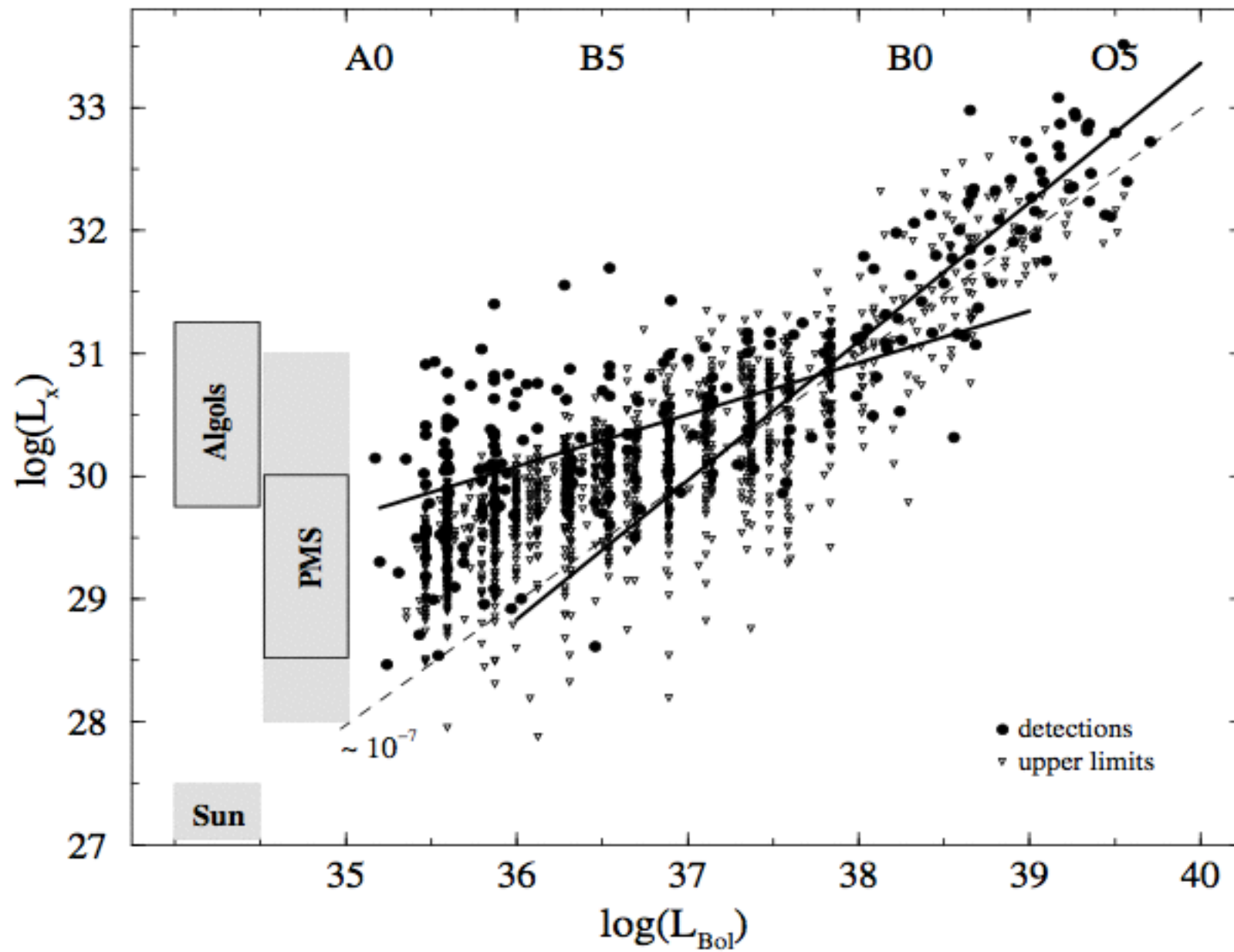


Fig. 4. X-ray luminosities L_x plotted versus bolometric luminosities L_{Bol} ; solid lines represent regression lines for $L_{\text{Bol}} < 10^{38} \text{ erg s}^{-1}$ and $L_{\text{Bol}} > 10^{38} \text{ erg s}^{-1}$, whereas the dashed line shows $L_x = 10^{-7} \times L_{\text{Bol}}$, grey bars at the left side show typical ranges for the X-ray luminosity of Algol-type systems, pre-main sequence stars (PMS), and our Sun.

The wind kinetic power is typically 10^4 times larger than the observed L_x

some process - which doesn't have to be very efficient - converts a small fraction of this kinetic power to heat

the observed X-rays are the thermal radiation from this hot stellar wind plasma

The line-deshadowing instability (LDI)

causes fast, rarefied wind plasma to slam into slower, denser wind plasma

the resulting shocks heat the plasma

the X-rays we see are the thermal emission from this hot wind plasma

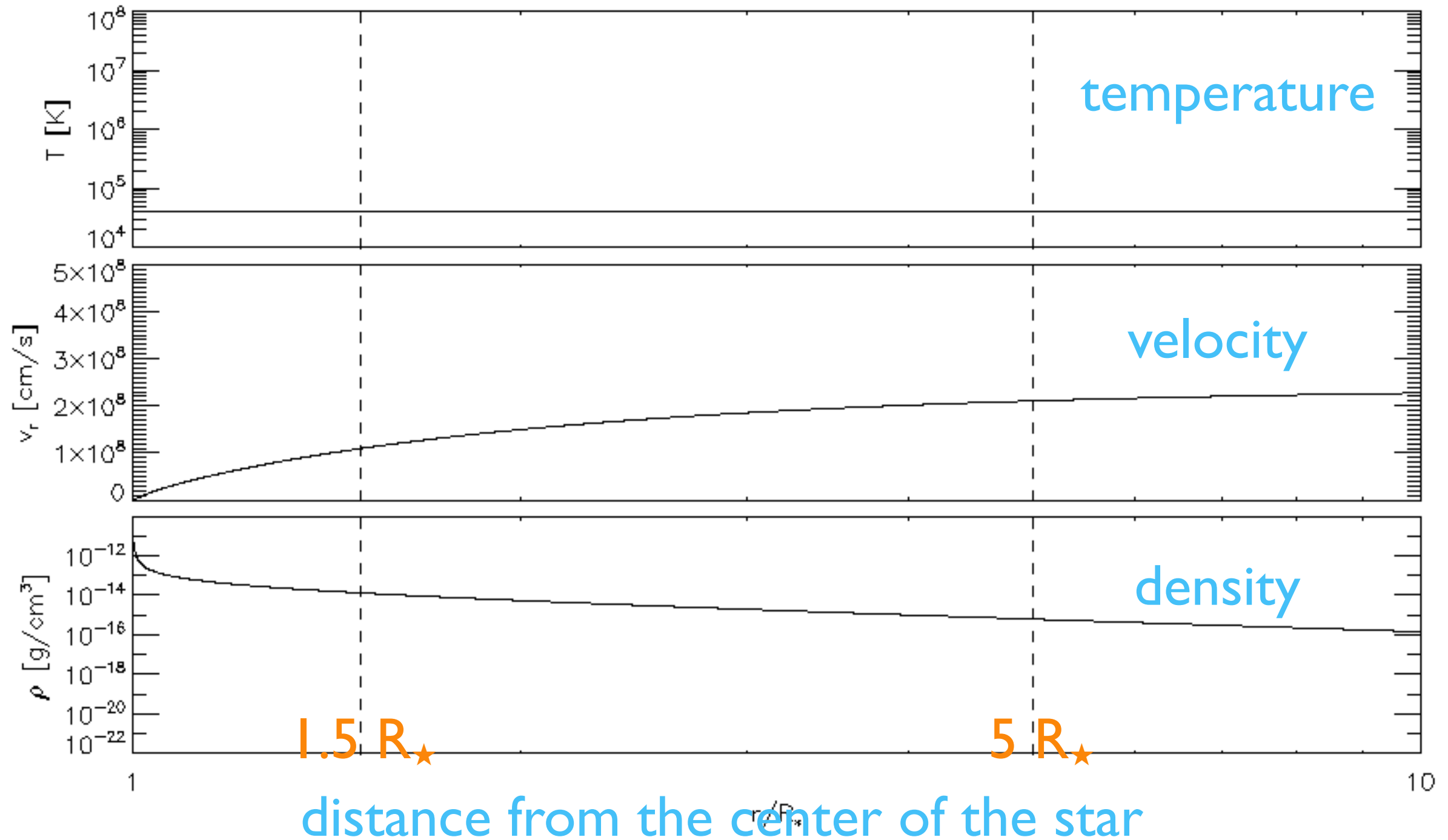
general result from shock theory:

$$T \sim 10^6 (\Delta v_{\text{shock}} / 300 \text{ km/s})^2$$

X-ray emitting plasma is embedded in the wind

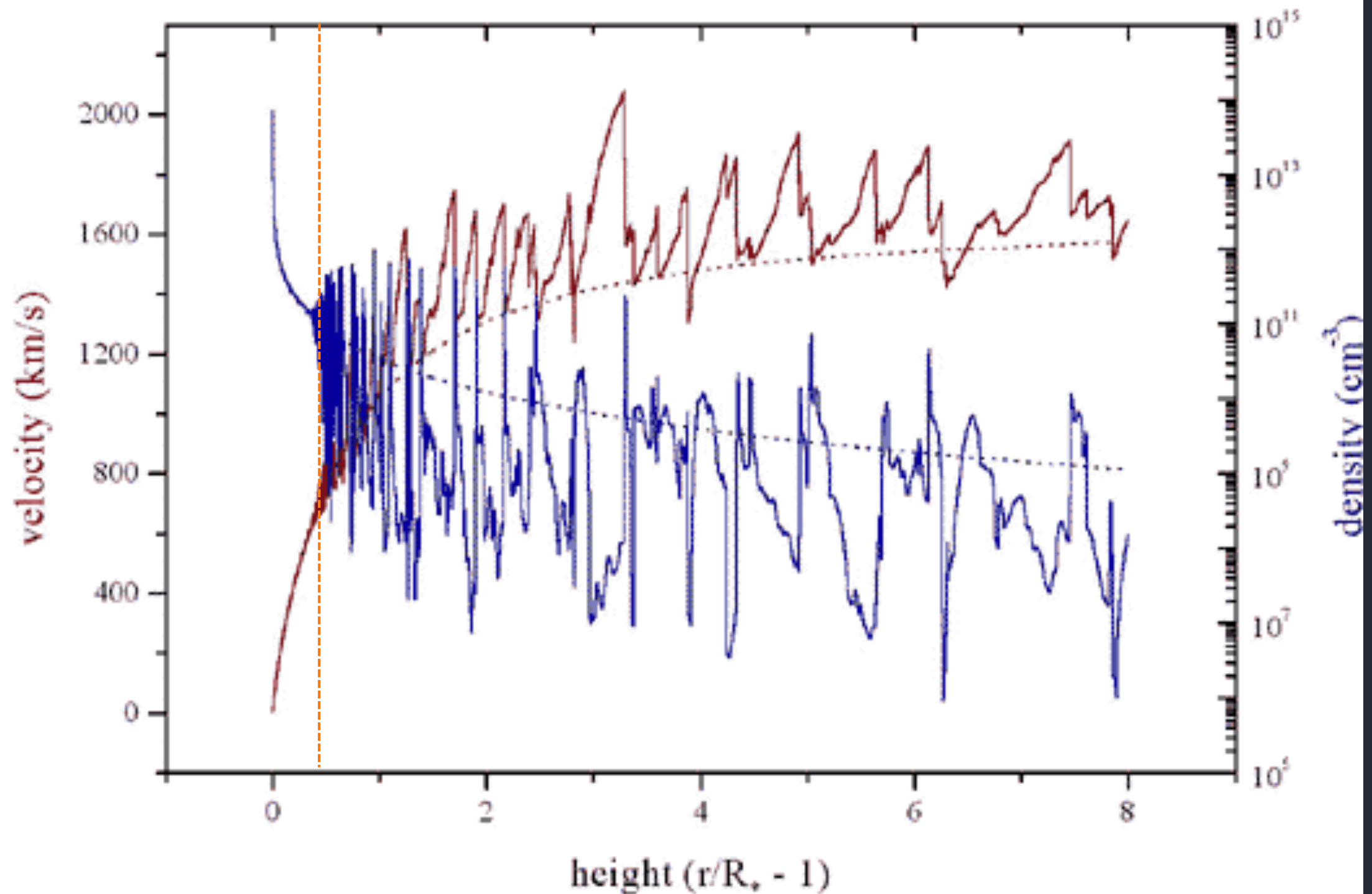
intrinsic instability of radiative driving, Line Deshadowing Instability (LDI), leads to shock-heating of the wind

astro.swarthmore.edu/~cohen/presentations/ifrc3_xmbkol.e-2.gif

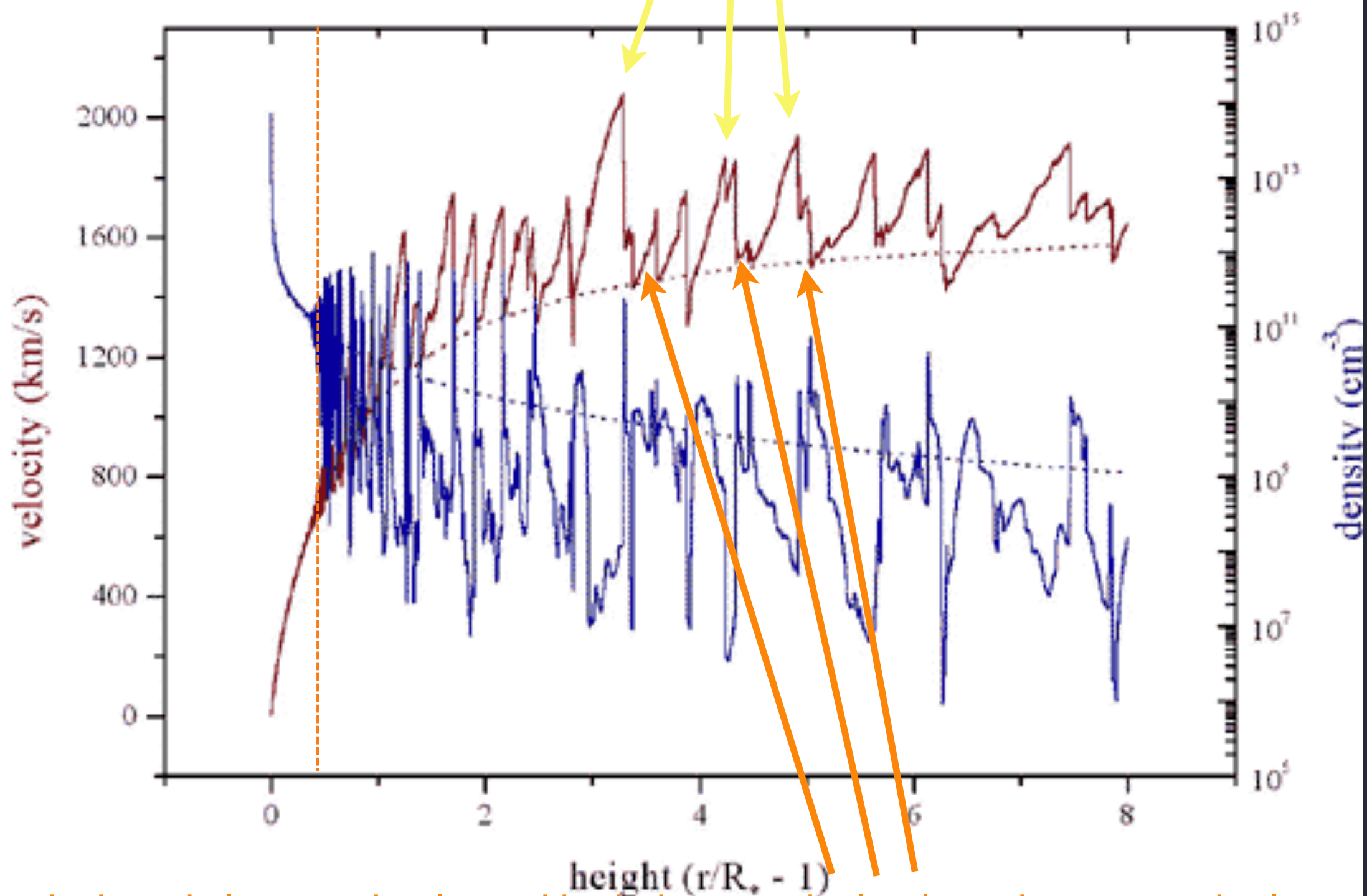


snapshot from the hydro simulation

$r \sim 1.5 R_{\star}$ numerous shock structures above $1.5 R_{\star}$

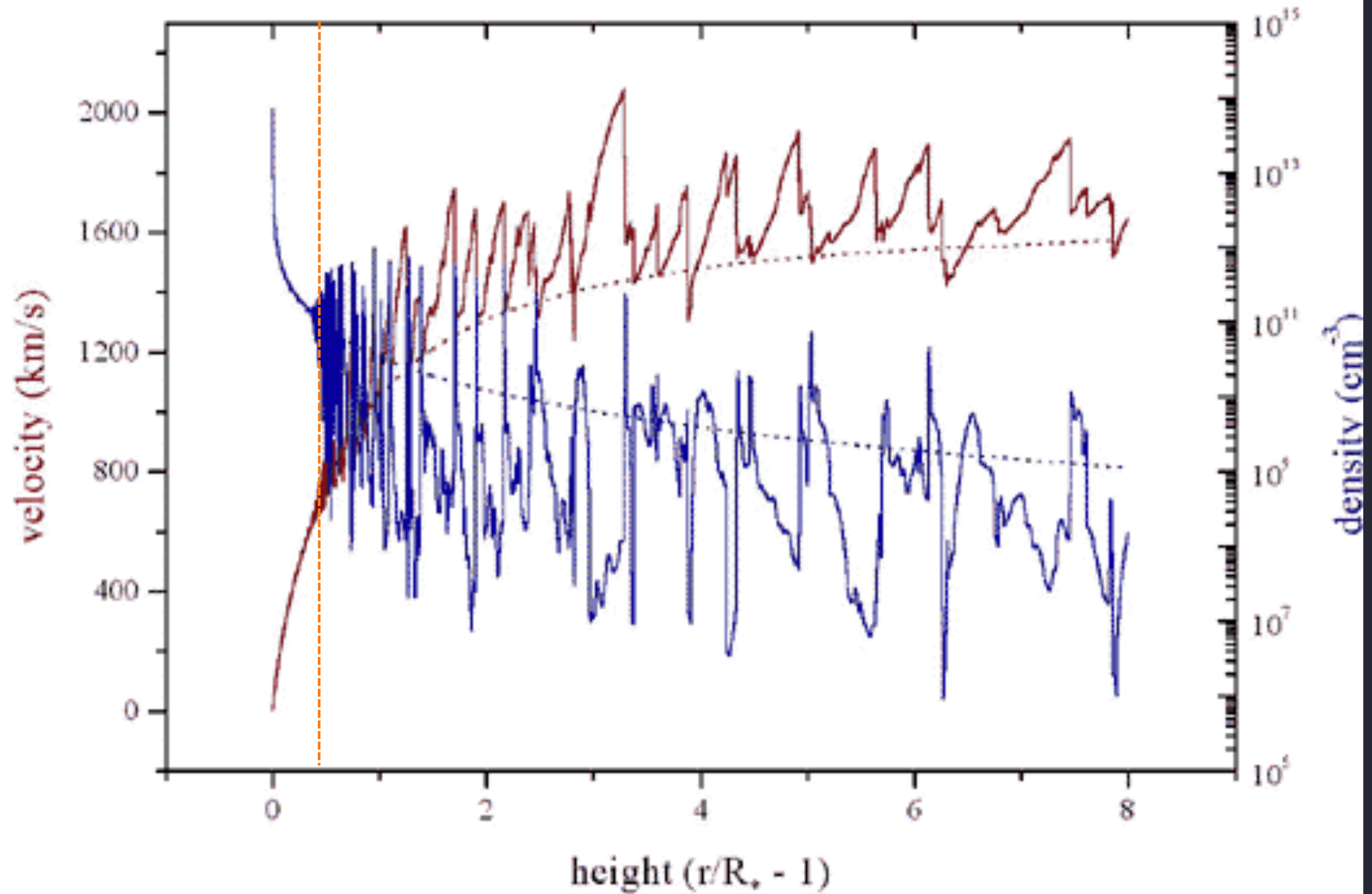


$V_{\text{shock}} \sim 300 \text{ km/s} : T \sim 10^6 \text{ K}$



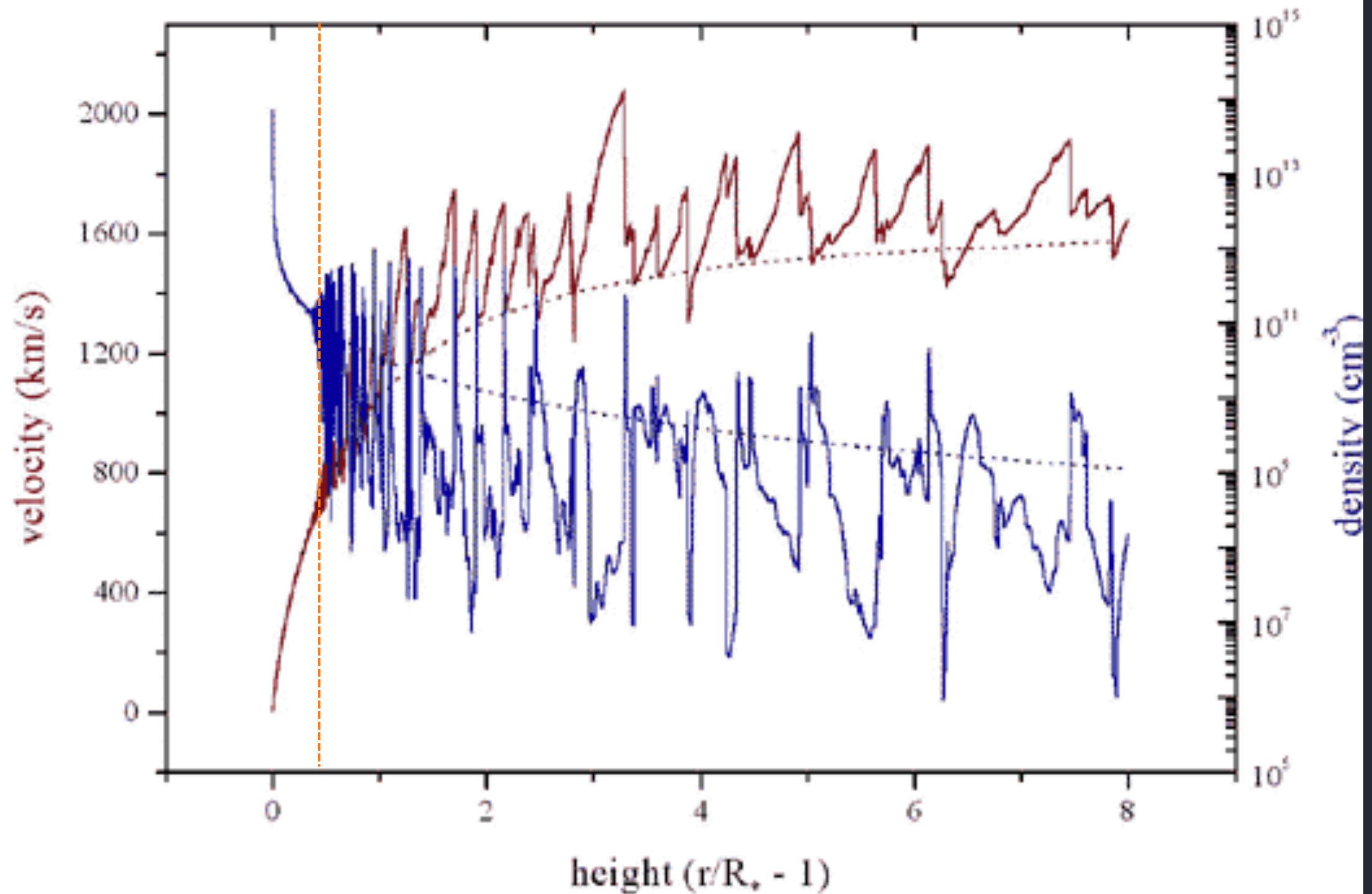
shocked wind plasma is decelerated back down to the local steady-state wind velocity

X-ray emission lines should be Doppler broadened



Less than 1% of the mass of the wind is emitting X-rays

>99% of the wind is cold and X-ray absorbing



Key points so far:

Massive stars emit X-rays

Their radiation-driven winds are the site of the X-ray emission (according to theory)

Next: X-ray spectroscopy of massive stars

X-ray spectroscopy confirms the general scenario embedded wind shocks (EWS)



Chandra launched in 1999 -
first high-resolution X-ray spectrograph

response to photons with
 $h\nu \sim 0.5 \text{ keV}$ up to a few
keV (corresp. $\sim 5\text{\AA}$ to 24\AA)

X-ray imaging? > 0.5 arc sec, at best (100s of AU)
spectroscopy ($\lambda/\Delta\lambda < 1000$ corresp. $v > 300 \text{ km/s}$)

Spectral resolution and velocity

“spectral resolution” how close can two lines be in a spectrum and still be seen as two separate lines?

“spectral resolution” how broad does an intrinsically narrow spectral line look in the spectrograph?

spectral resolution, $R = \lambda/\Delta\lambda$

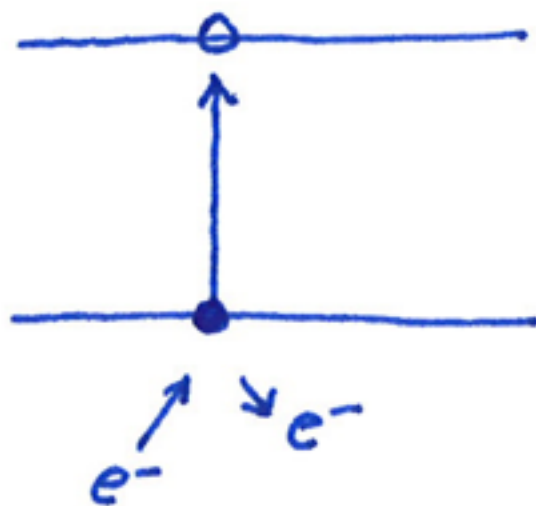
Doppler shift, $\Delta\lambda/\lambda = v/c$

X-ray emission process

thermal emission from collisional plasma

X-ray emission

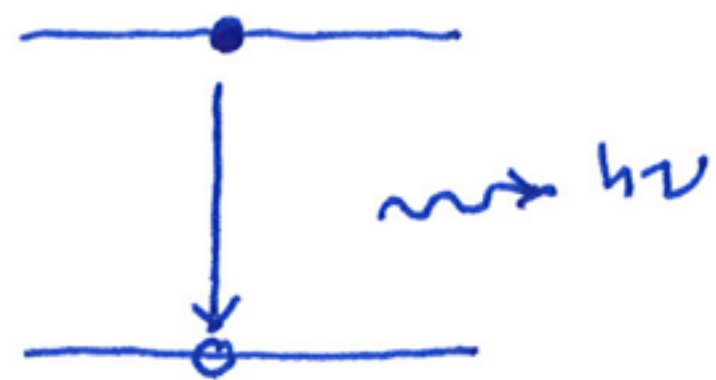
collisional
excitation



followed
by

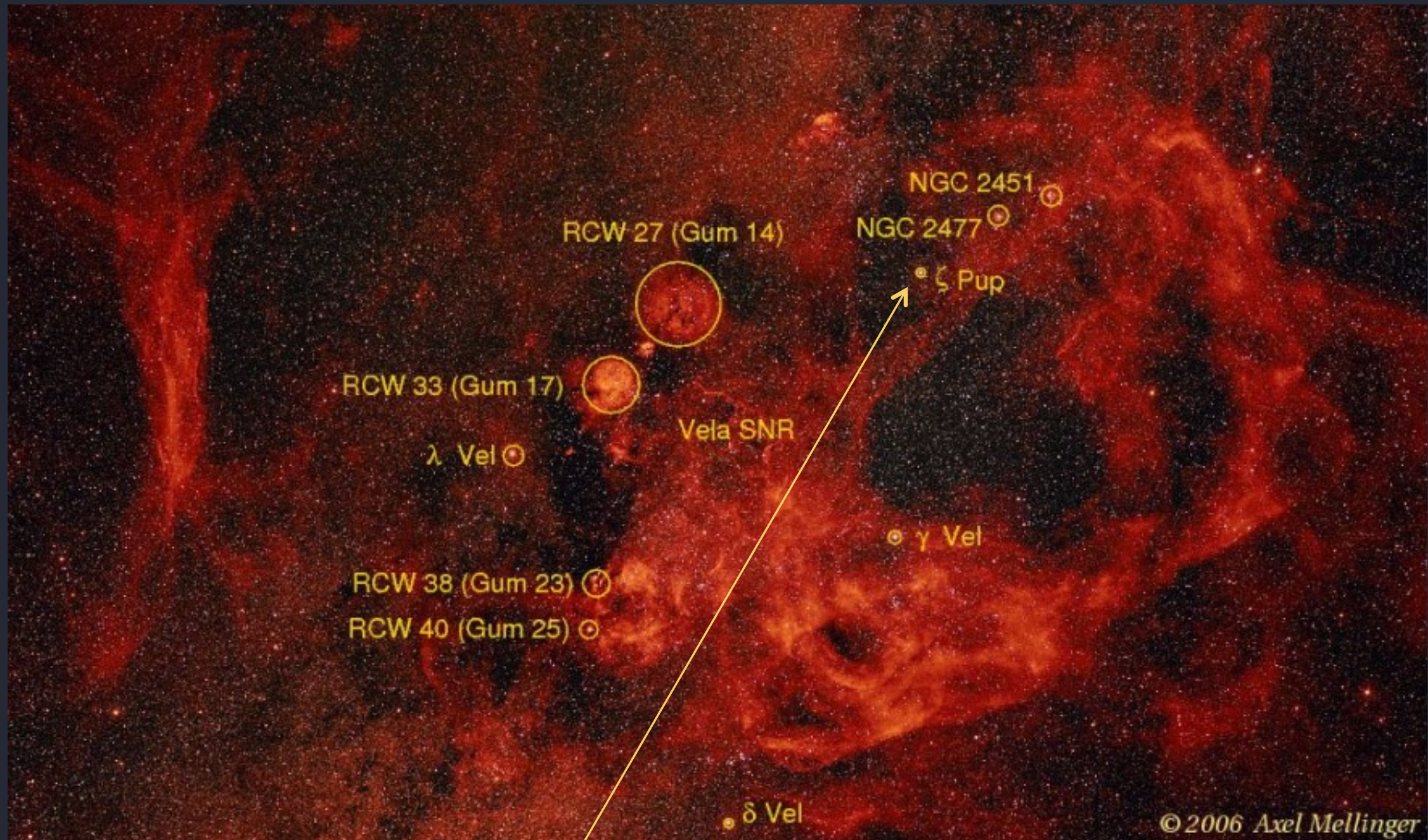


spontaneous
emission



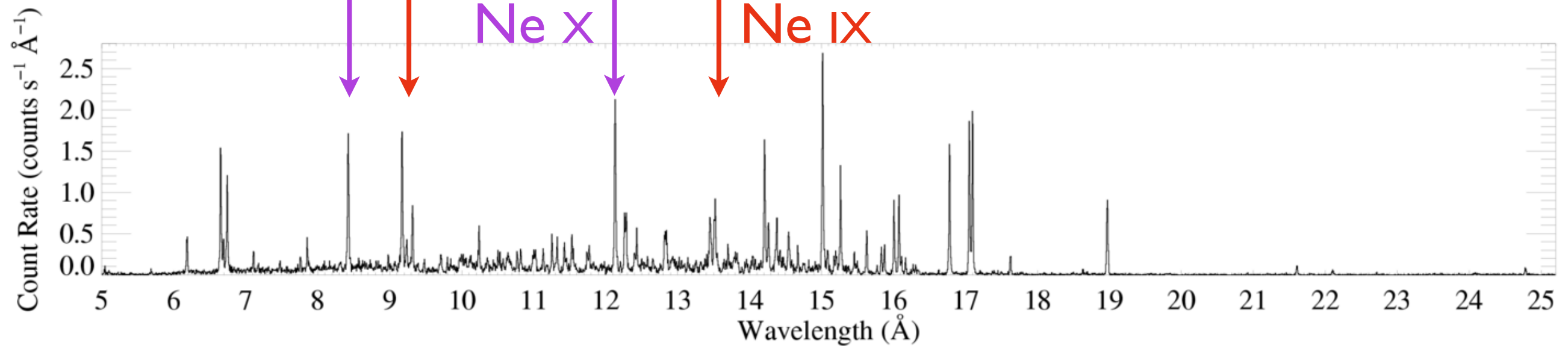
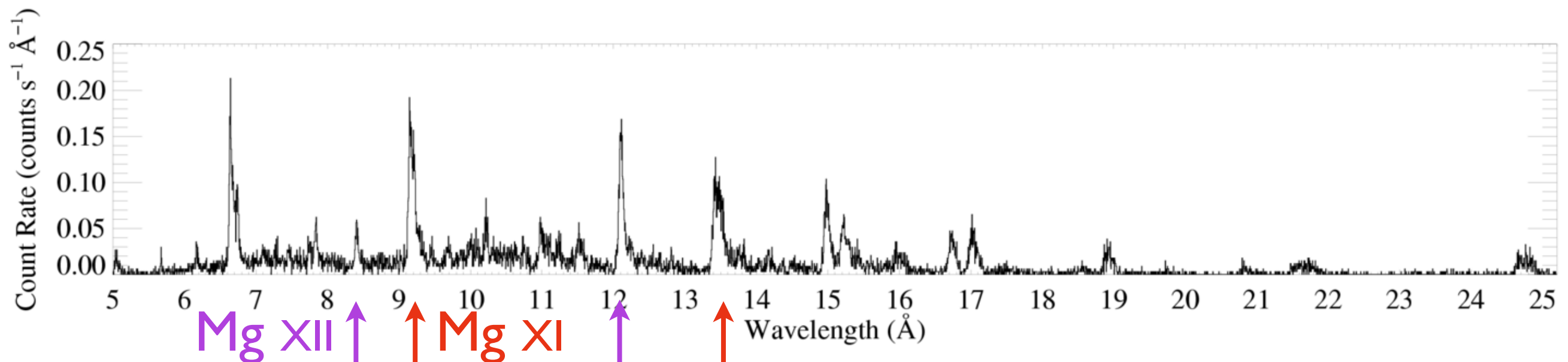
Chandra grating spectroscopy

ζ Pup (O4 If)



Chandra grating (HETGS/MEG) spectra

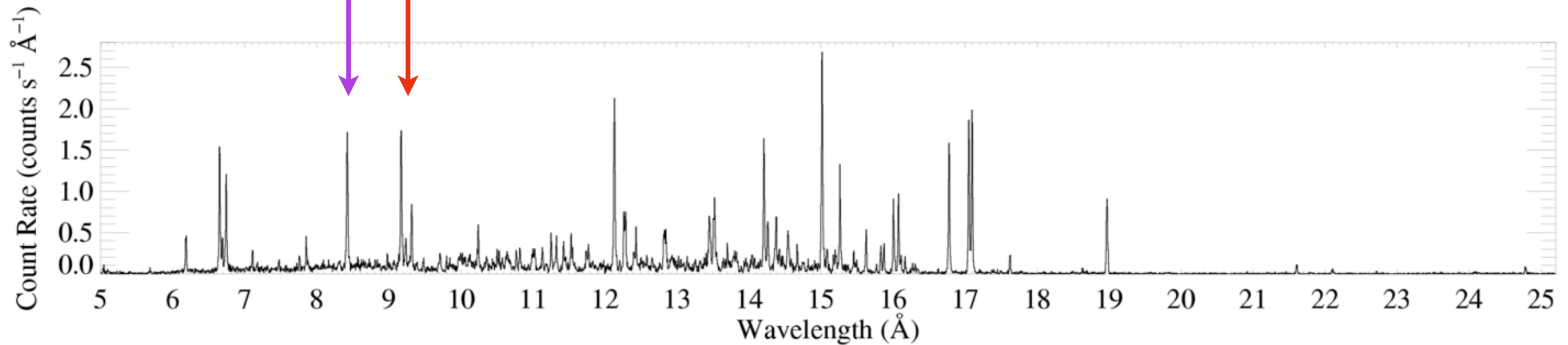
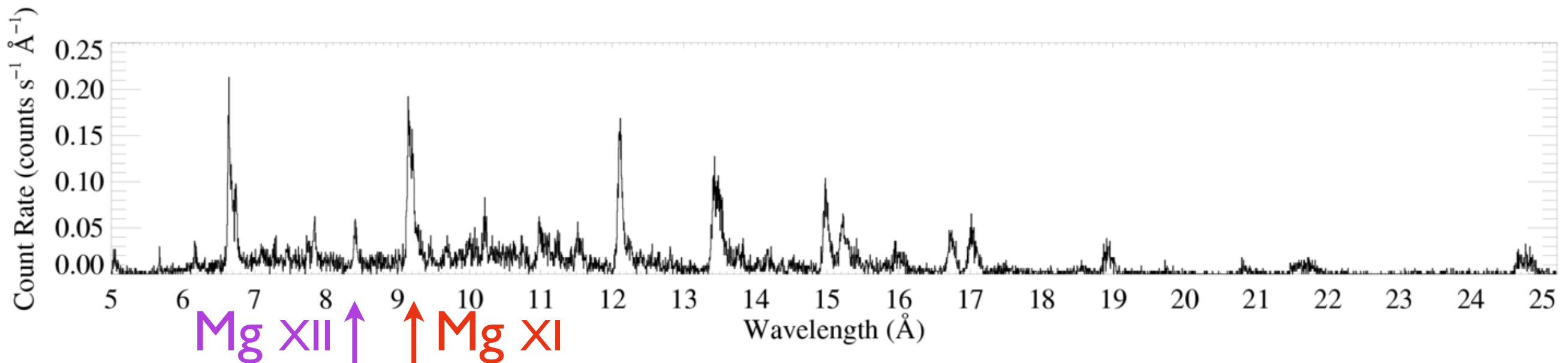
ζ Pup (O4 If)



Capella (G5 III)

typical temperatures $T \sim \text{few } 10^6 \text{ K}$
(late-type stellar coronae tend to be hotter)

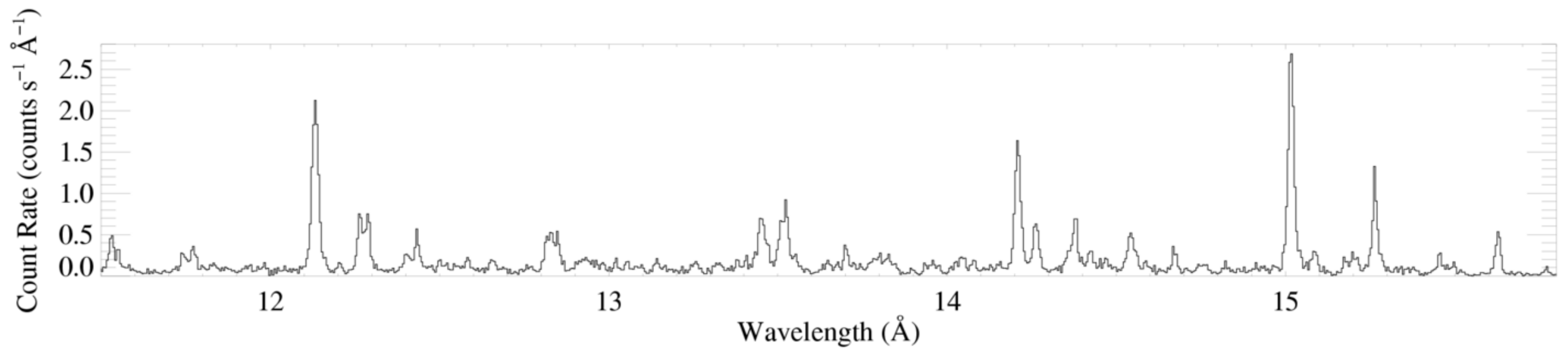
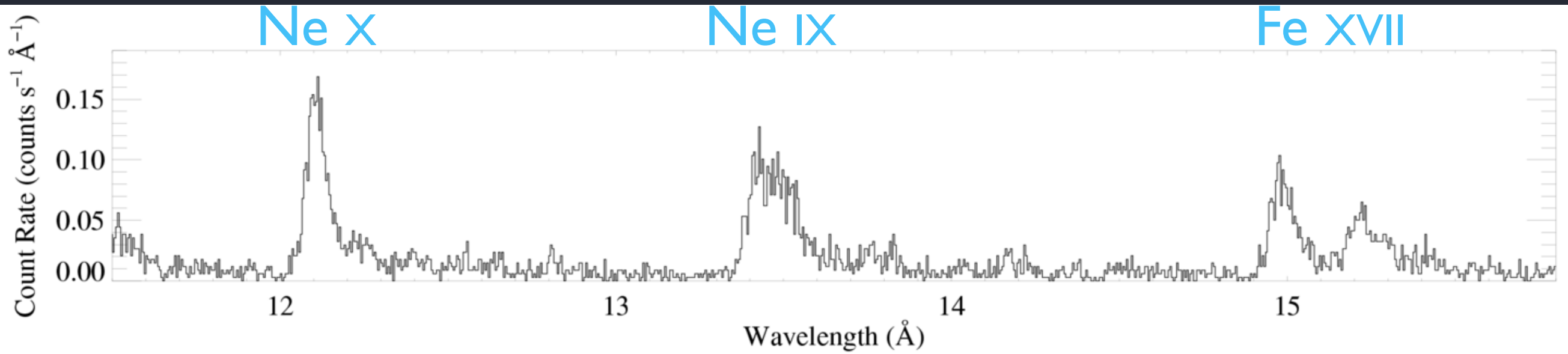
$\zeta \text{ Pup (O4 If)}$



Capella (G5 III)

Zoom in

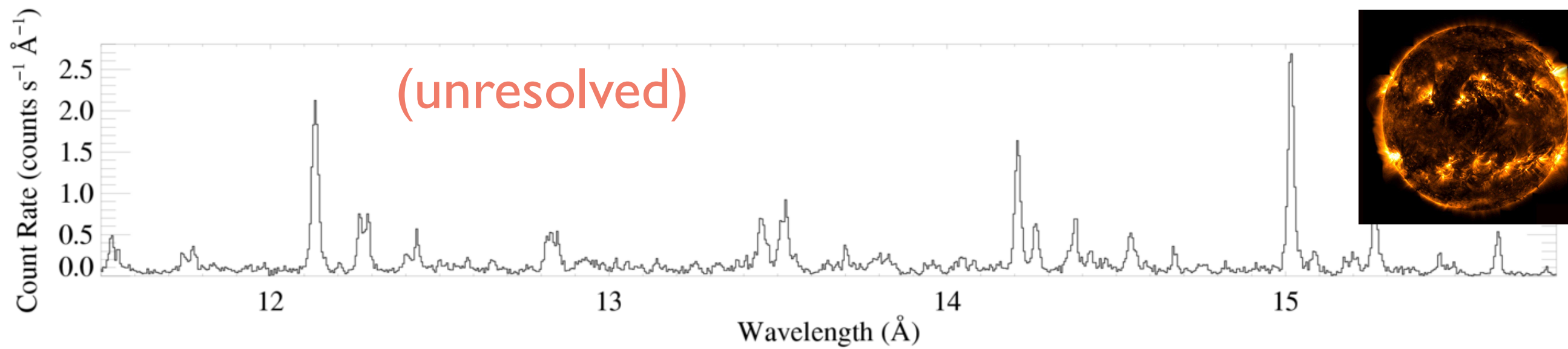
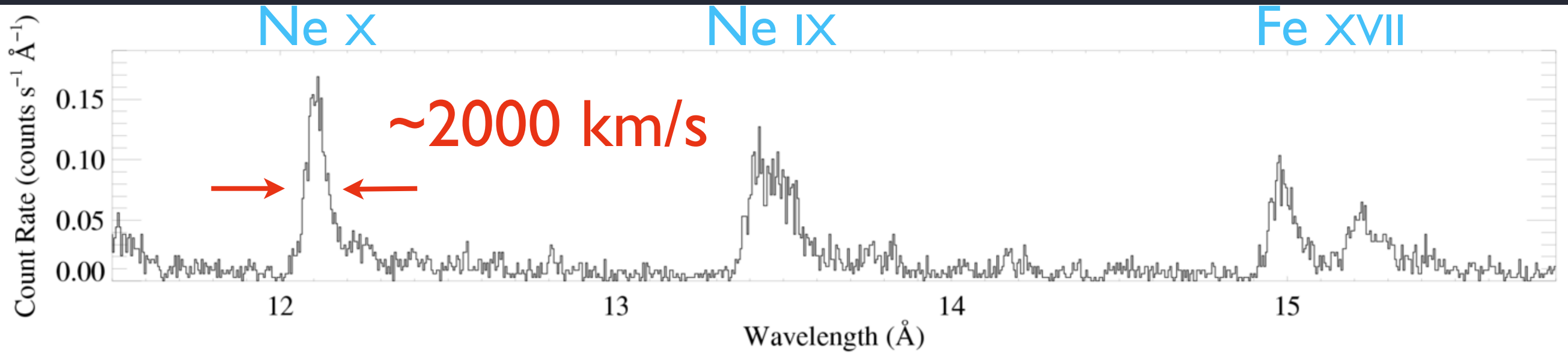
ζ Pup (O4 If)



Capella (G5 III)

Zoom in

ζ Pup (O4 If)

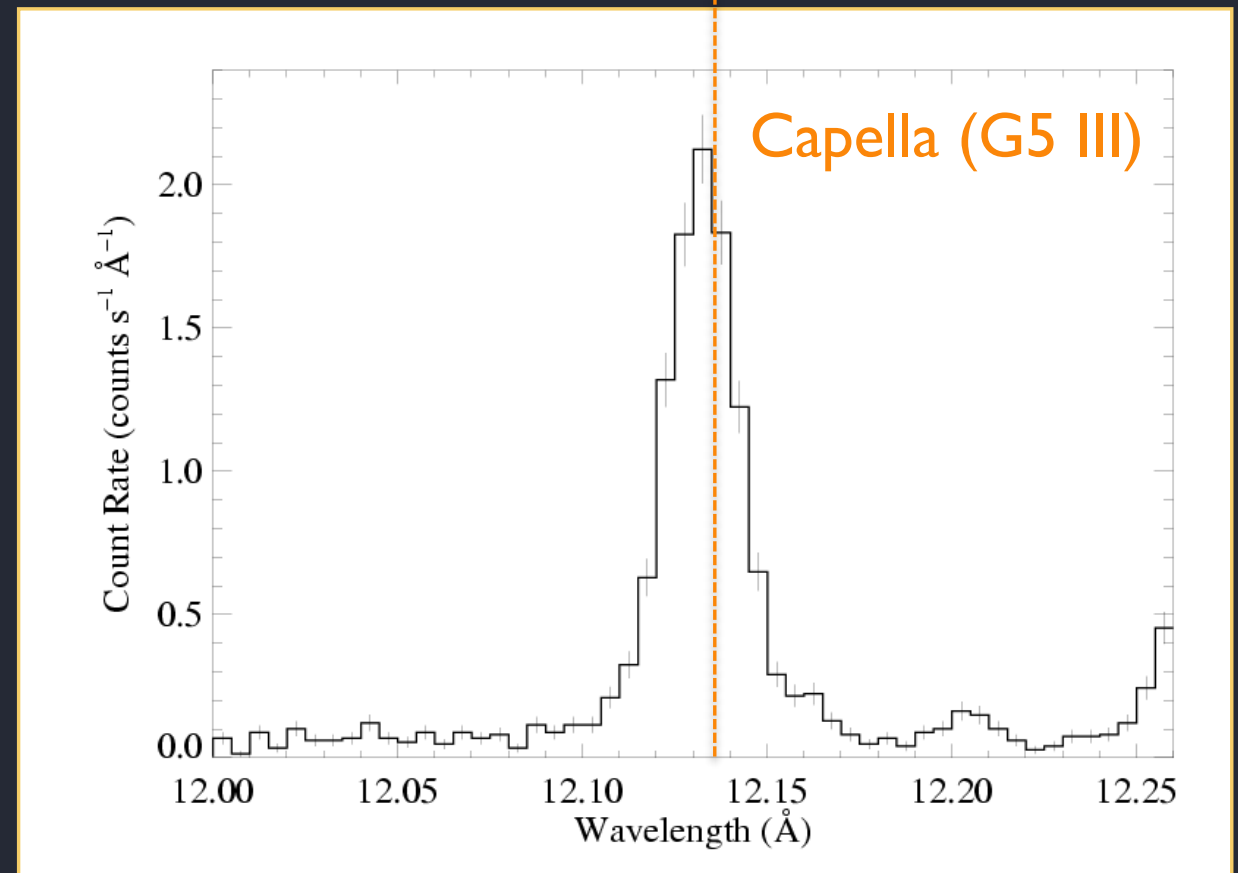
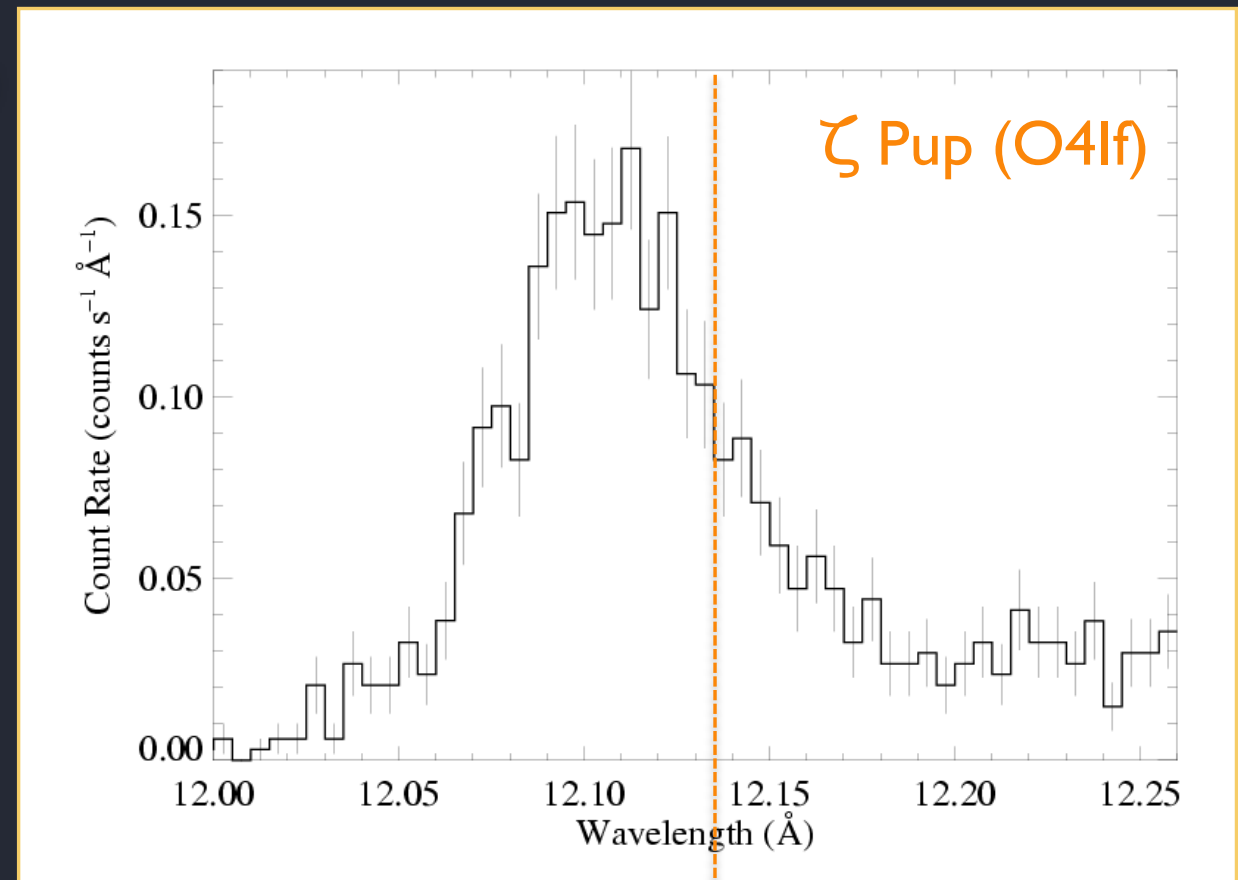


Capella (G5 III)

A careful look at the individual emission lines

characteristic *asymmetry*

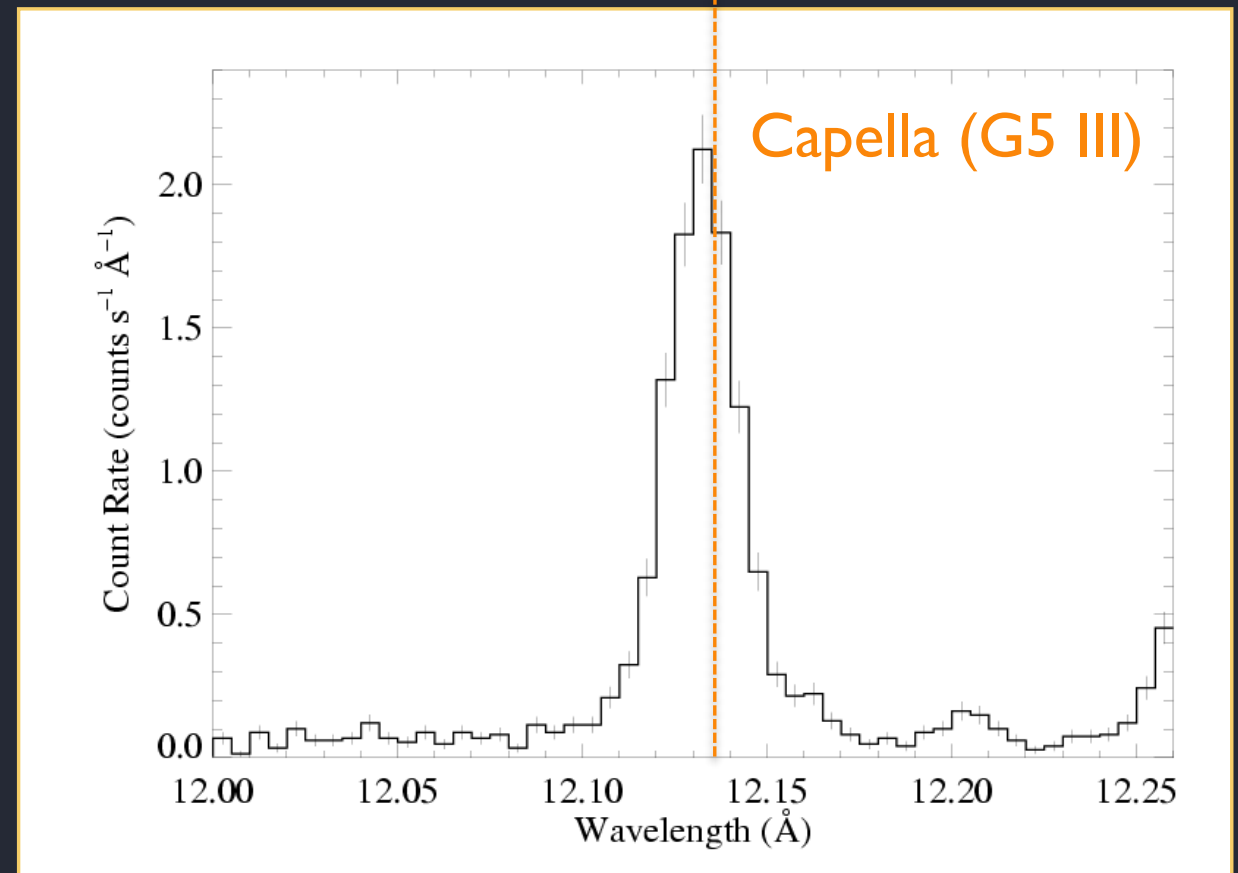
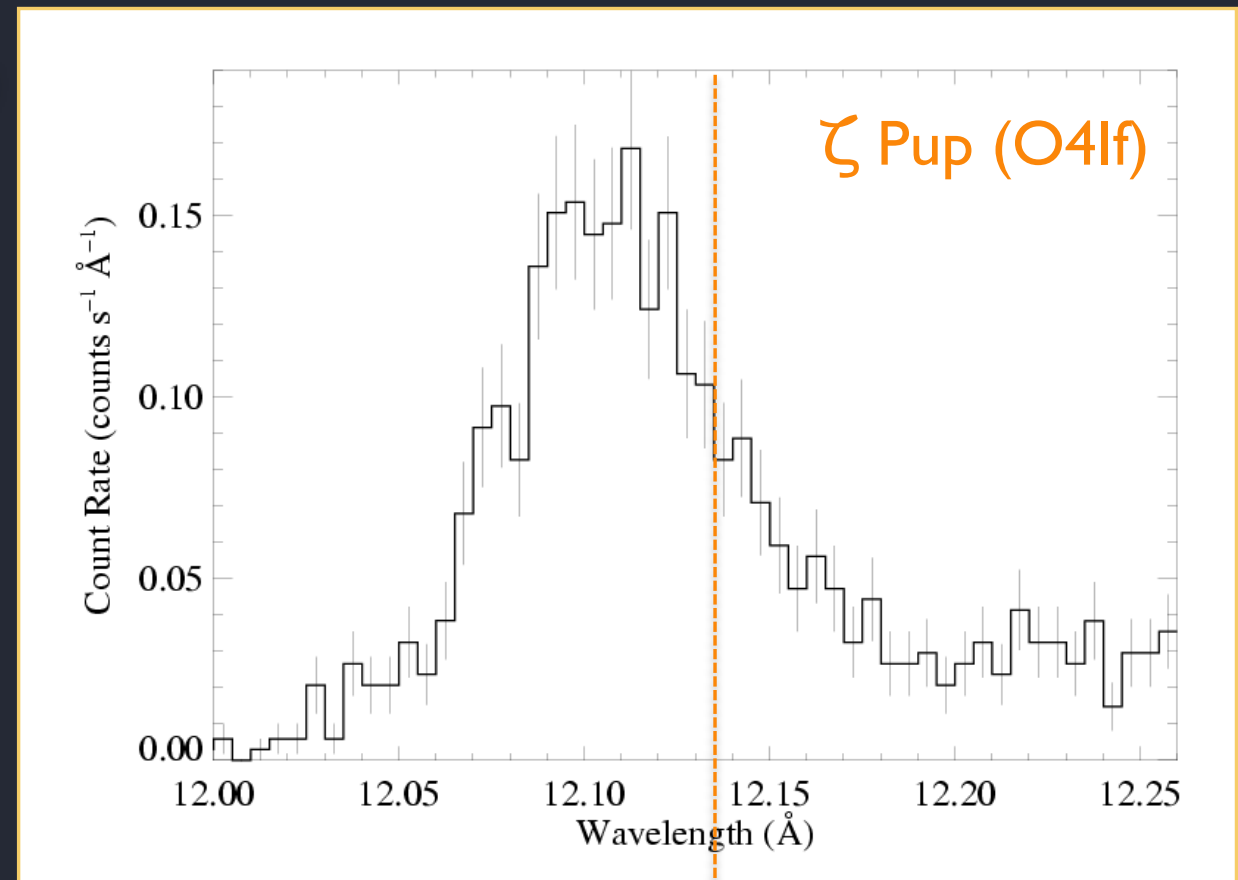
blue-shifted peak
& skewness



A careful look at the individual emission lines

characteristic *asymmetry*

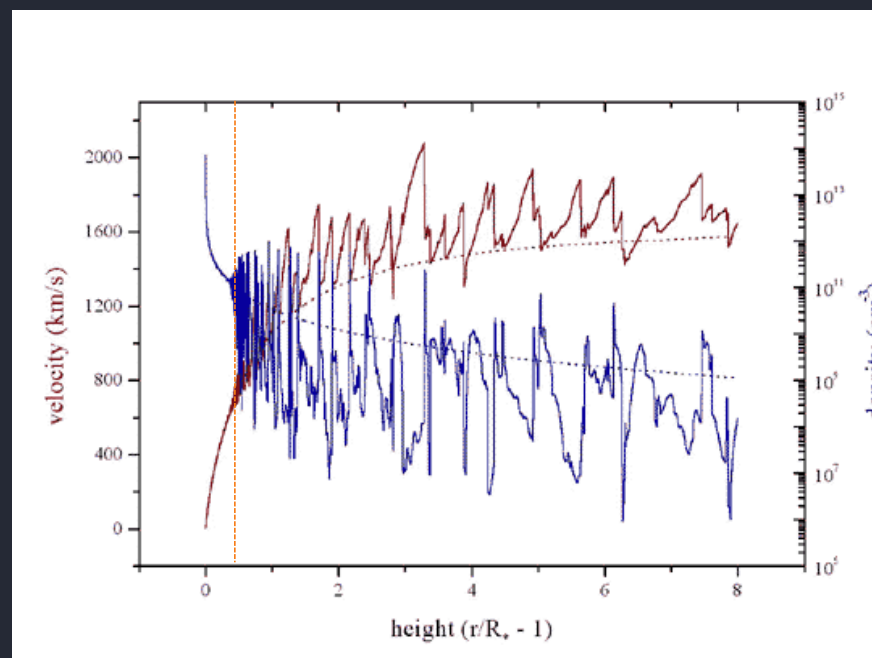
How can this be explained in the context of embedded wind shocks (EWS)?



We need a model that...

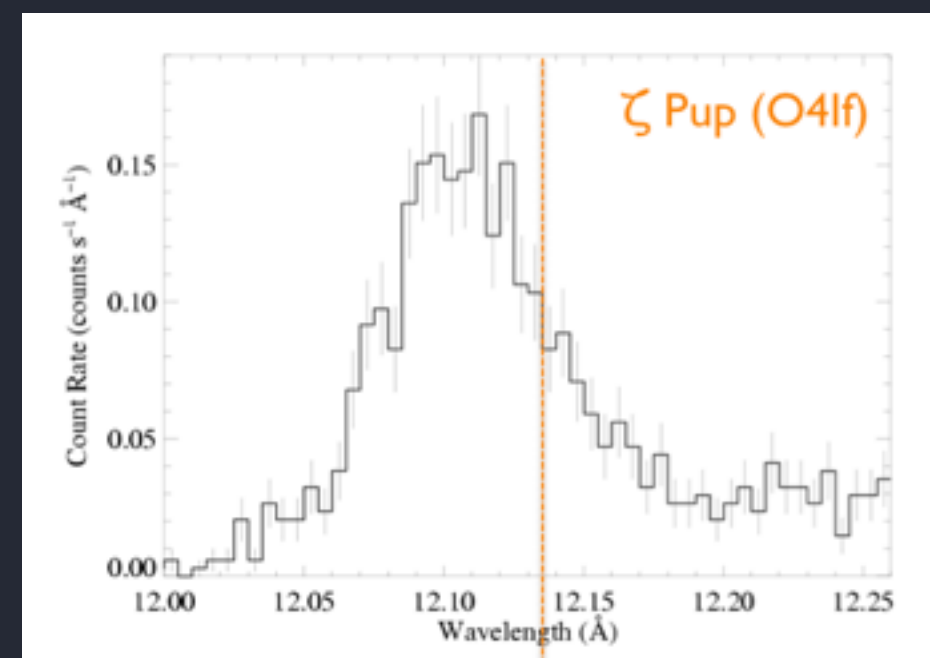
captures the basic physical properties of
the hydro simulations of the LDI

but is simple enough to parameterize and
fit to data



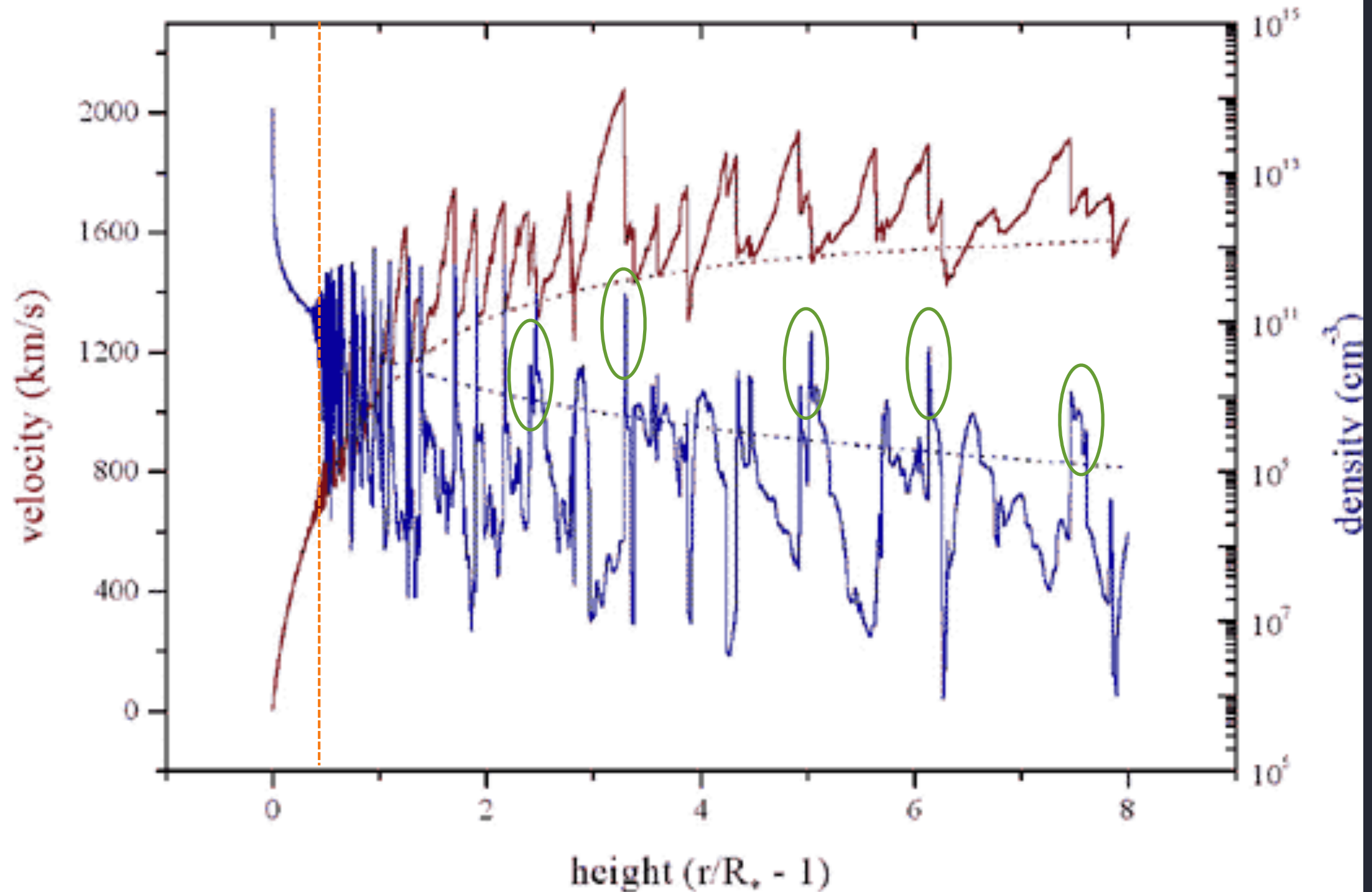
??

←→



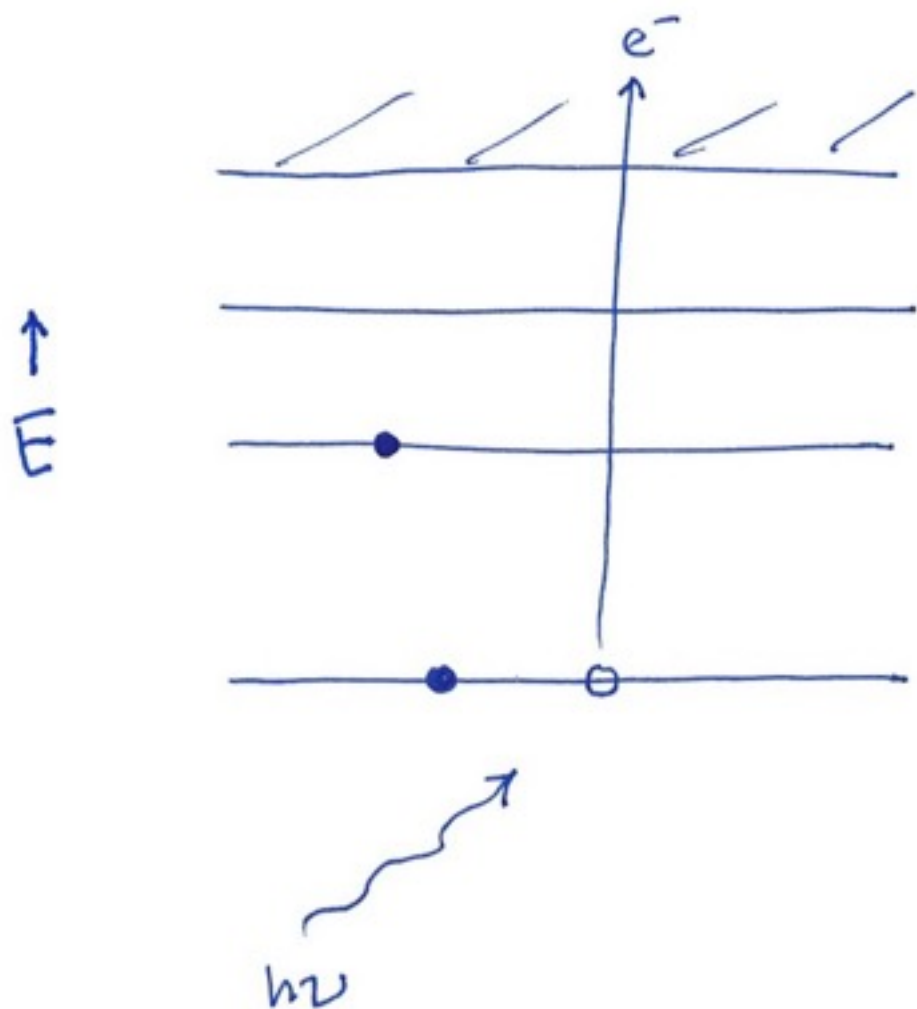
Recall that most of the wind is cold

>99% of the wind is cold and X-ray absorbing

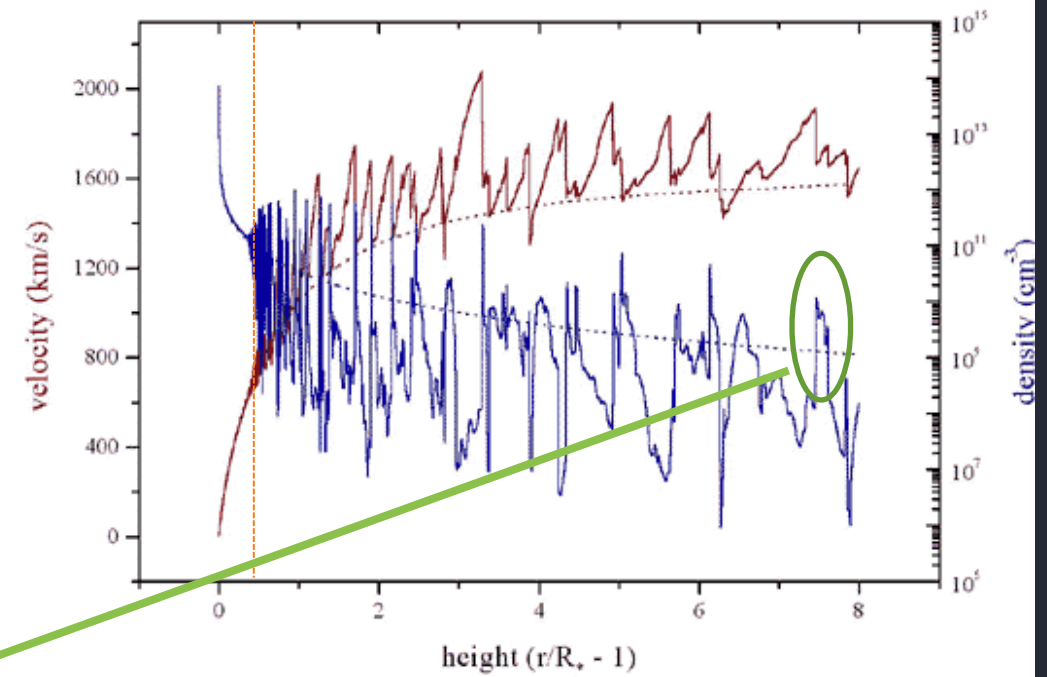


>99% of the wind is cold and X-ray absorbing

inner-shell
photoionization

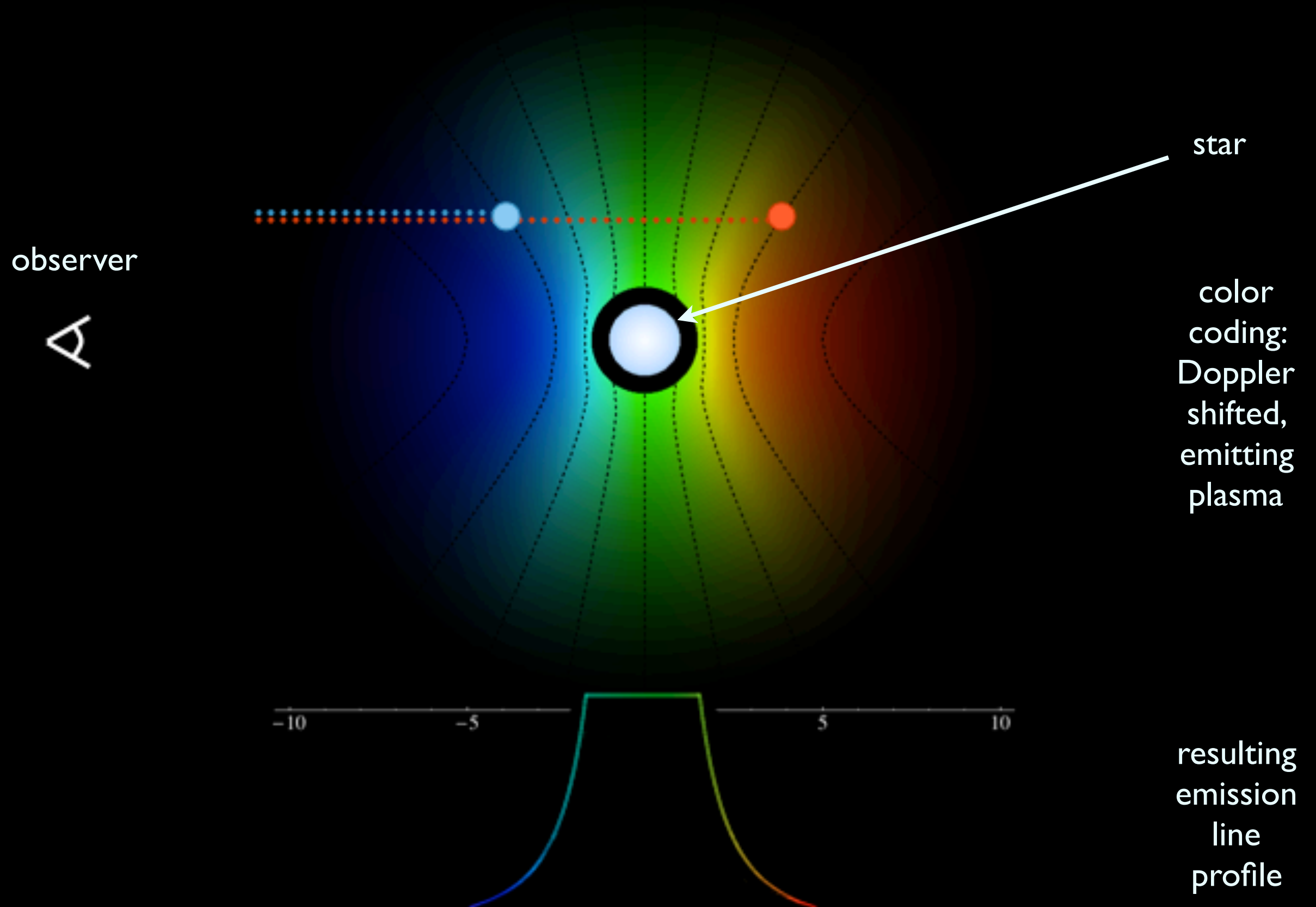


I.P. ~ 1 keV

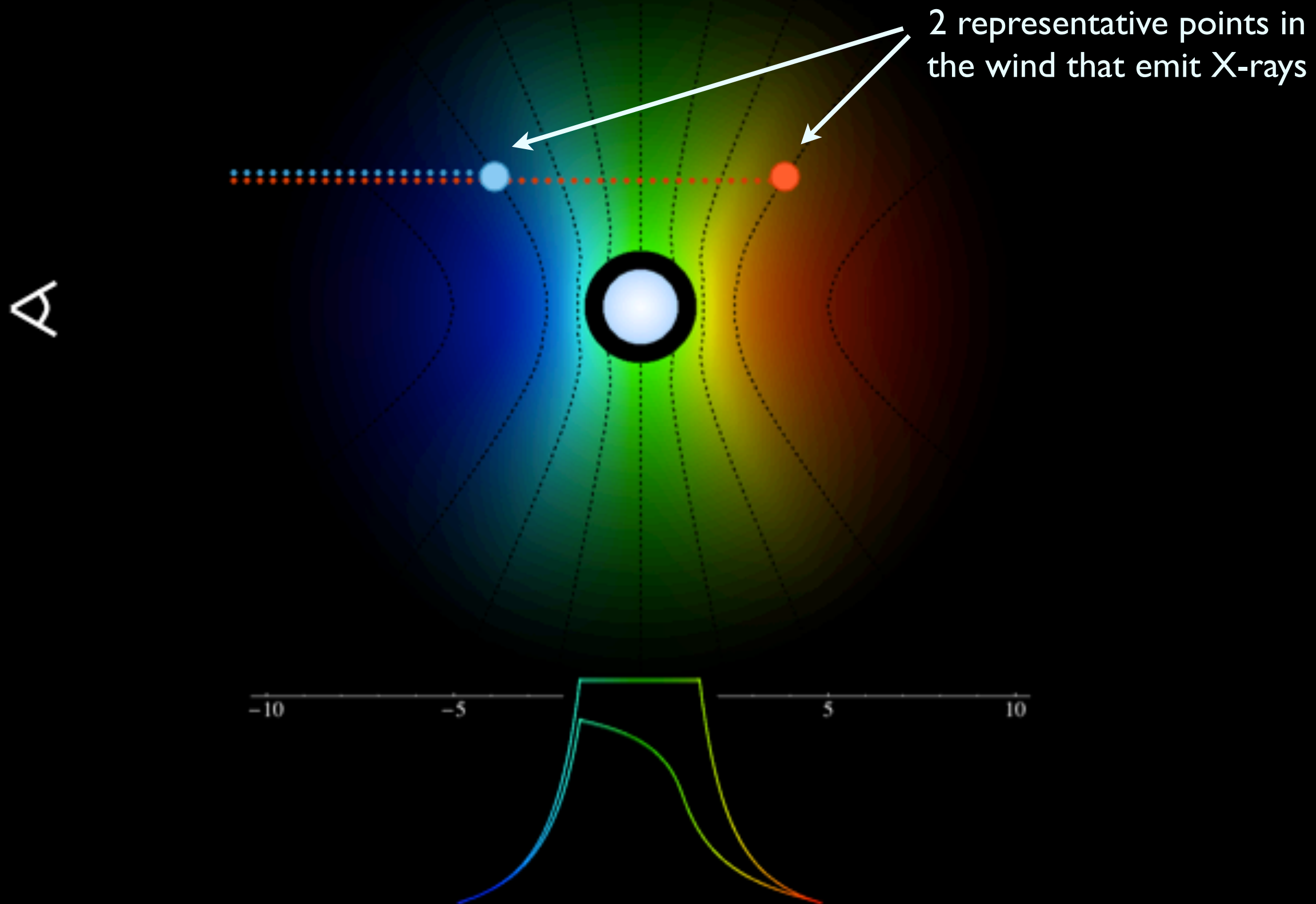


Line Asymmetry

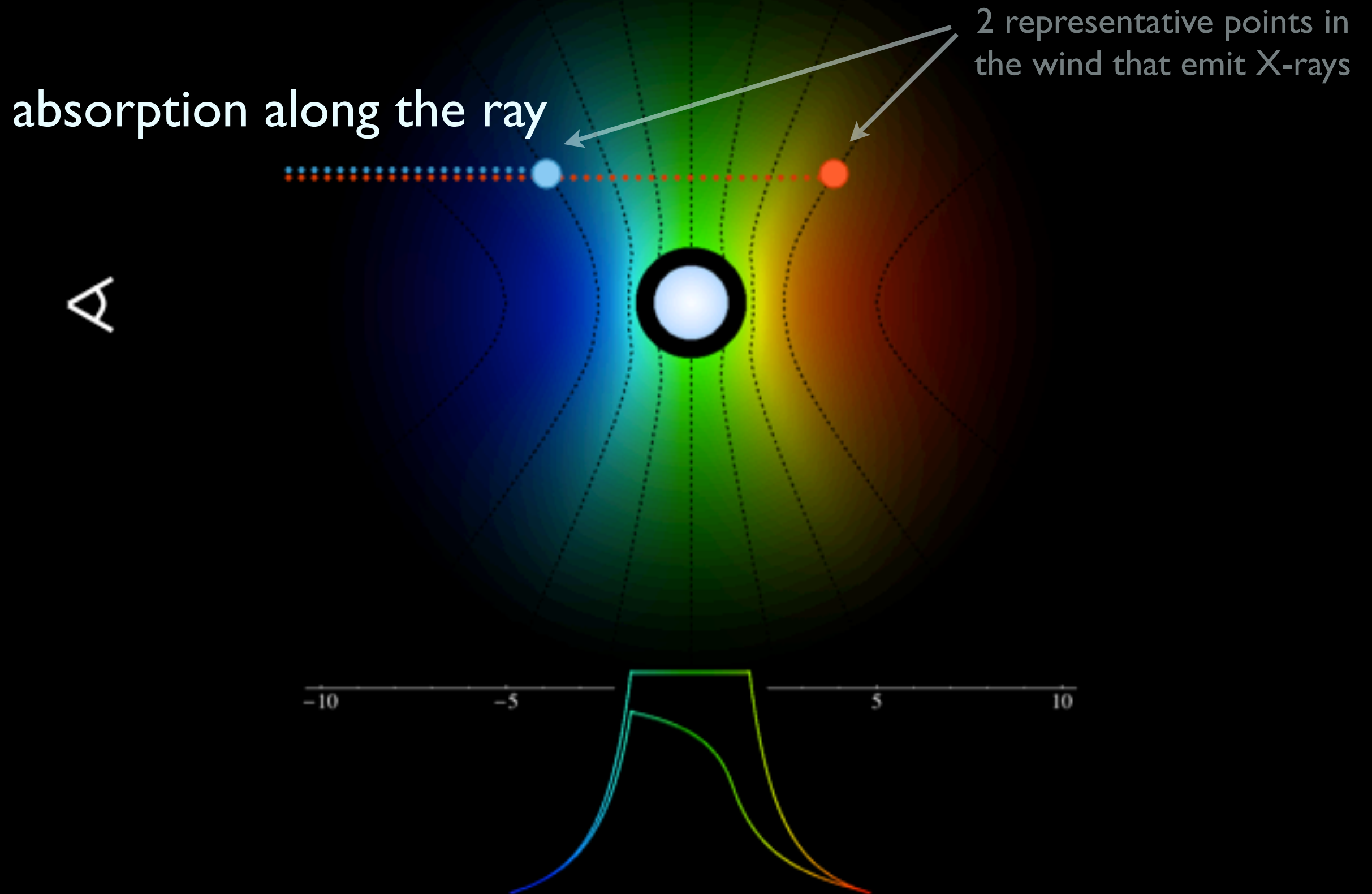
Emma Wollman ('09)
Roban Kramer ('03)



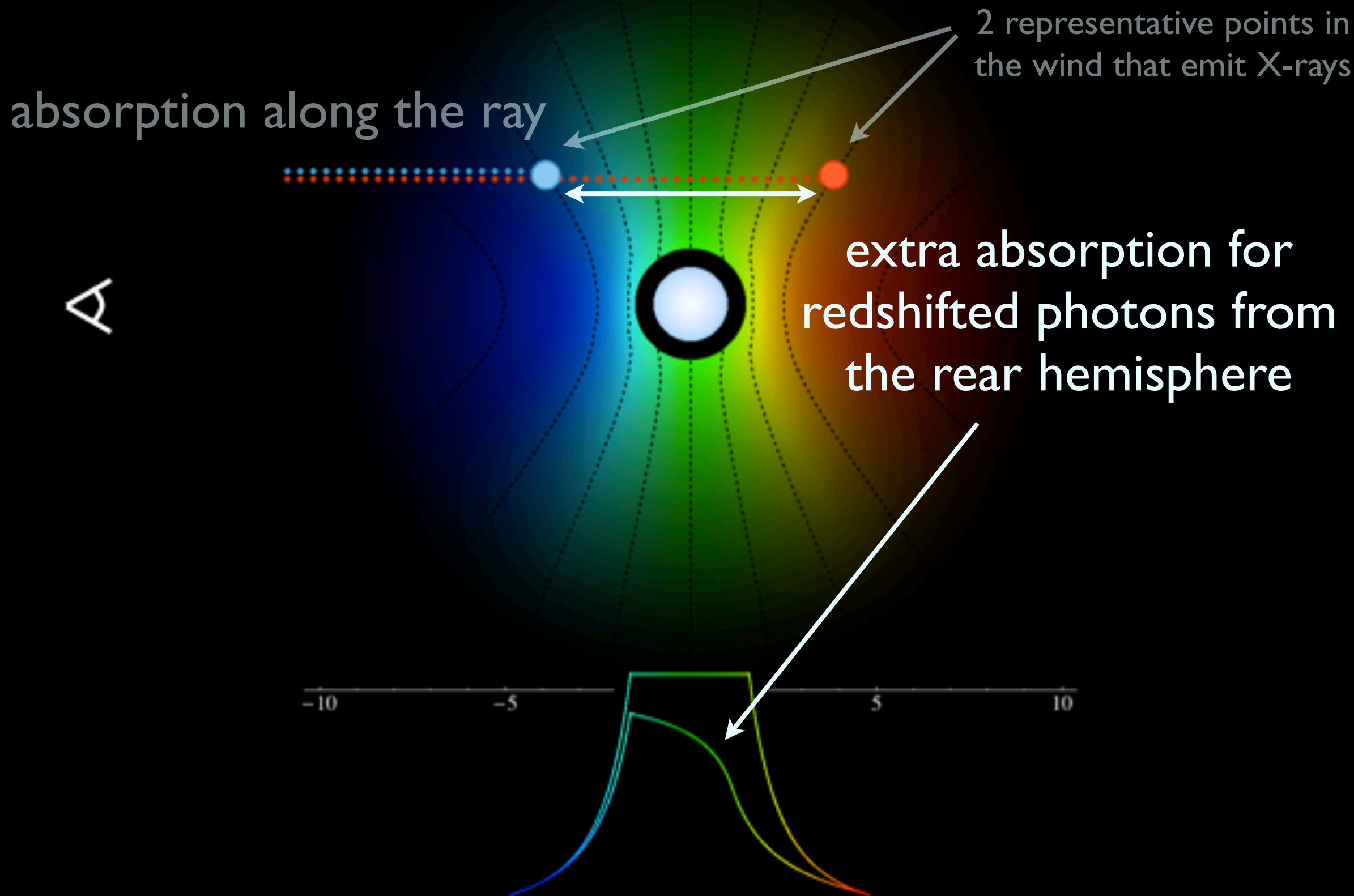
Line Asymmetry



Line Asymmetry

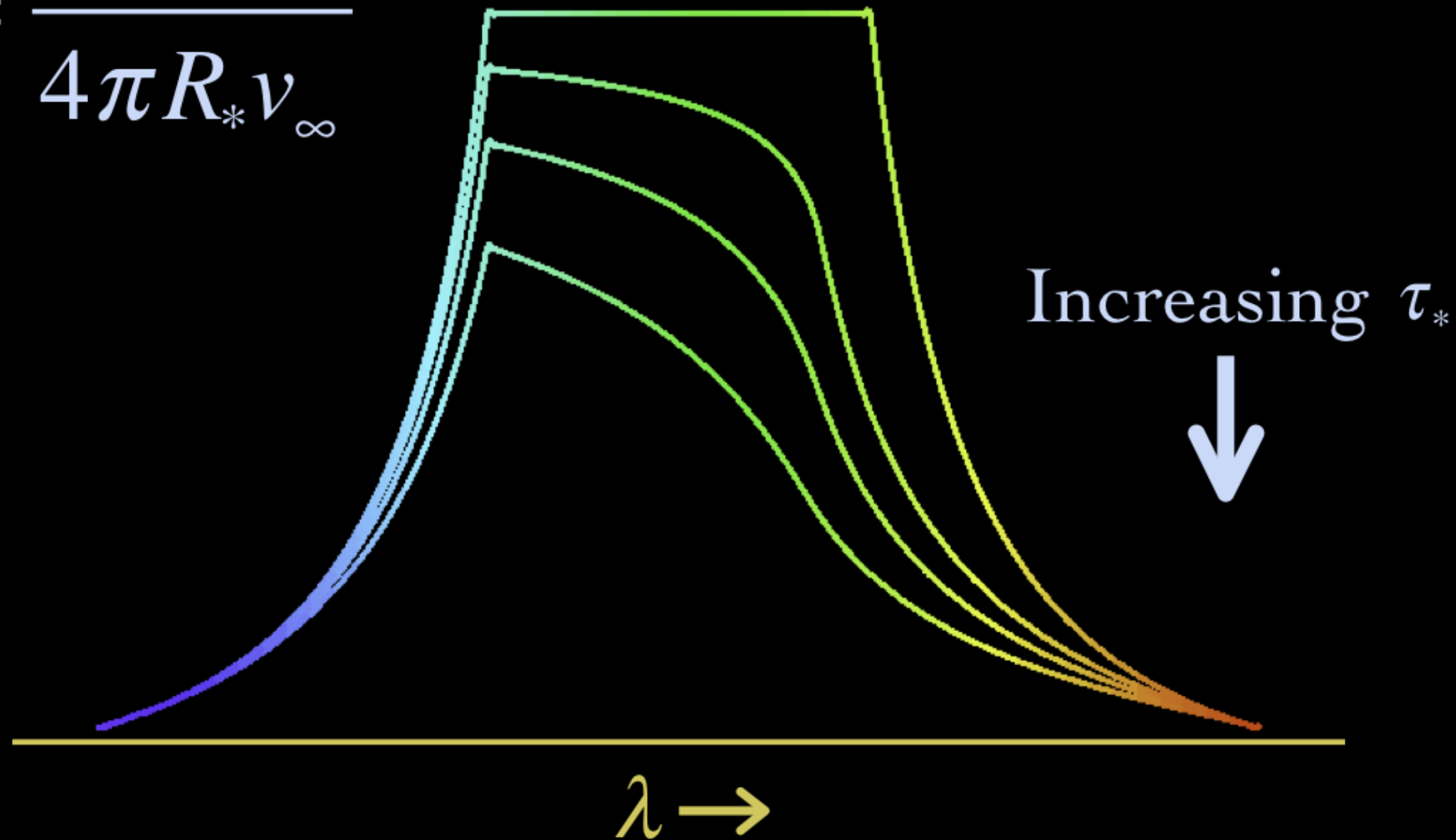


Line Asymmetry



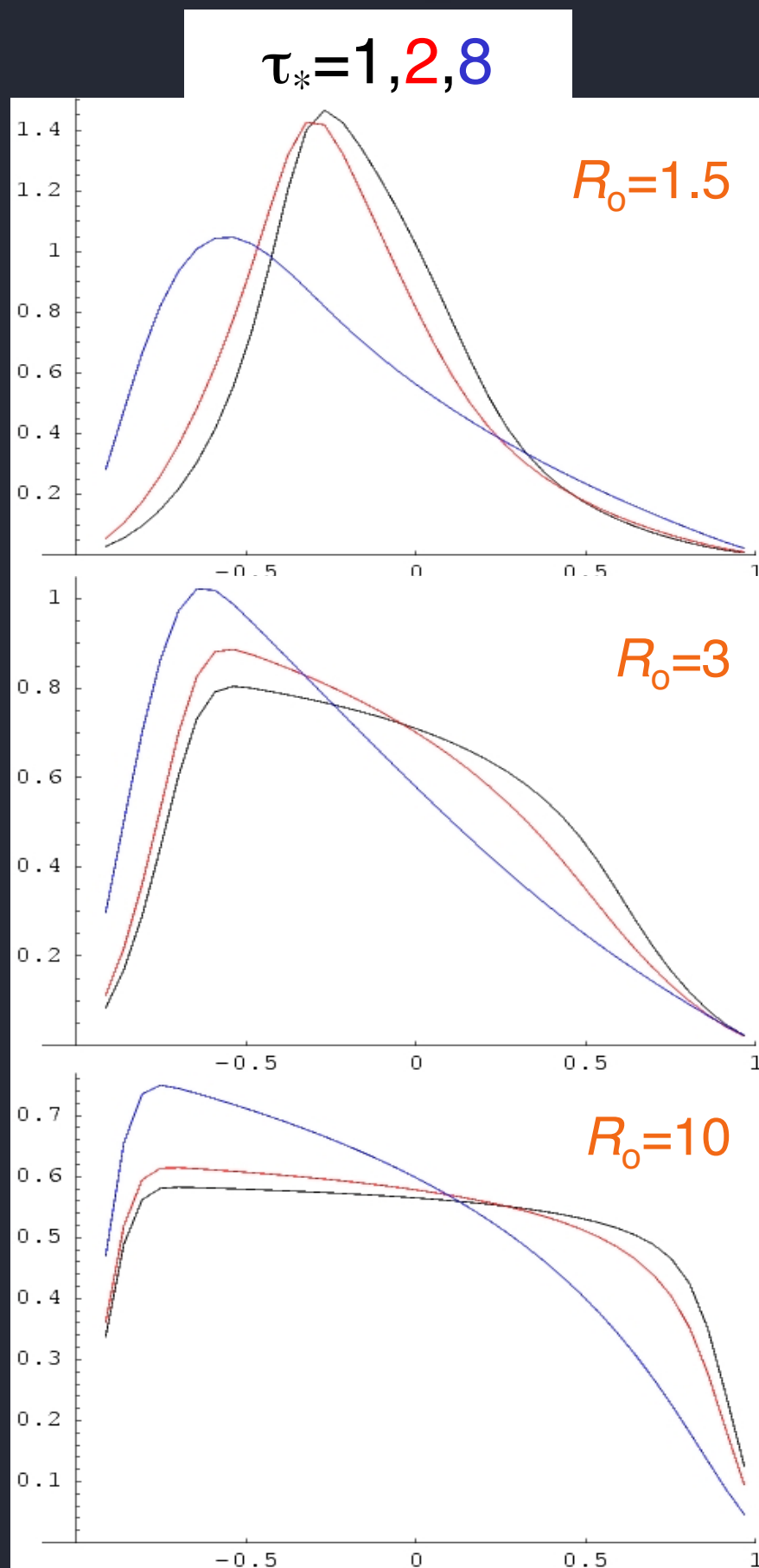
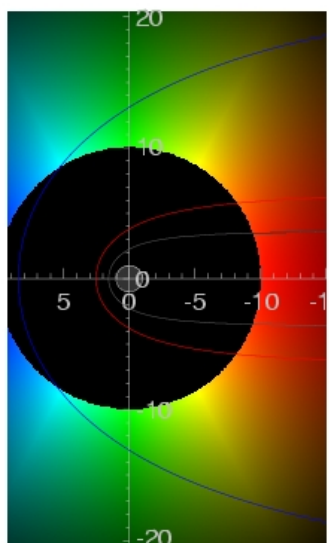
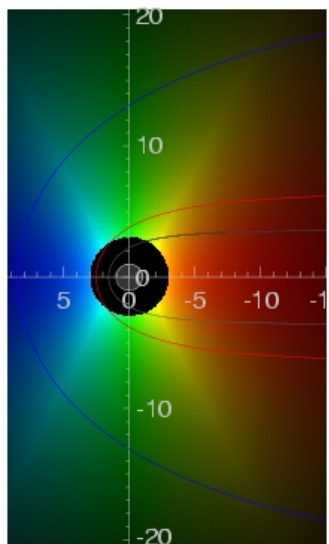
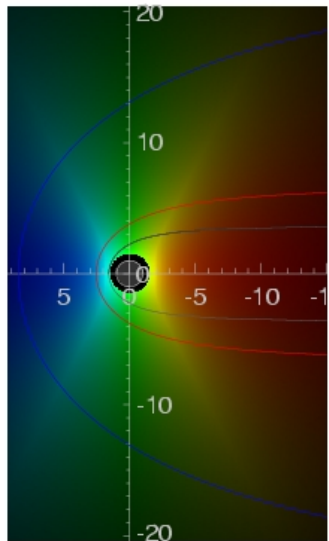
Wind Profile Model

$$\tau_* = \frac{\kappa \dot{M}}{4\pi R_* v_\infty}$$



Line profile shapes

key parameters: R_0 & τ_*



$$v = v_\infty (1 - r/R_*)^\beta$$

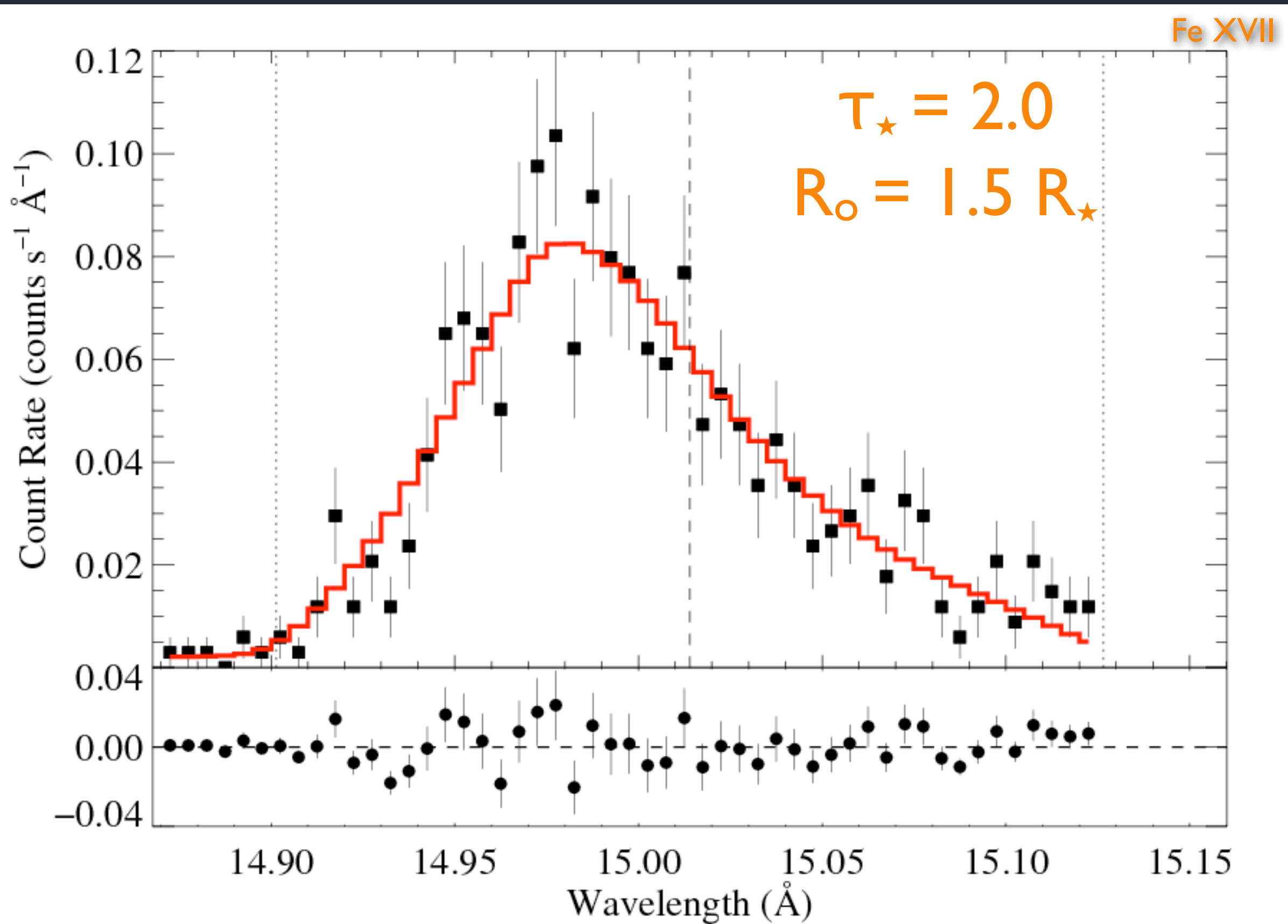
$$j \sim \rho^2 \text{ for } r/R_* > R_0, \\ = 0 \text{ otherwise}$$

$$\tau = \tau_* \int_z^\infty \frac{R_* dz'}{r'^2 (1 - R_*/r')^\beta}$$

$$\tau_* \equiv \frac{\kappa \dot{M}}{4\pi R_* v_\infty}$$

Model is fit to data

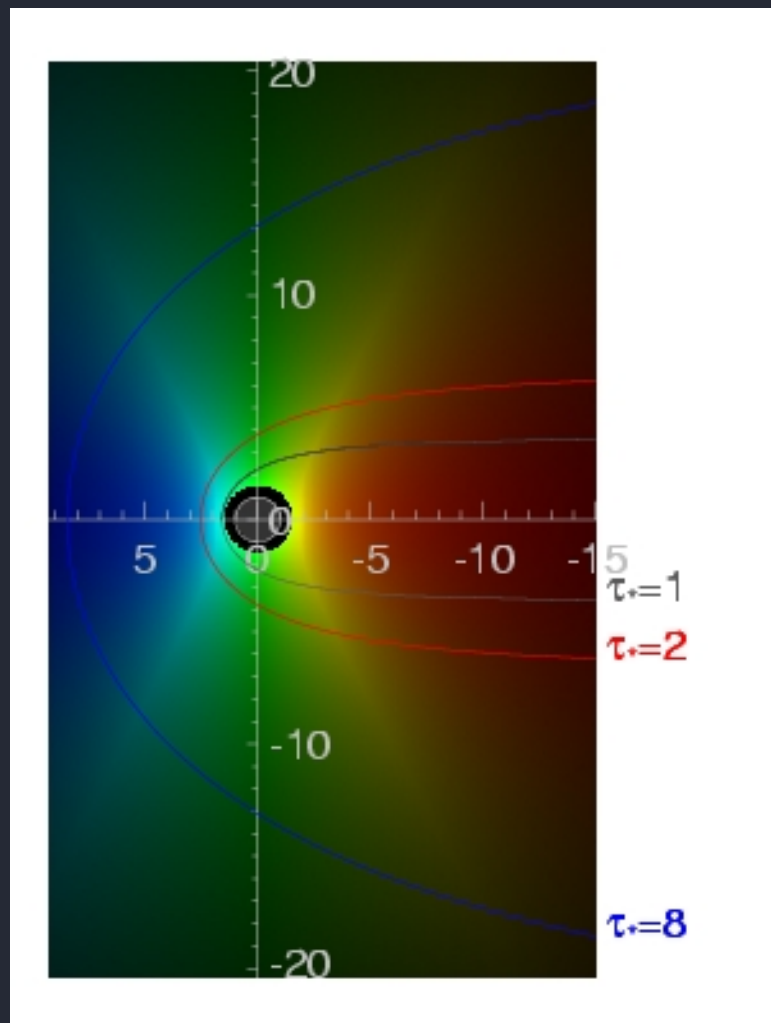
ζ Pup: *Chandra*



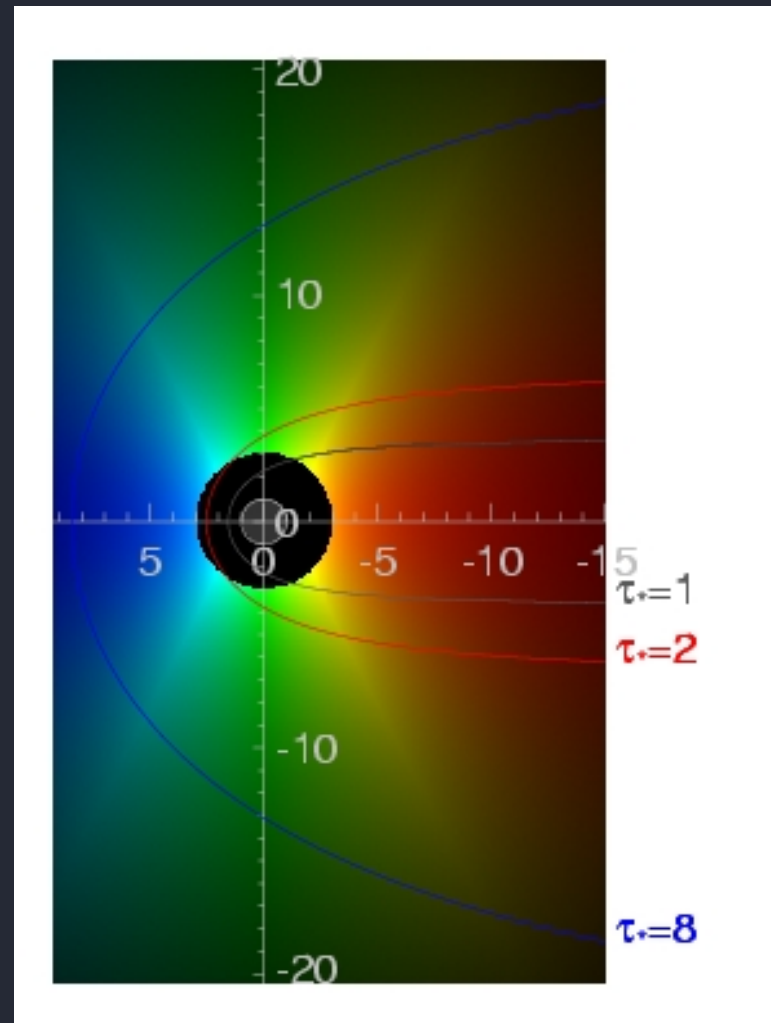
Hot plasma kinematics and location

R_o controls the line width via $v(r)$

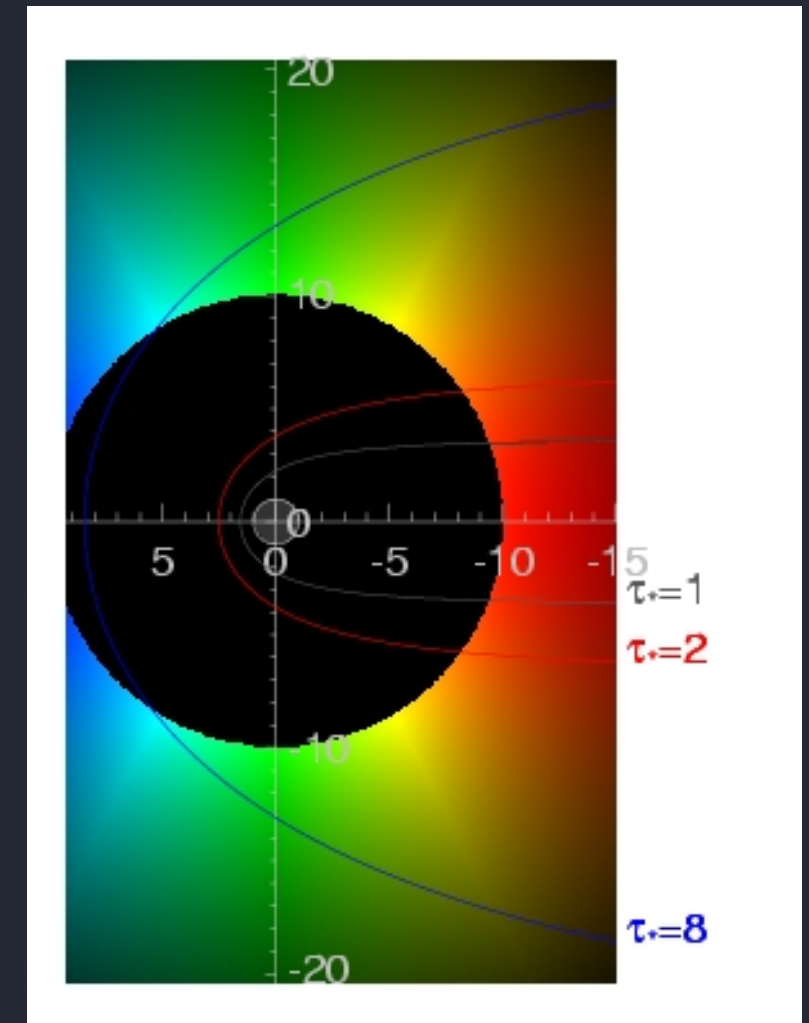
$R_o = 1.5 R_\star$



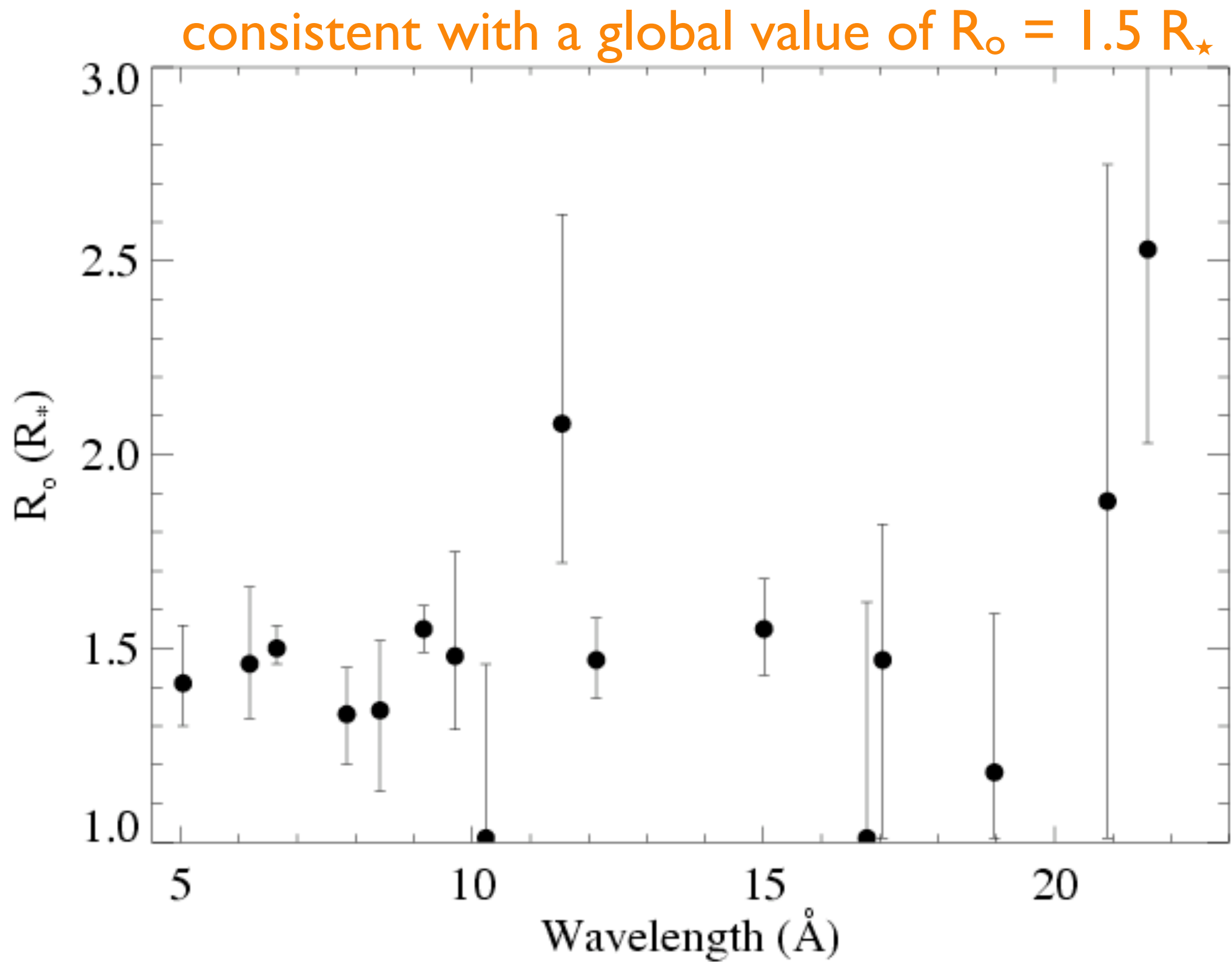
$R_o = 3 R_\star$



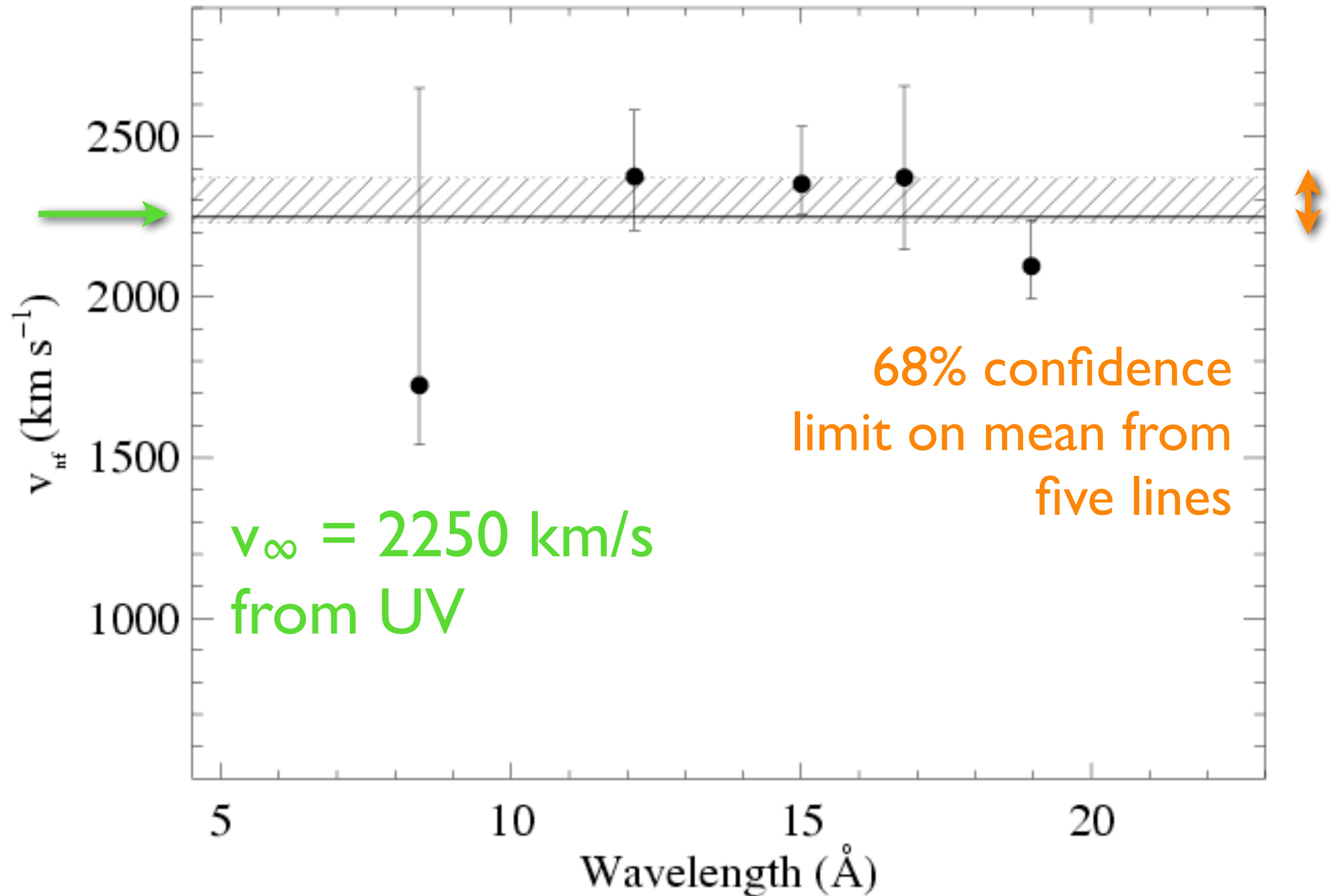
$R_o = 10 R_\star$



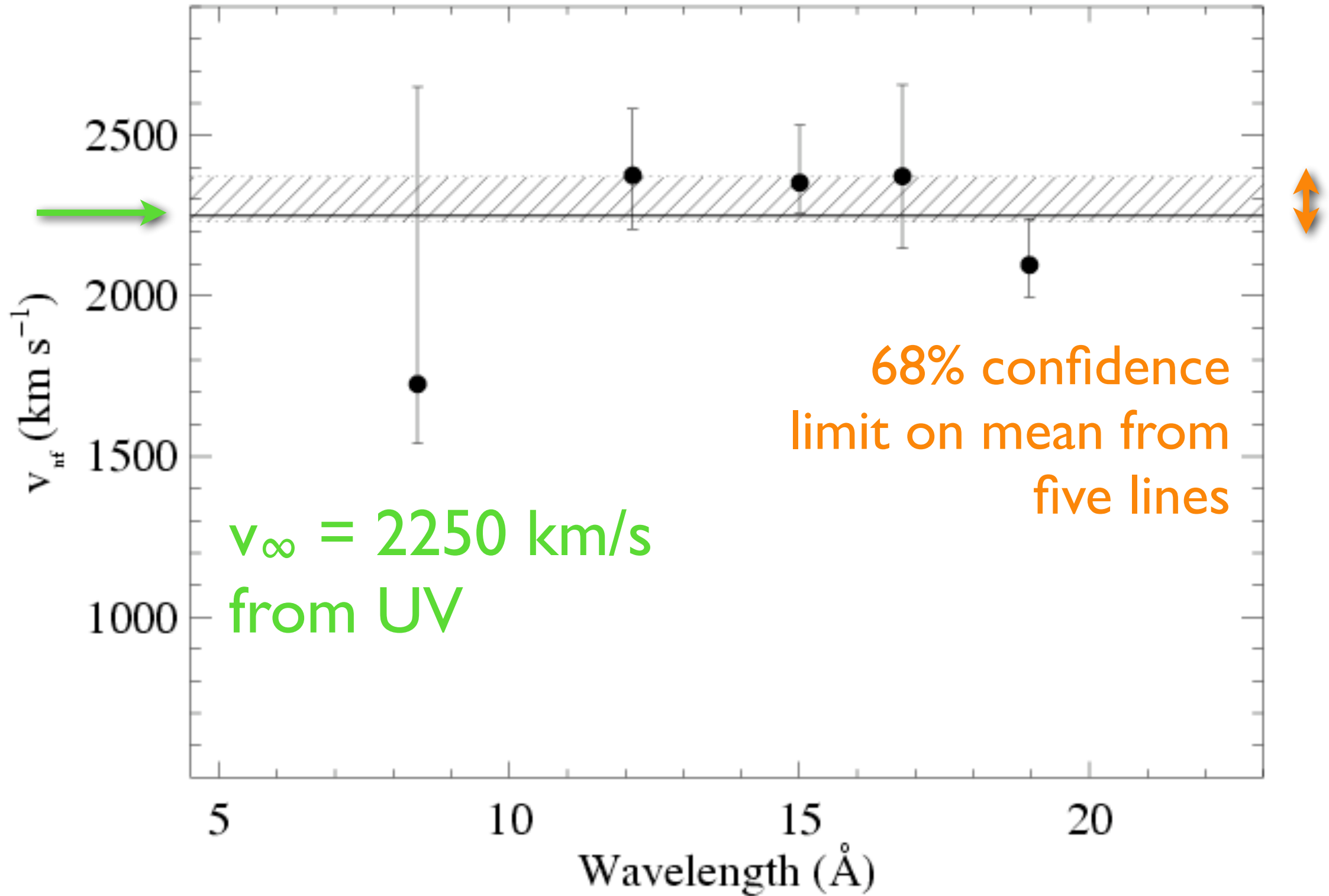
Distribution of R_o values for ζ Pup



v_∞ can be constrained by the line fitting too



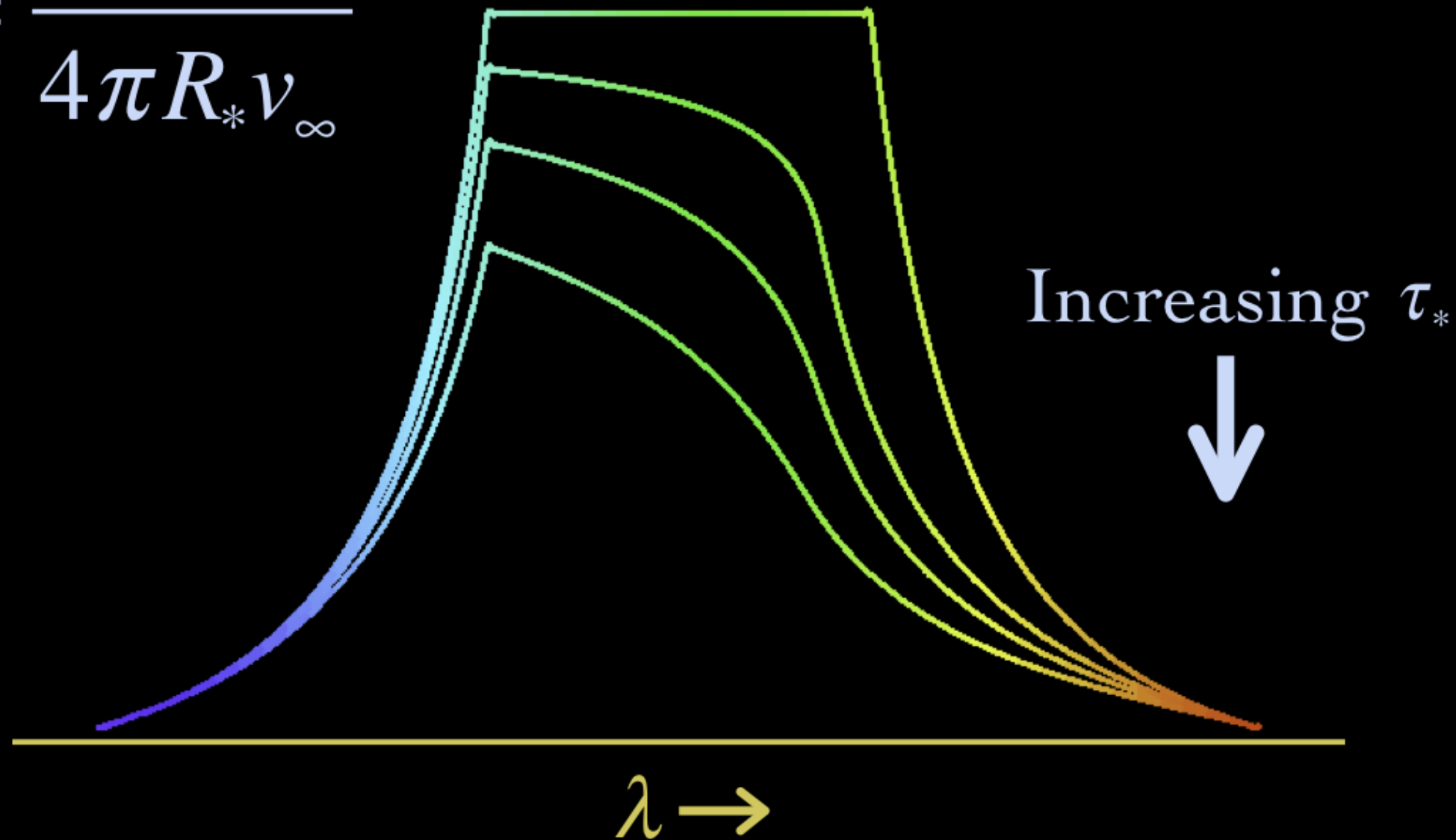
X-ray plasma and mean wind have same kinematics



The profiles also tell us about the level of
wind absorption

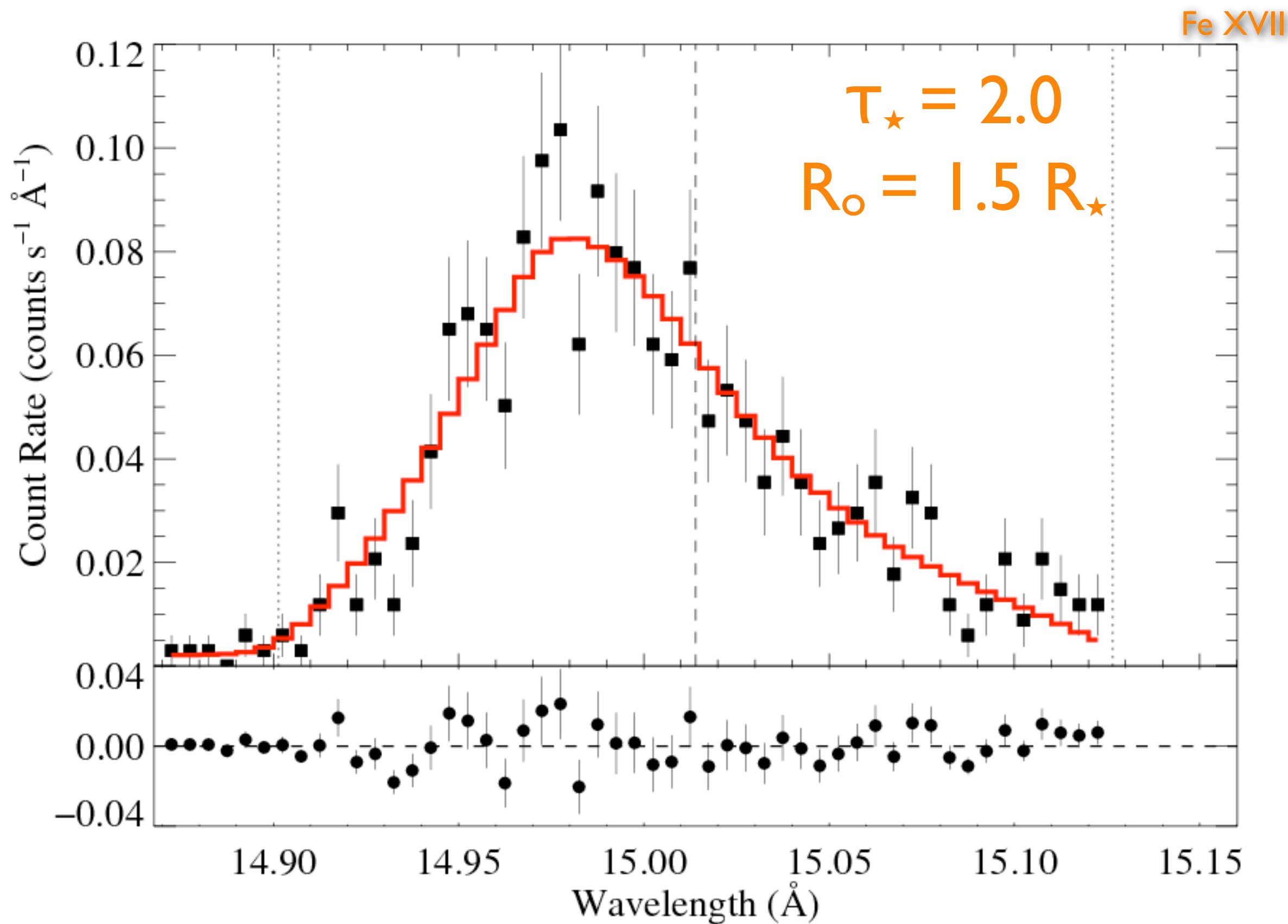
Wind Profile Model

$$\tau_* = \frac{\kappa \dot{M}}{4\pi R_* v_\infty}$$



Model is fit to data

ζ Pup: *Chandra*



Quantifying the wind optical depth

opacity of the cold wind component (due to bound-free transitions in C, N, O, Ne, Fe)

wind mass-loss rate

$$\dot{M} = 4\pi r^2 v \rho$$

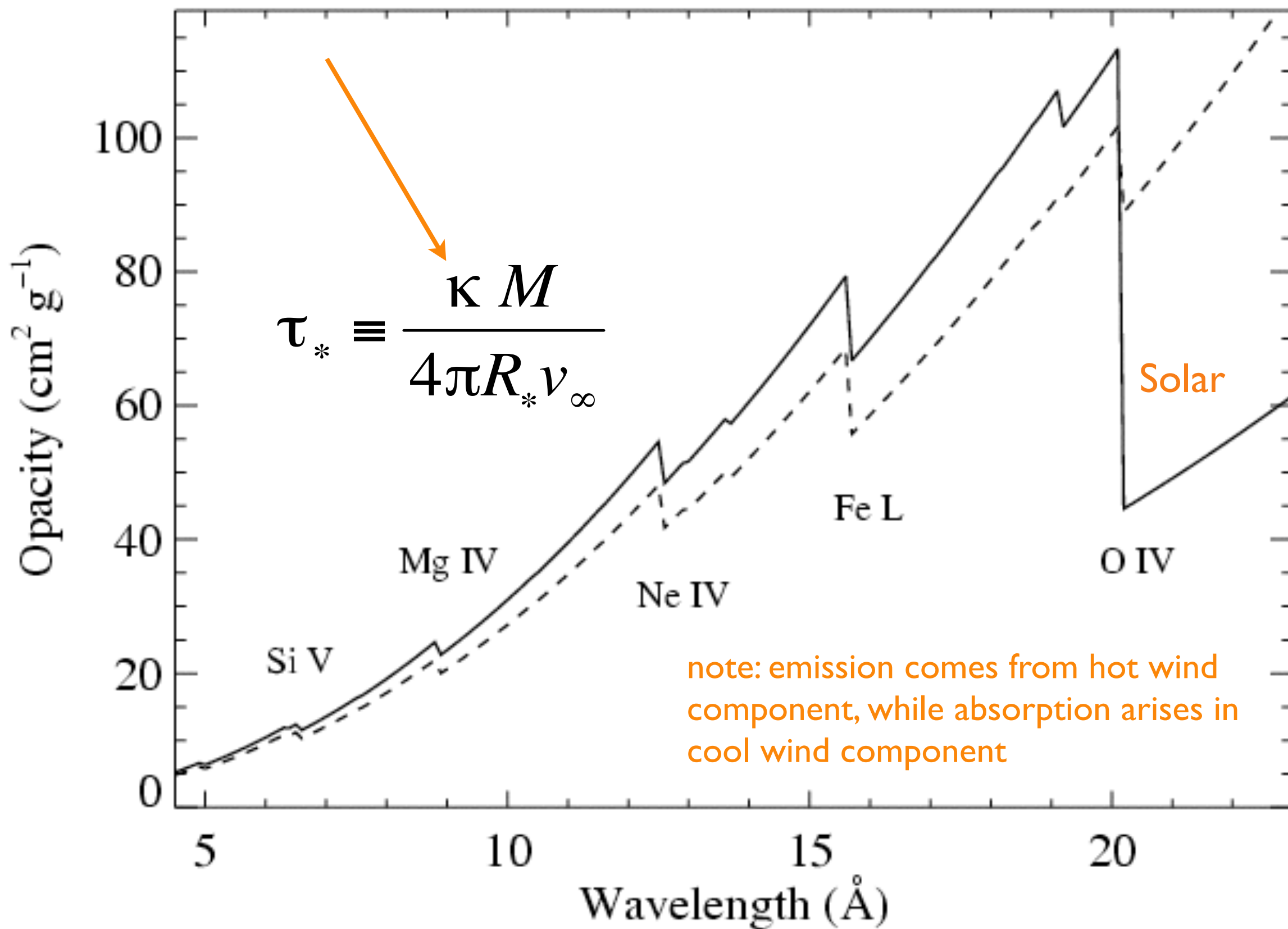
$$\tau_* \equiv \frac{\kappa \dot{M}}{4\pi R_* v_\infty}$$

stellar radius

wind terminal velocity

soft X-ray wind opacity

CNO processed

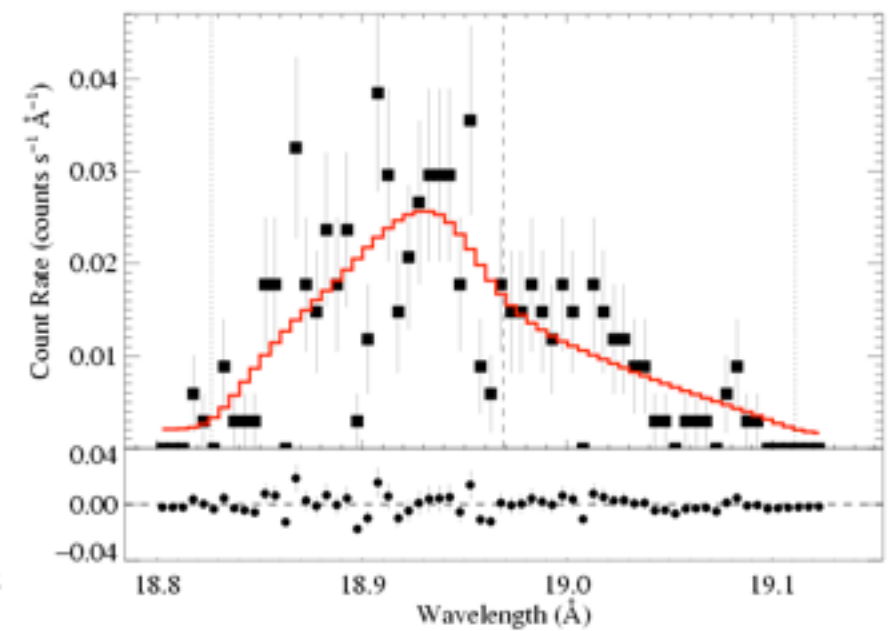
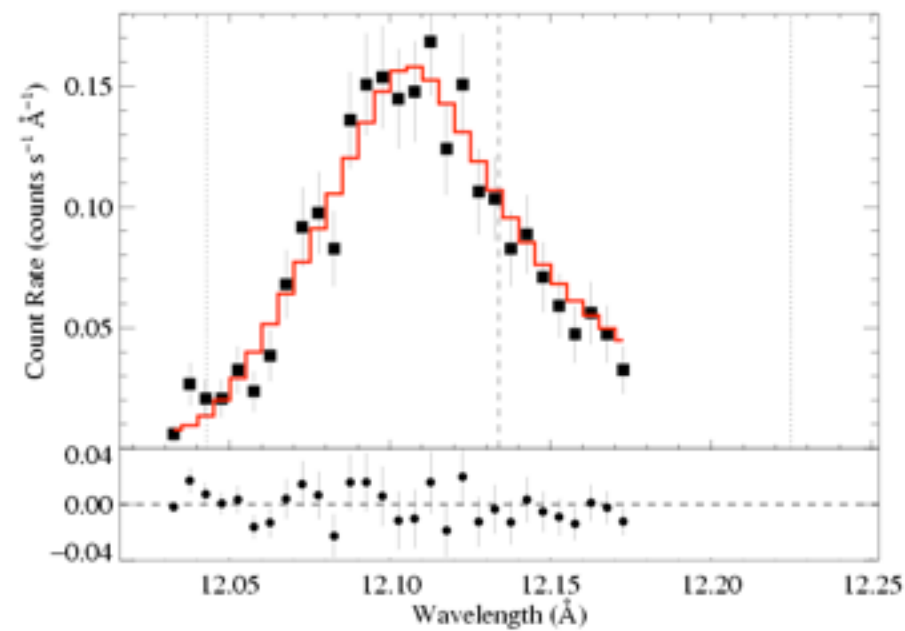
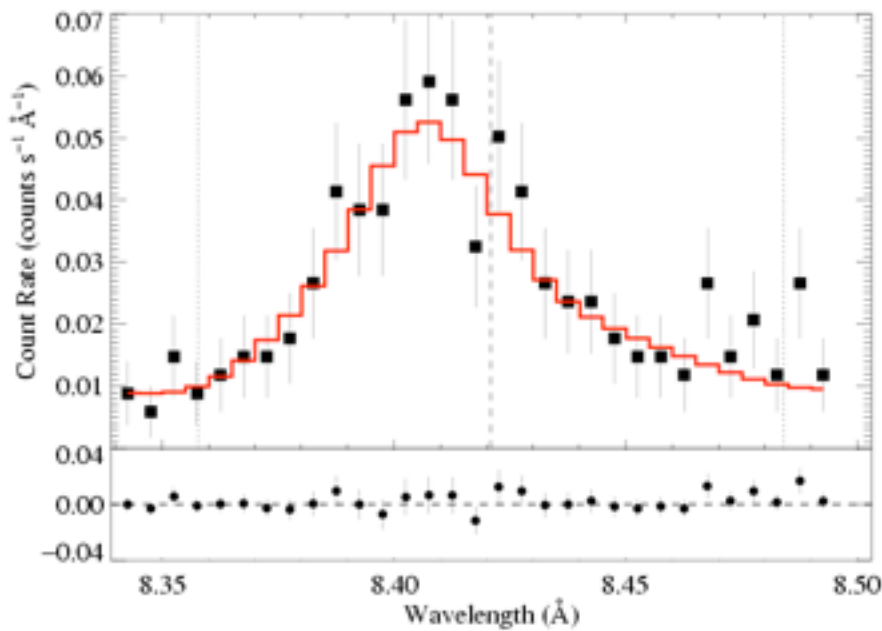


ζ Pup *Chandra*: three emission lines

Mg Ly α : 8.42 Å

Ne Ly α : 12.13 Å

O Ly α : 18.97 Å



$\tau_* \sim 1$

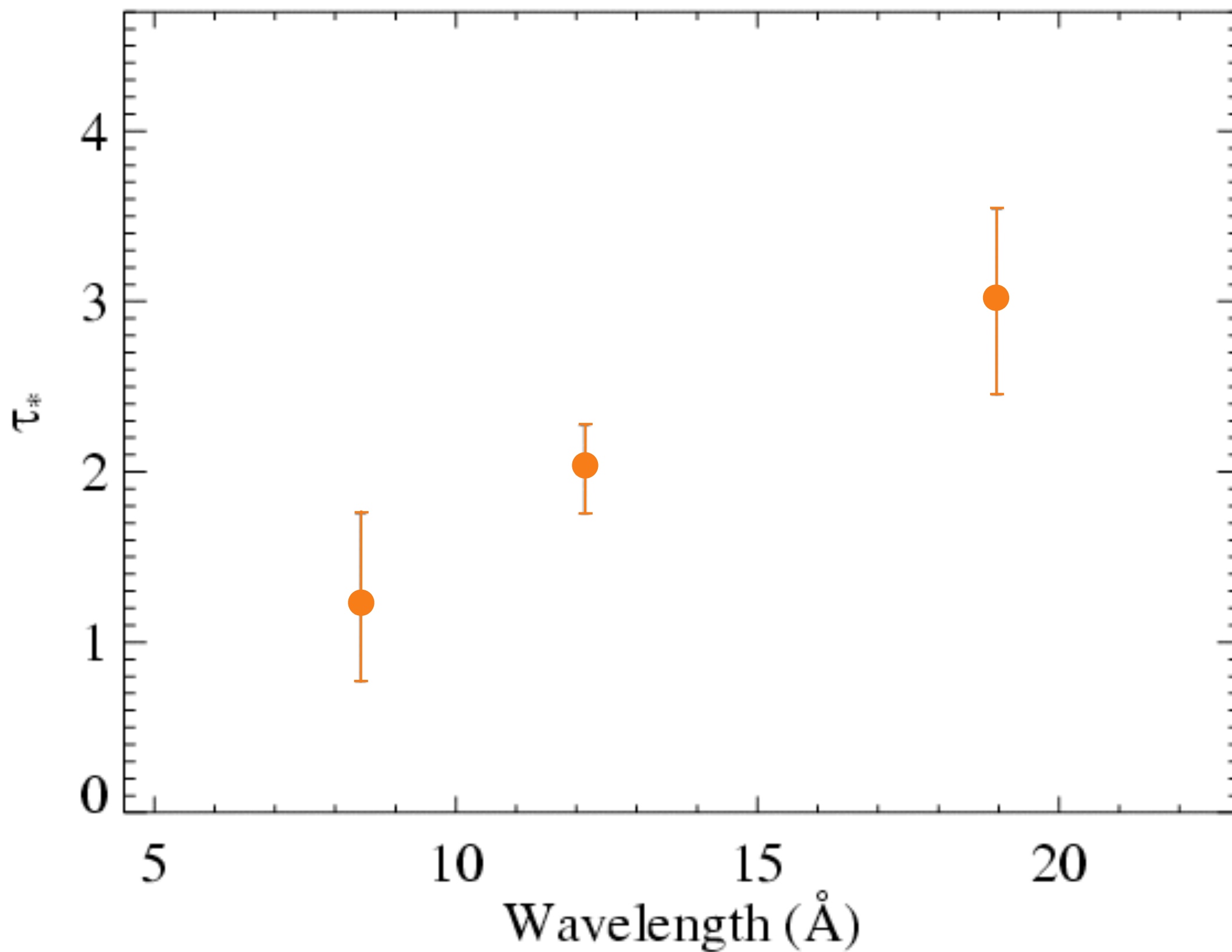
$\tau_* \sim 2$

$\tau_* \sim 3$

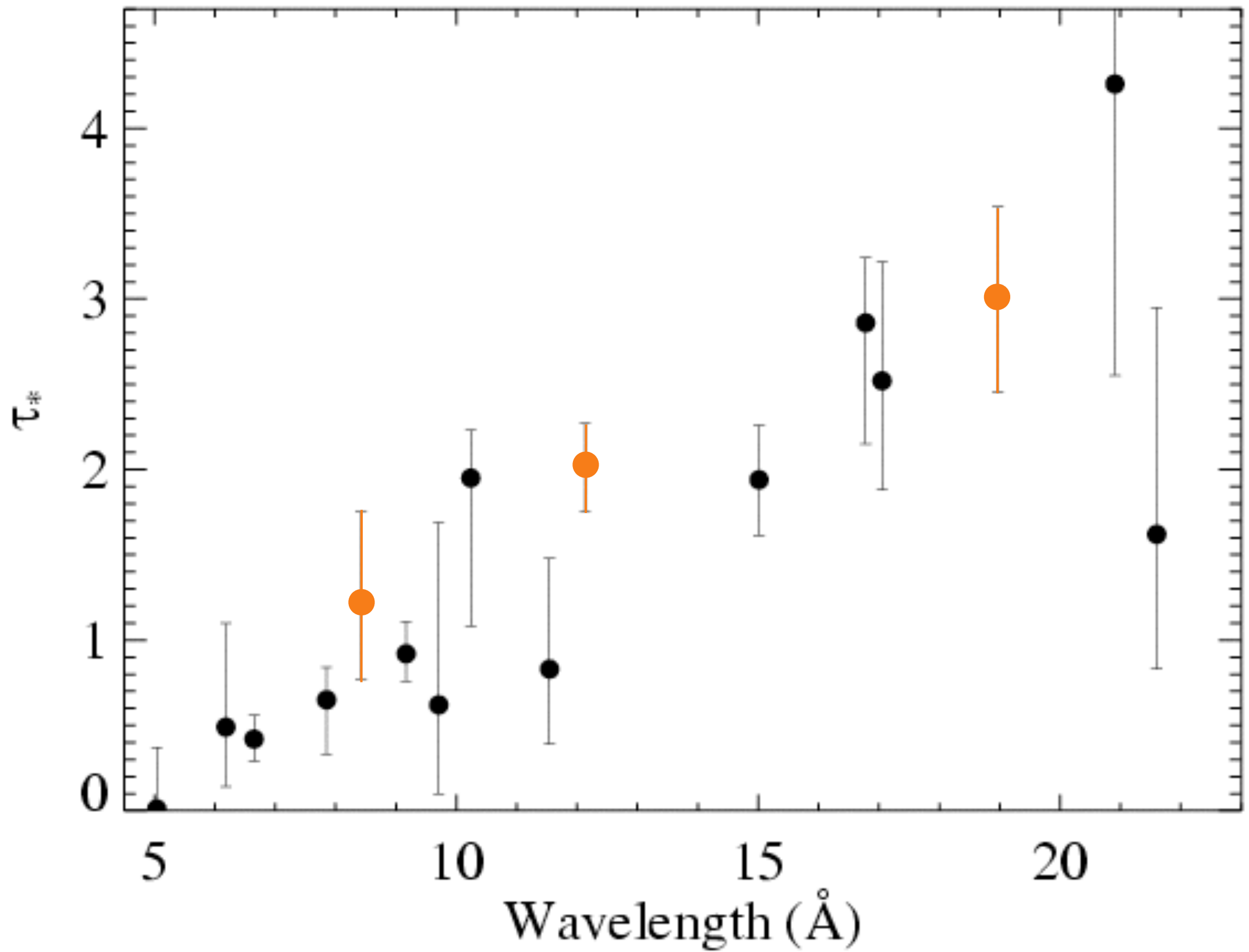
Recall:

$$\tau_* \equiv \frac{\kappa \dot{M}}{4\pi R_* v_\infty}$$

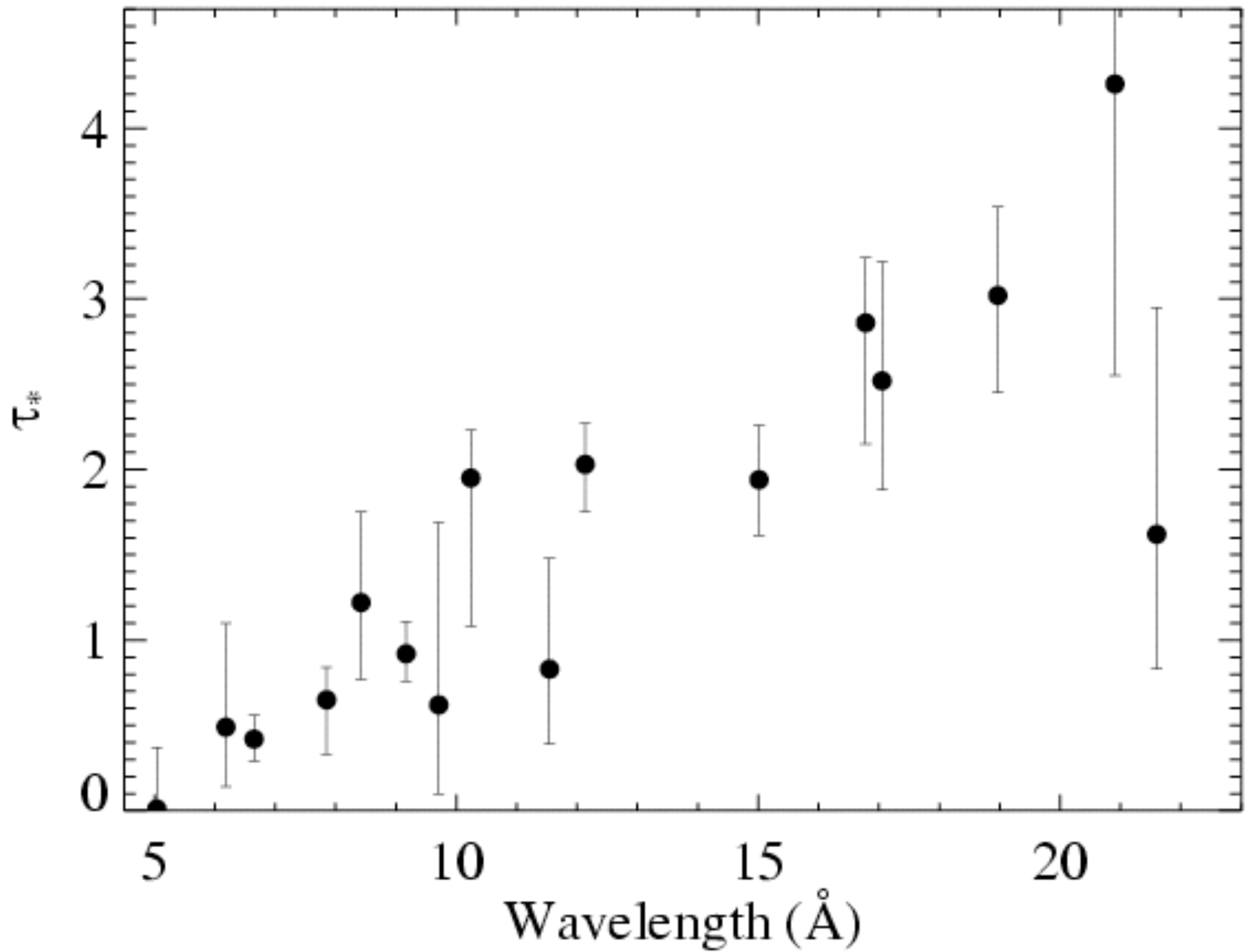
Results from the 3 line fits shown previously



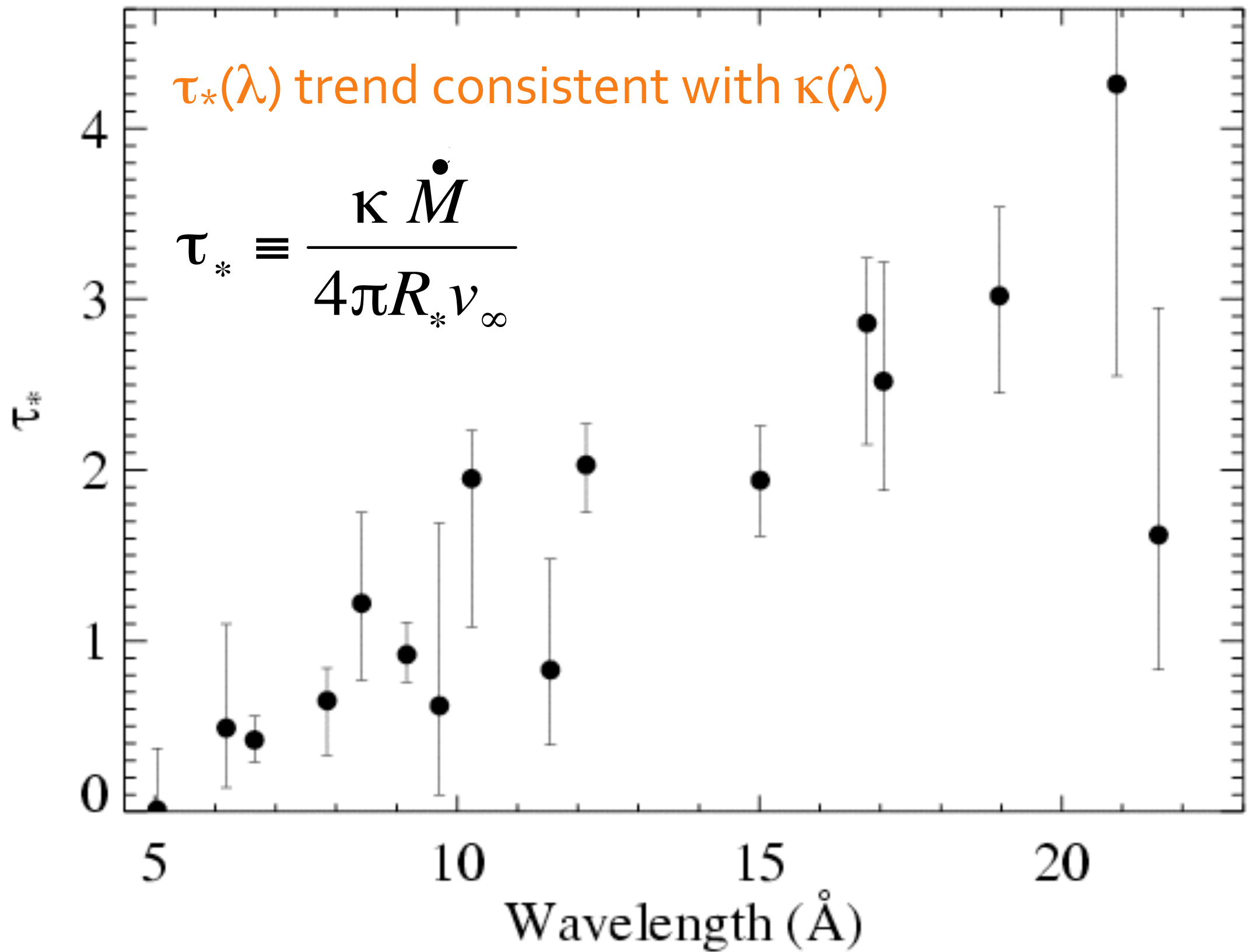
Fits to 16 lines in the *Chandra* spectrum of ζ Pup



Fits to 16 lines in the *Chandra* spectrum of ζ Pup

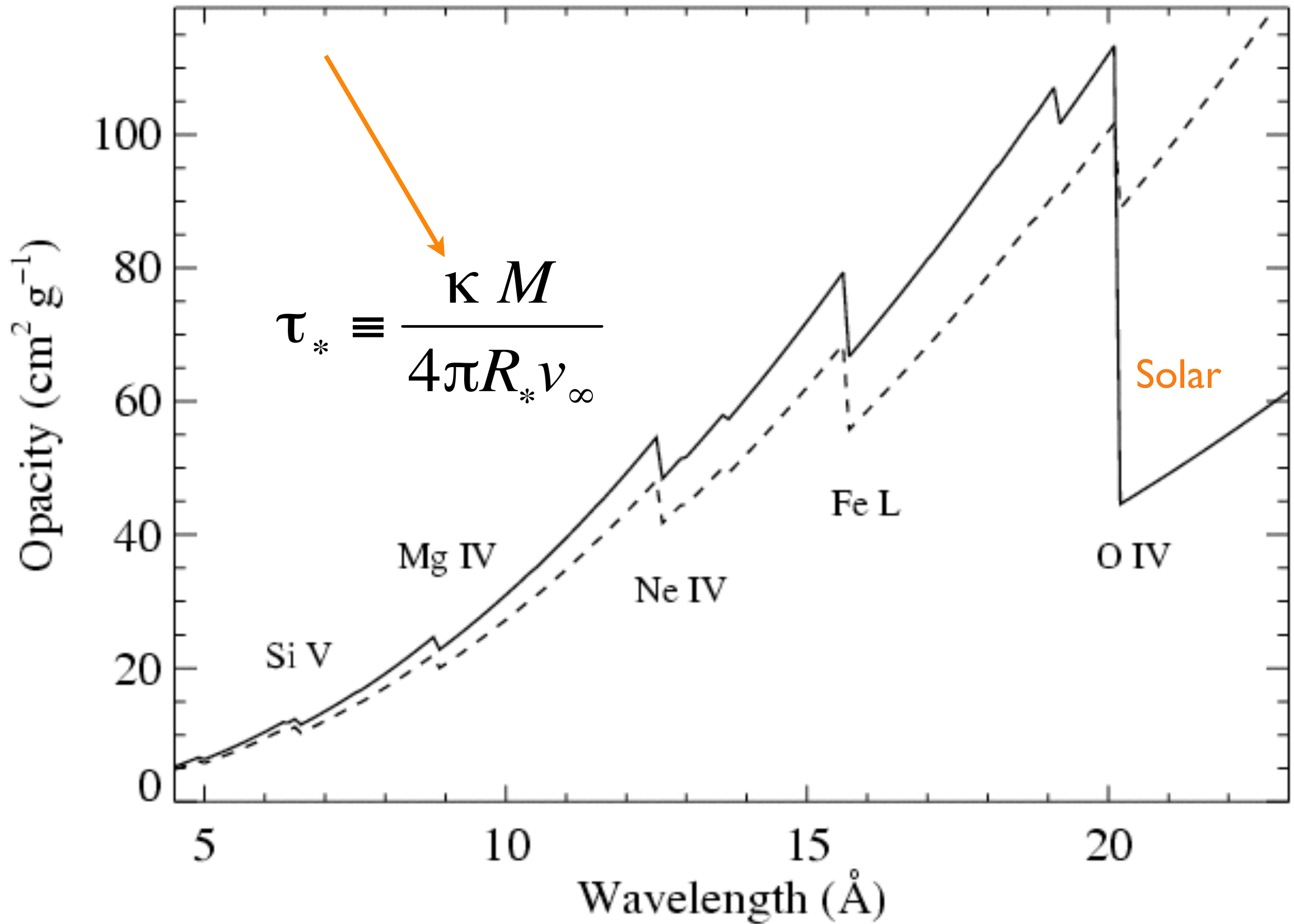


Fits to 16 lines in the *Chandra* spectrum of ζ Pup



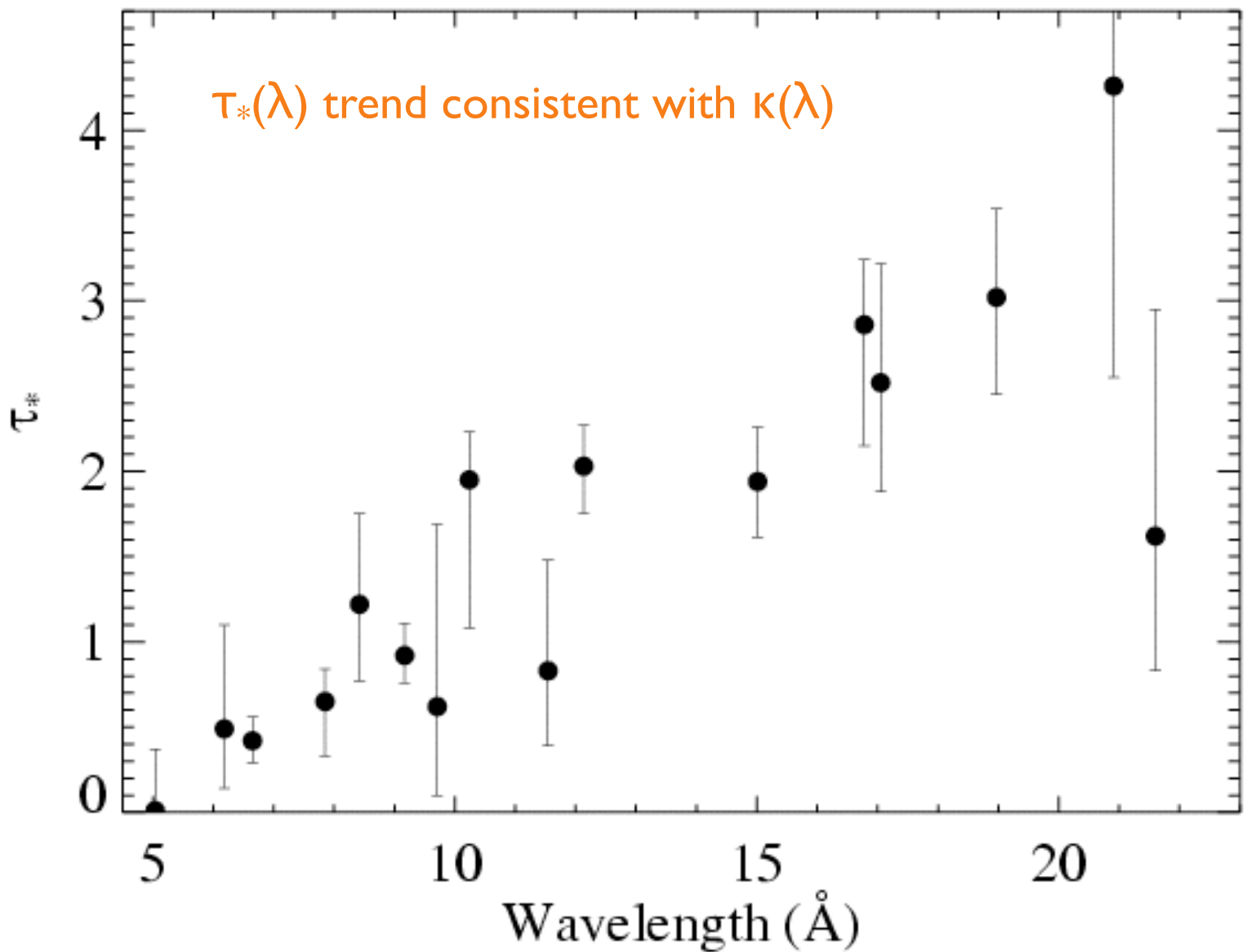
soft X-ray wind opacity

CNO processed



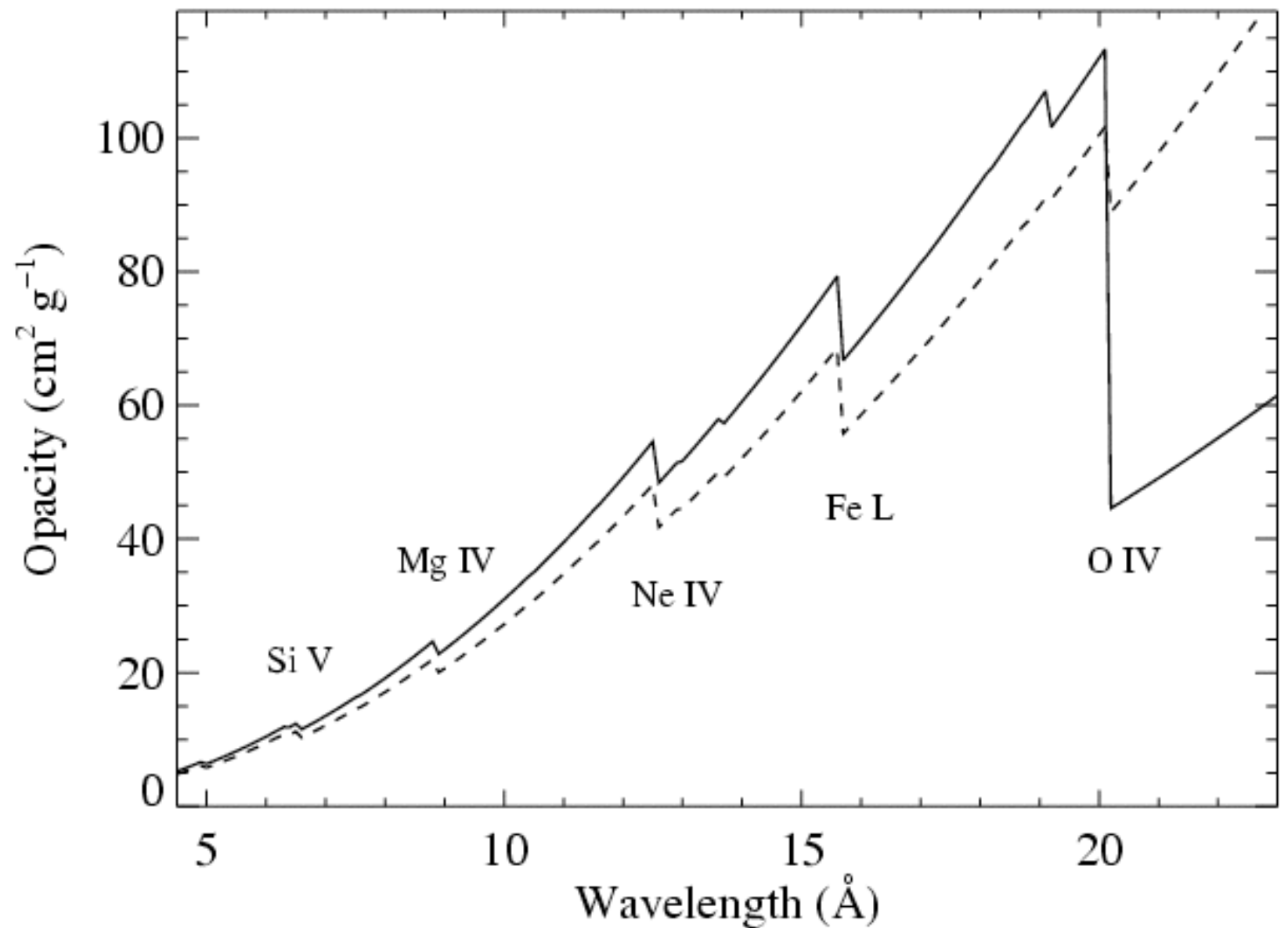
$$\tau_* \equiv \frac{\kappa \dot{M}}{4\pi R_* v_\infty}$$

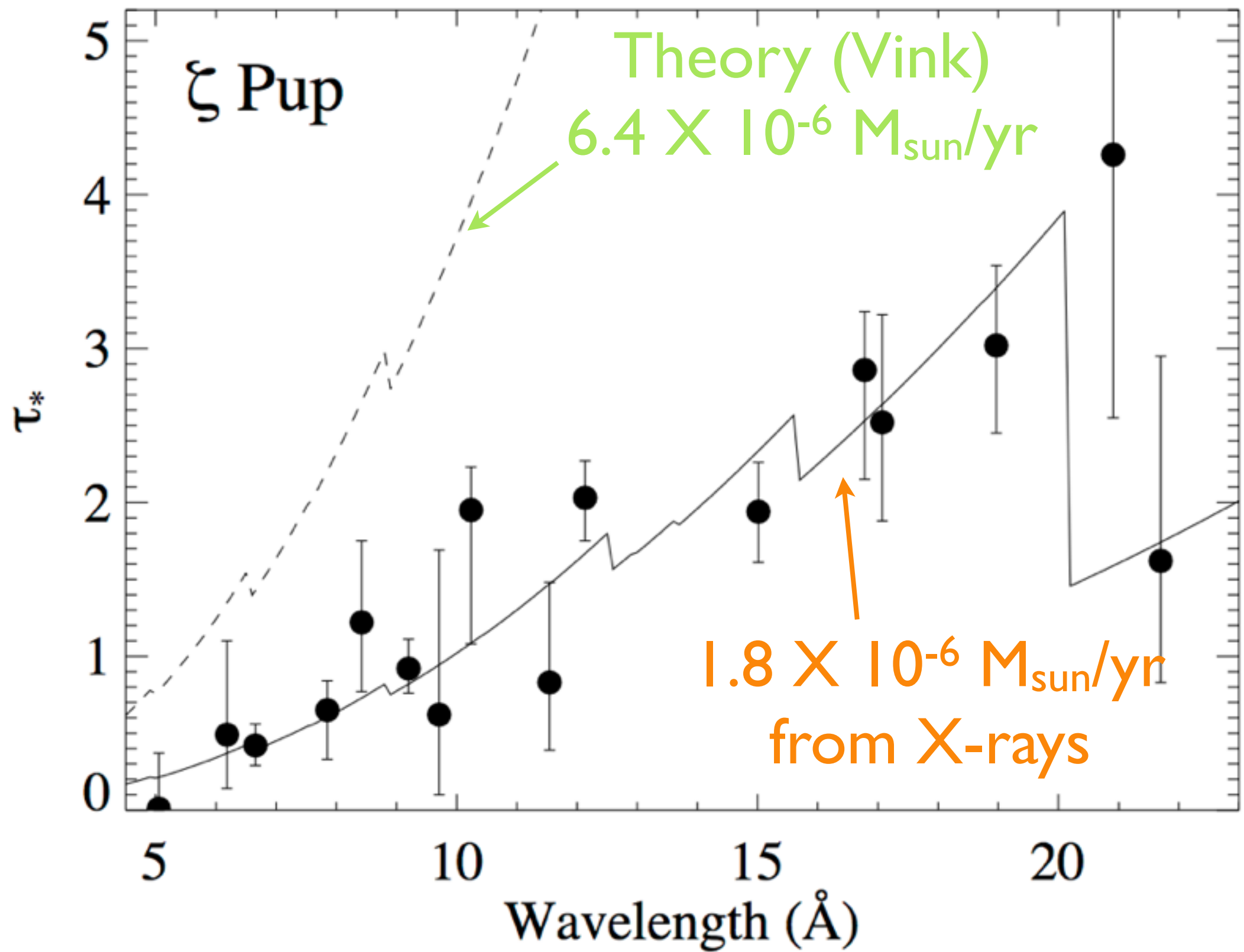
\dot{M} becomes the free parameter of the fit to the $\tau_*(\lambda)$ trend

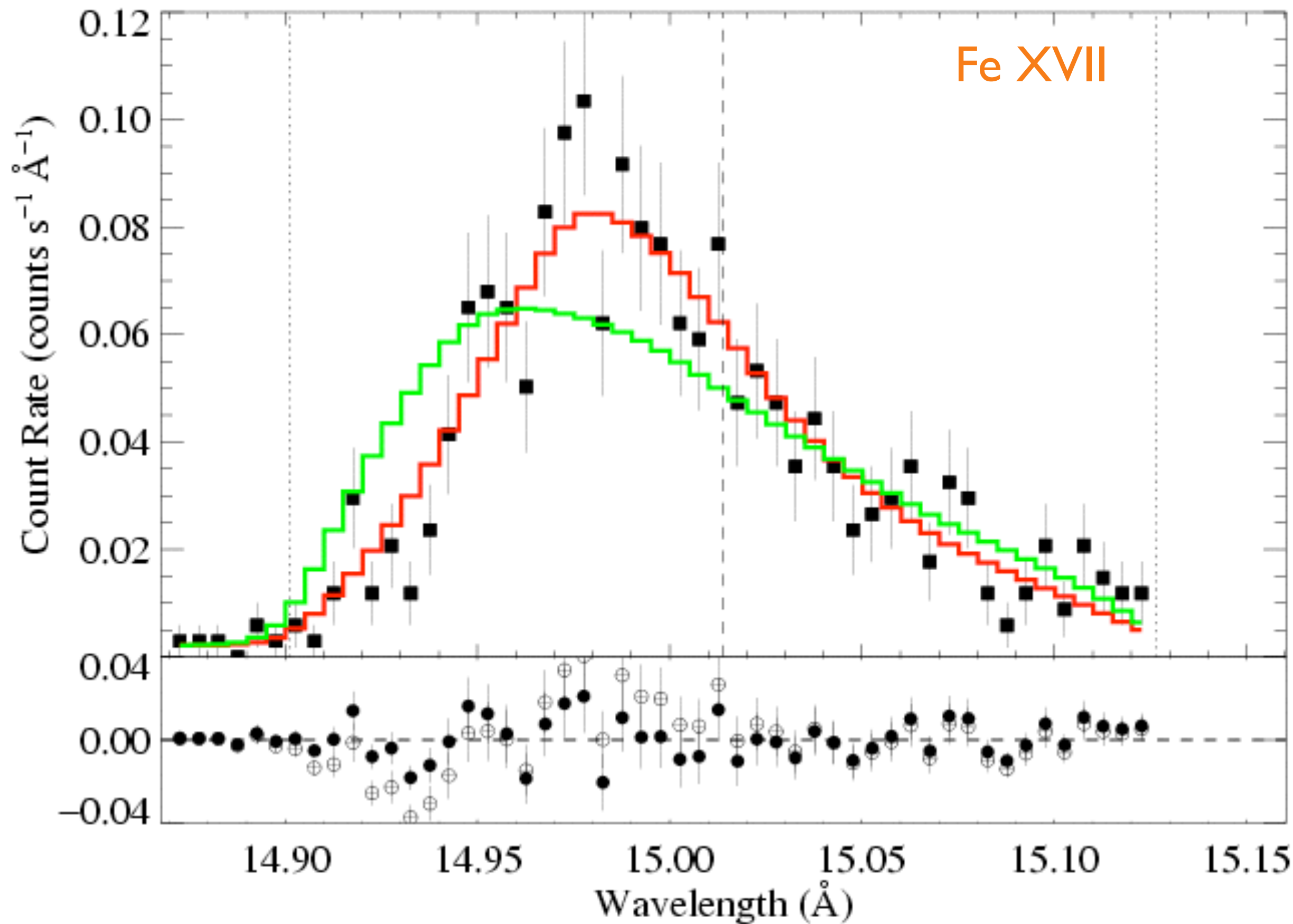


$$\tau_* \equiv \frac{\kappa \dot{M}}{4\pi R_* v_\infty}$$

\dot{M} becomes the free parameter of the fit to the $\tau_*(\lambda)$ trend







Preliminary Conclusions

1. Doppler-broadened line profiles tell us the kinematics of the shock-heated wind plasma
2. Line profile asymmetry tells us about the wind absorption; joint analysis of an ensemble of lines tells us the mass-loss rate of the wind

Preliminary Conclusions

1. Doppler-broadened line profiles tell us the kinematics of the shock-heated wind plasma

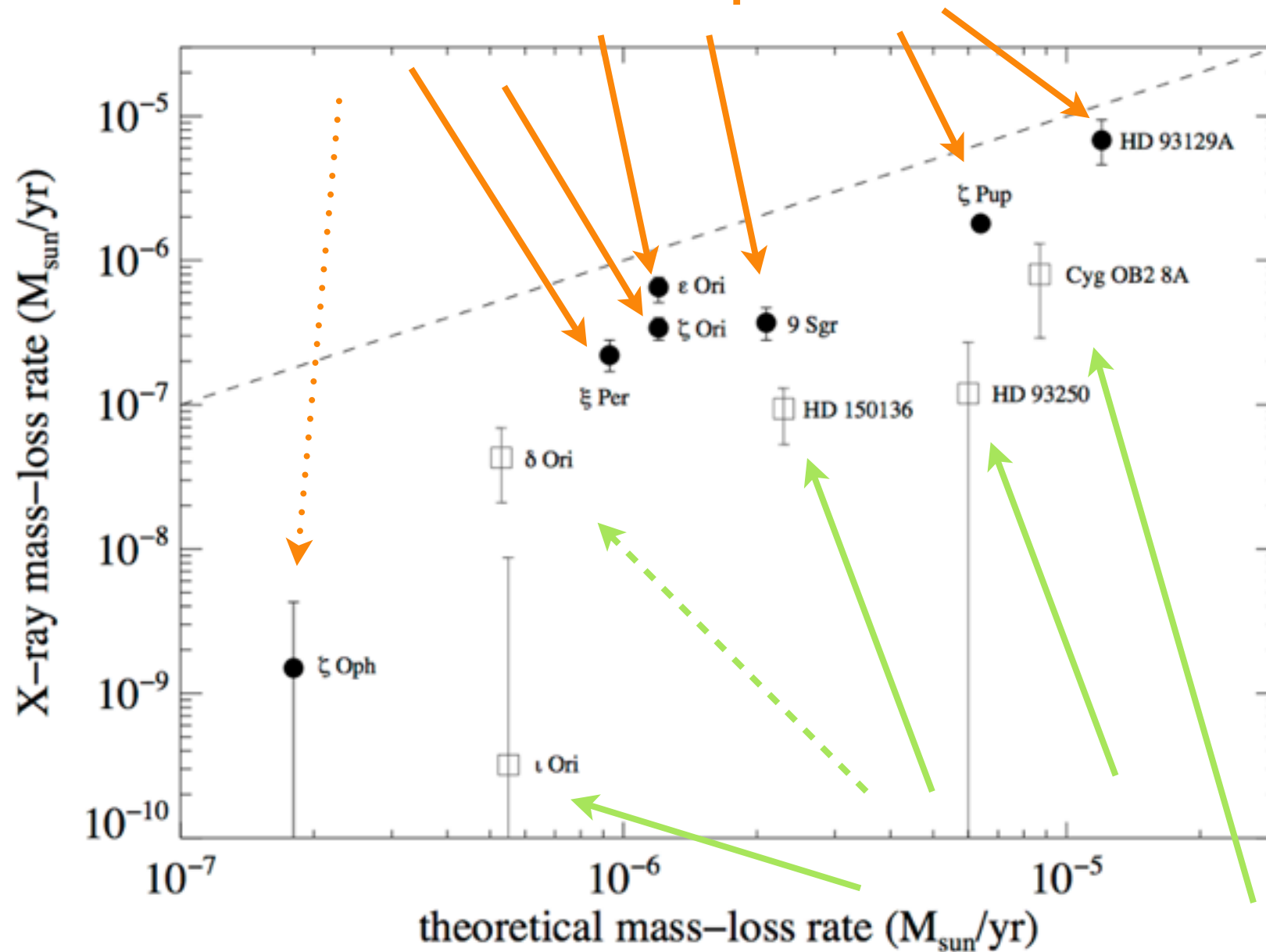
consistent with hydro simulation predictions

2. Line profile asymmetry tells us about the wind absorption; joint analysis of an ensemble of lines tells us the mass-loss rate of the wind

mass-loss rate factor ~ 3 lower than theoretically expected value

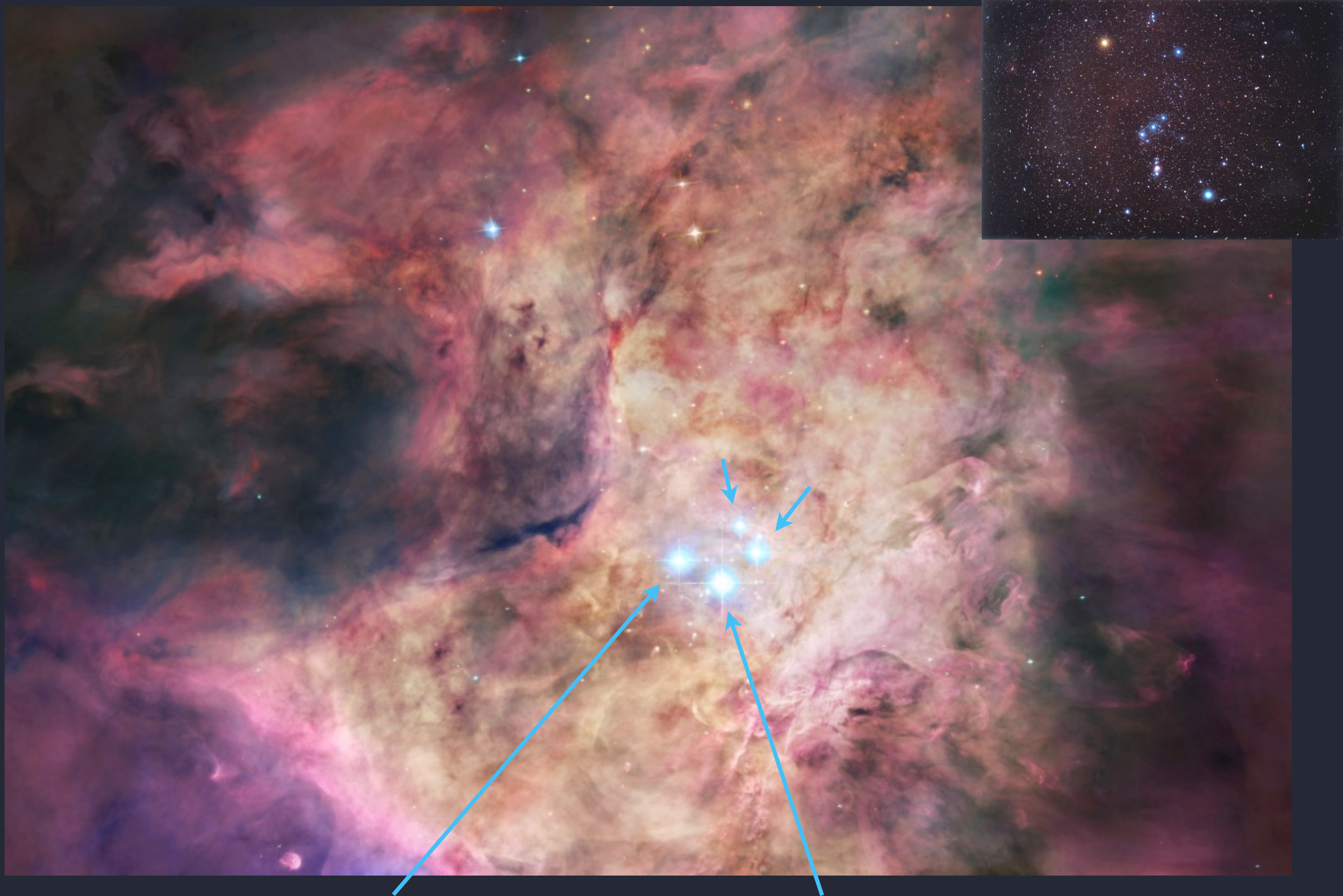
Survey of a dozen O stars

X-ray mass-loss rates: a few times less than theoretical predictions



binary wind-wind
interaction X-rays

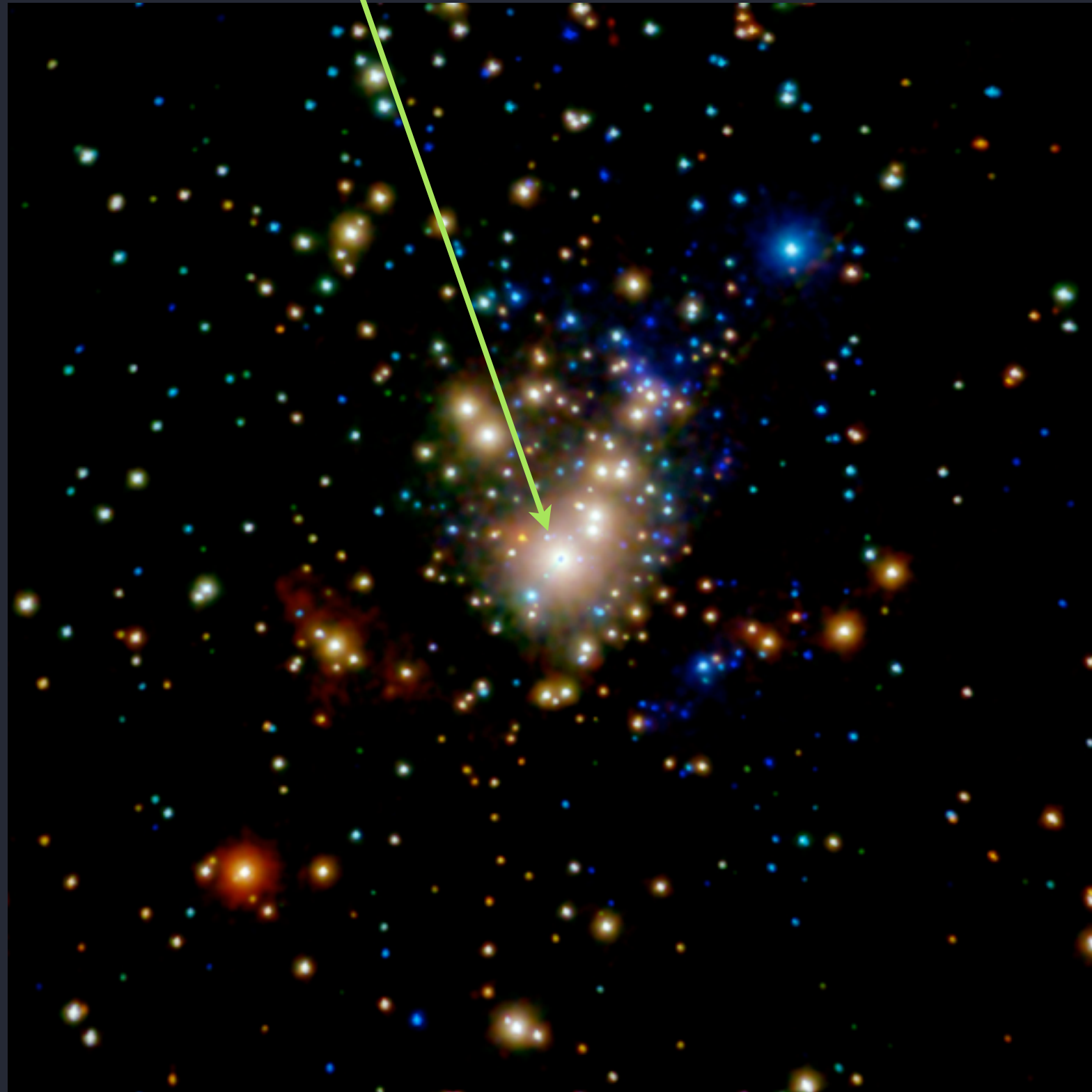
Recall the O star that ionizes the Orion Nebula



θ^1 Ori C: only O star here

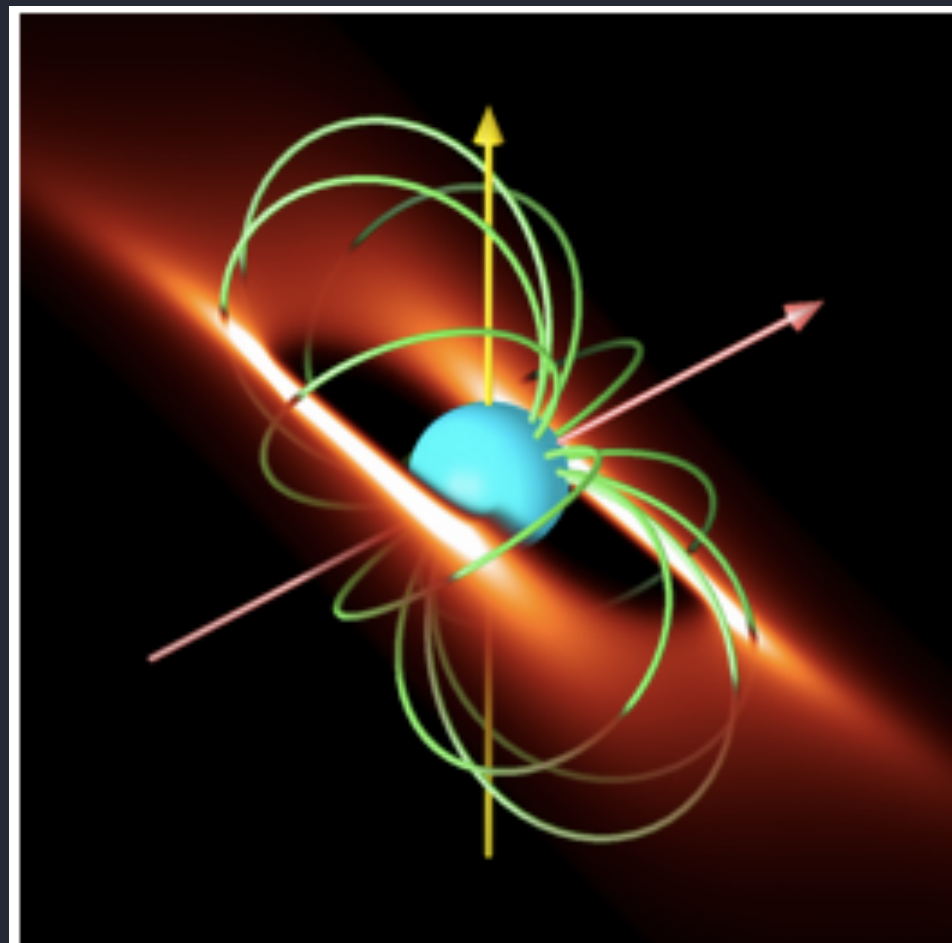
Chandra X-ray image of the Orion Nebula Cluster

θ^1 Ori C: very X-ray bright



~10% of massive stars are magnetic!

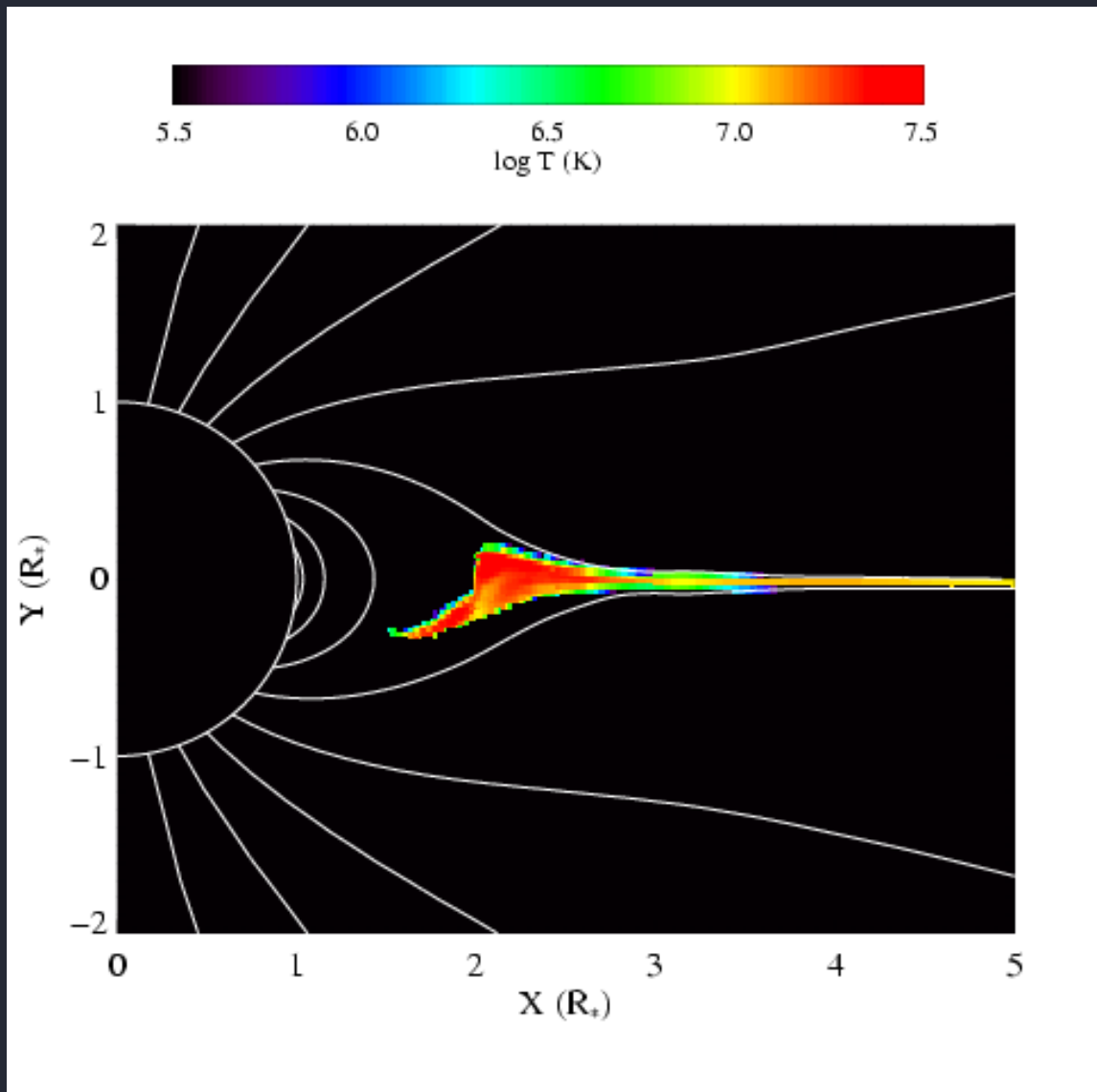
unlike solar type magnetism, though:
time-constant, not dynamo generated, often
large-scale dipole



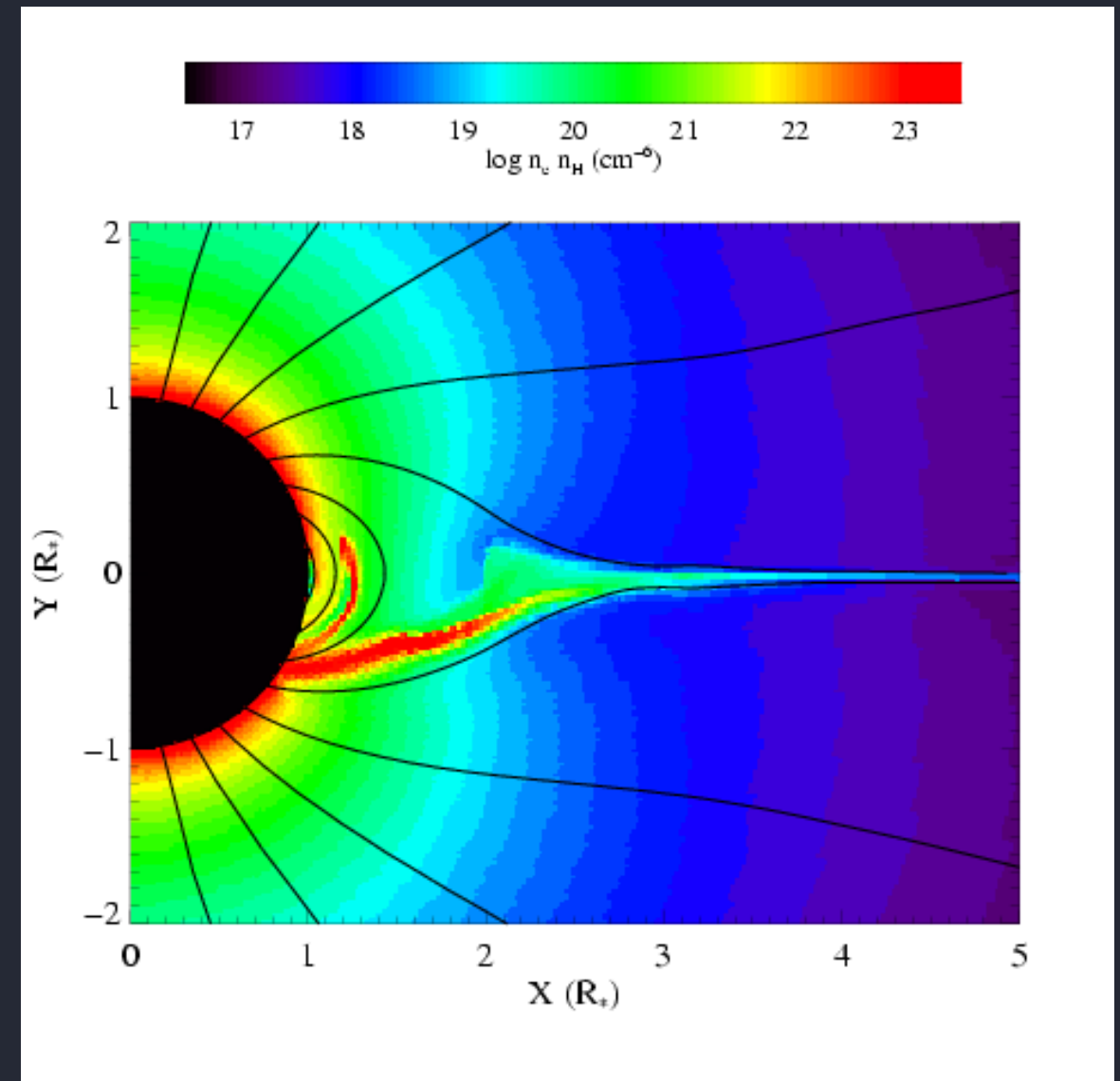
A simulation of the circumstellar matter distribution of σ Ori E, as predicted by the Rigidly Rotating Magnetosphere mode

θ^1 Ori C: prototype magnetic O star

temperature



emission measure



simulations by A. ud-Doula; Gagné et al. (2005)

The line-deshadowing instability (LDI)

causes fast, rarefied wind plasma to slam into slower, denser wind plasma

the resulting shocks heat the plasma

the X-rays we see are the thermal emission from this hot wind plasma

general result from shock theory:

$$T \sim 10^6 (\Delta v_{\text{shock}} / 300 \text{ km/s})^2$$

Magnetically Channeled Wind Shock model

magnetic channeling causes wind flows from opposite hemispheres to collide in the magnetic equator

the resulting shocks heat the plasma

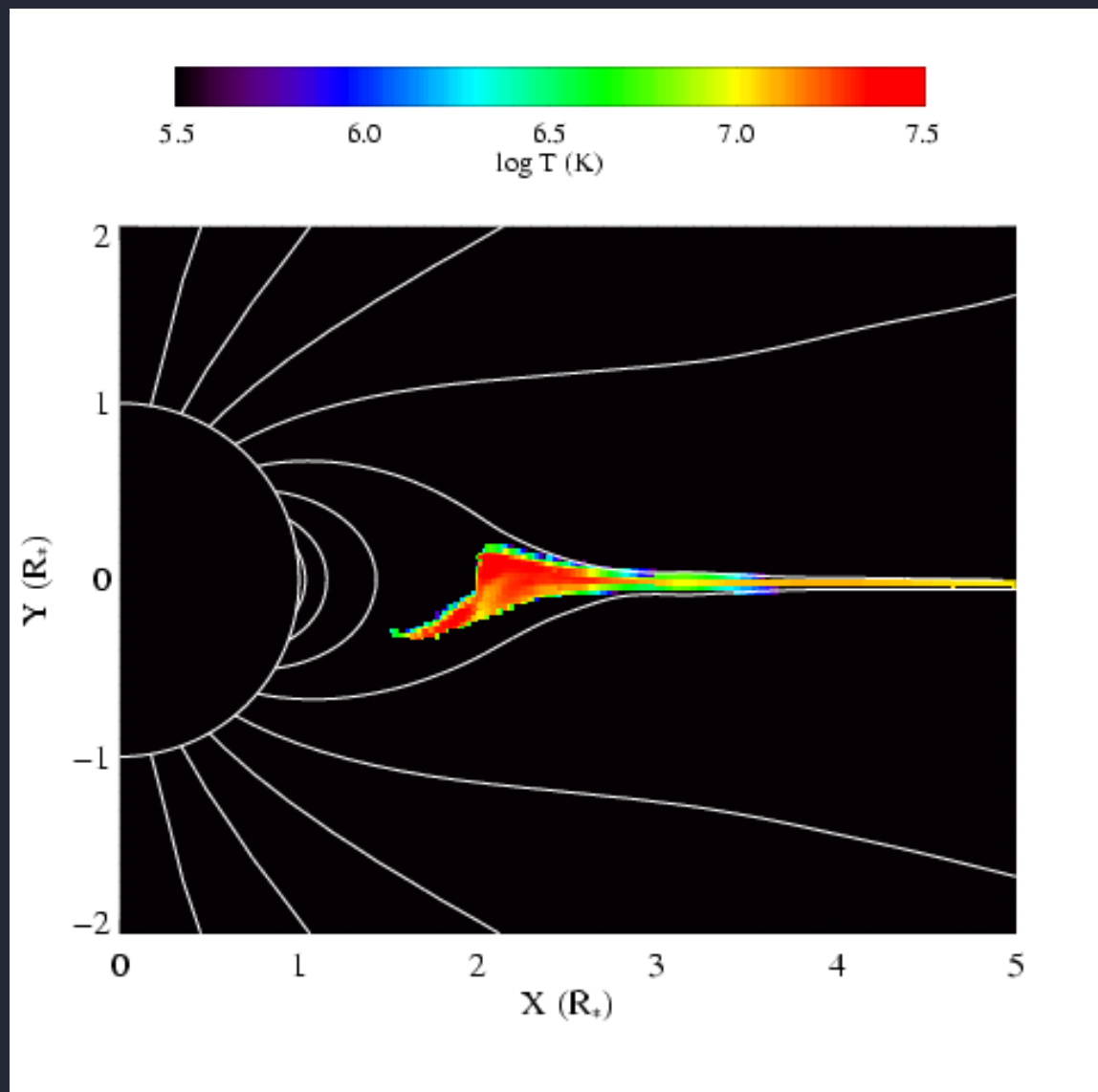
the X-rays we see are the thermal emission from this hot wind plasma

general result from shock theory:

$$T \sim 10^6 (\Delta v_{\text{shock}} / 300 \text{ km/s})^2$$

θ^1 Ori C: prototype magnetic O star

temperature



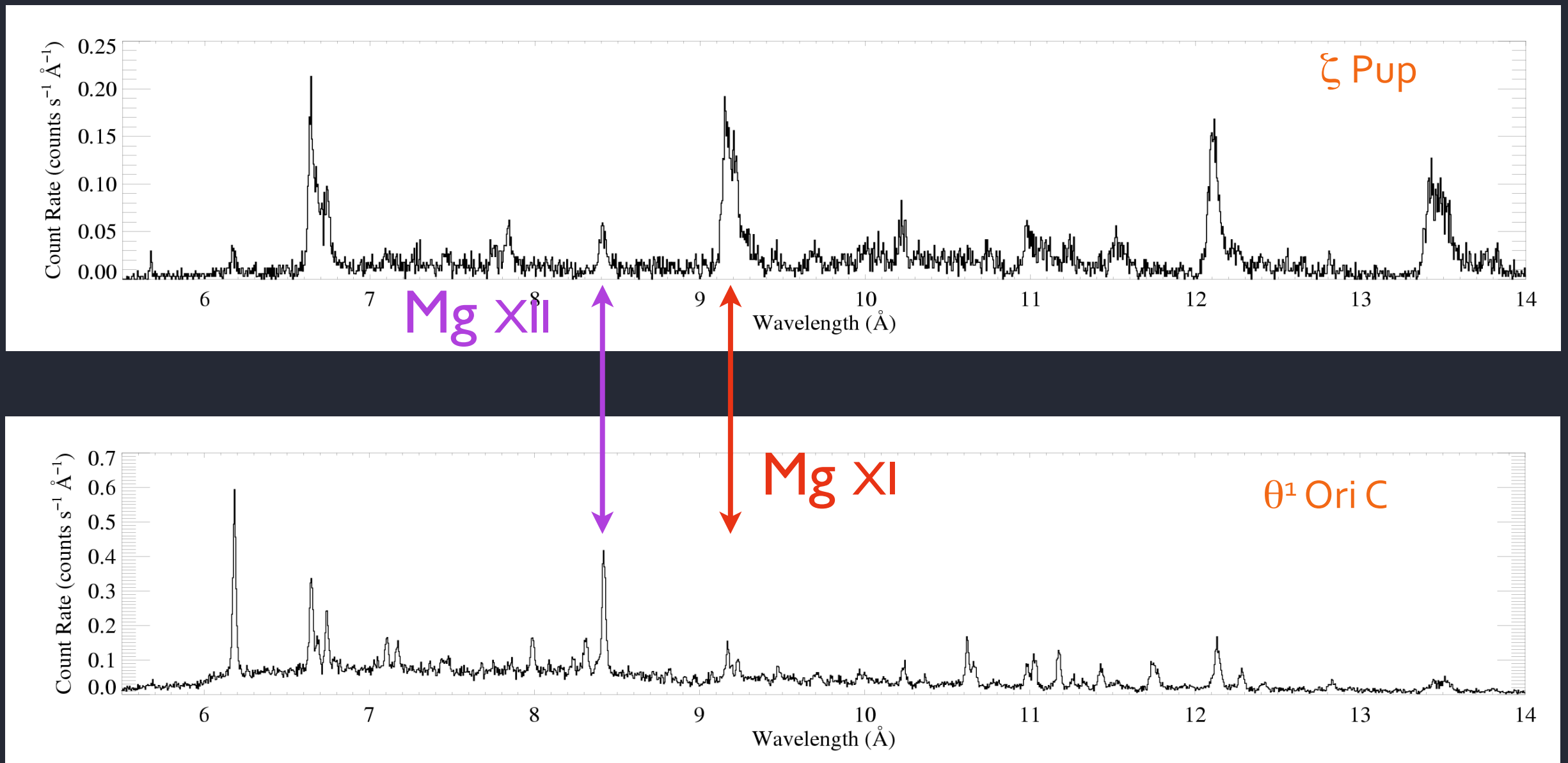
magnetic channeling : strong shocks = hotter plasma

magnetic confinement : low post-shock velocity = narrower lines

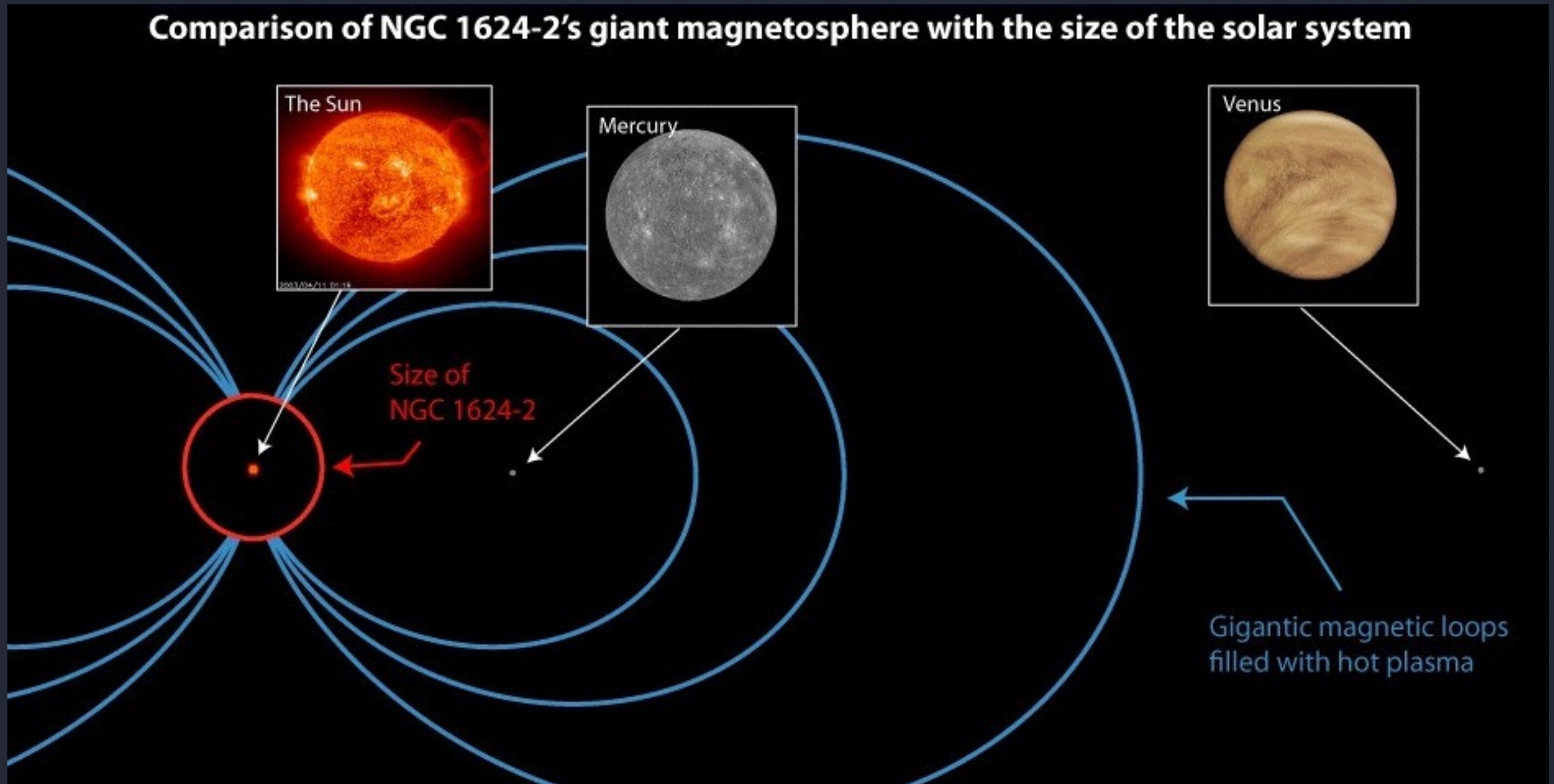
simulations by A. ud-Doula; Gagné et al. (2005)

θ^1 Ori C: hotter plasma, narrower lines

Mg XII / Mg XI is proportional to temperature

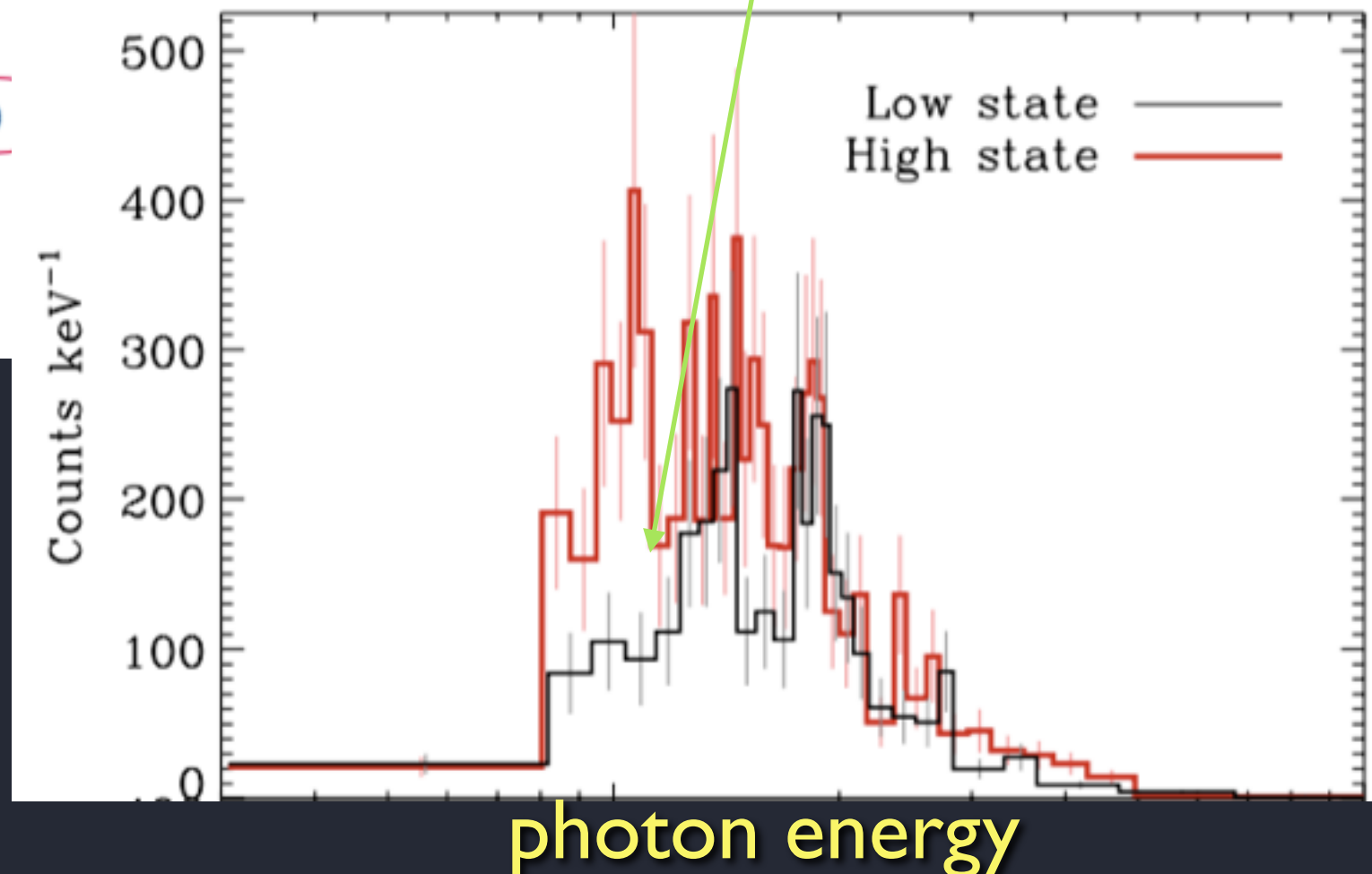
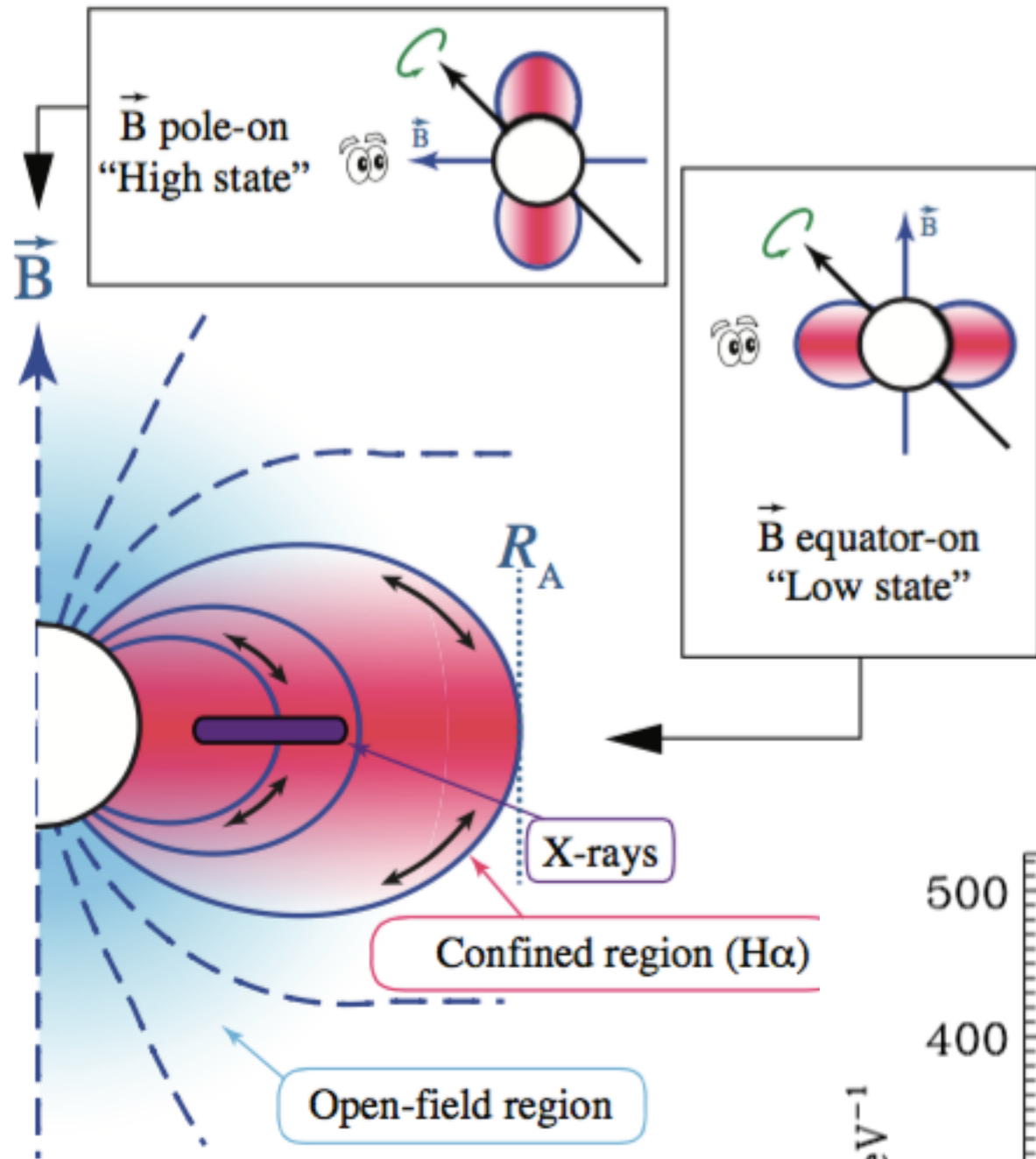


recently discovered largest O star magnetosphere (team includes Prof.V. Petit)



Chandra observations at two phases

more absorption when
viewed edge-on



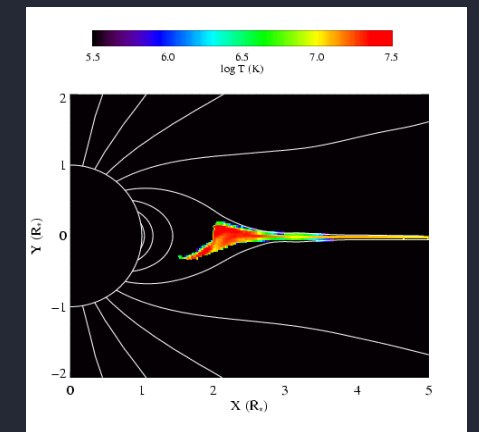
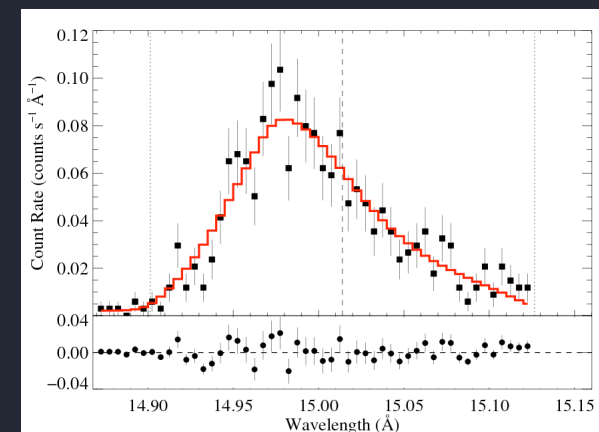
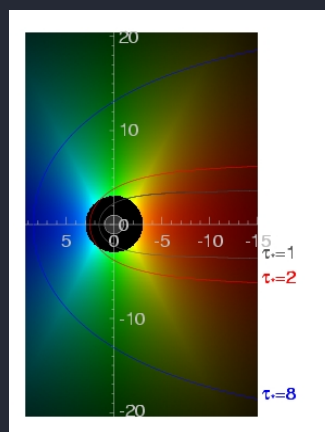
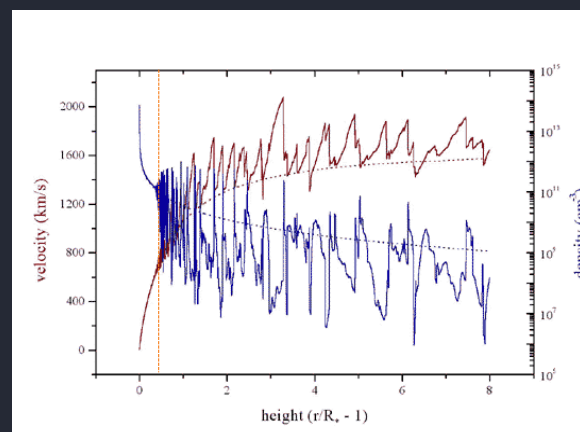
Preliminary Conclusions

1. Magnetic massive stars produce X-rays via wind shocks in their magnetospheres
2. X-ray observations show that this process is more efficient than LDI-generated embedded wind shocks in non-magnetic O stars

Overall Conclusions

1. Shock heating extracts kinetic energy from radiation-driven winds, producing the X-rays

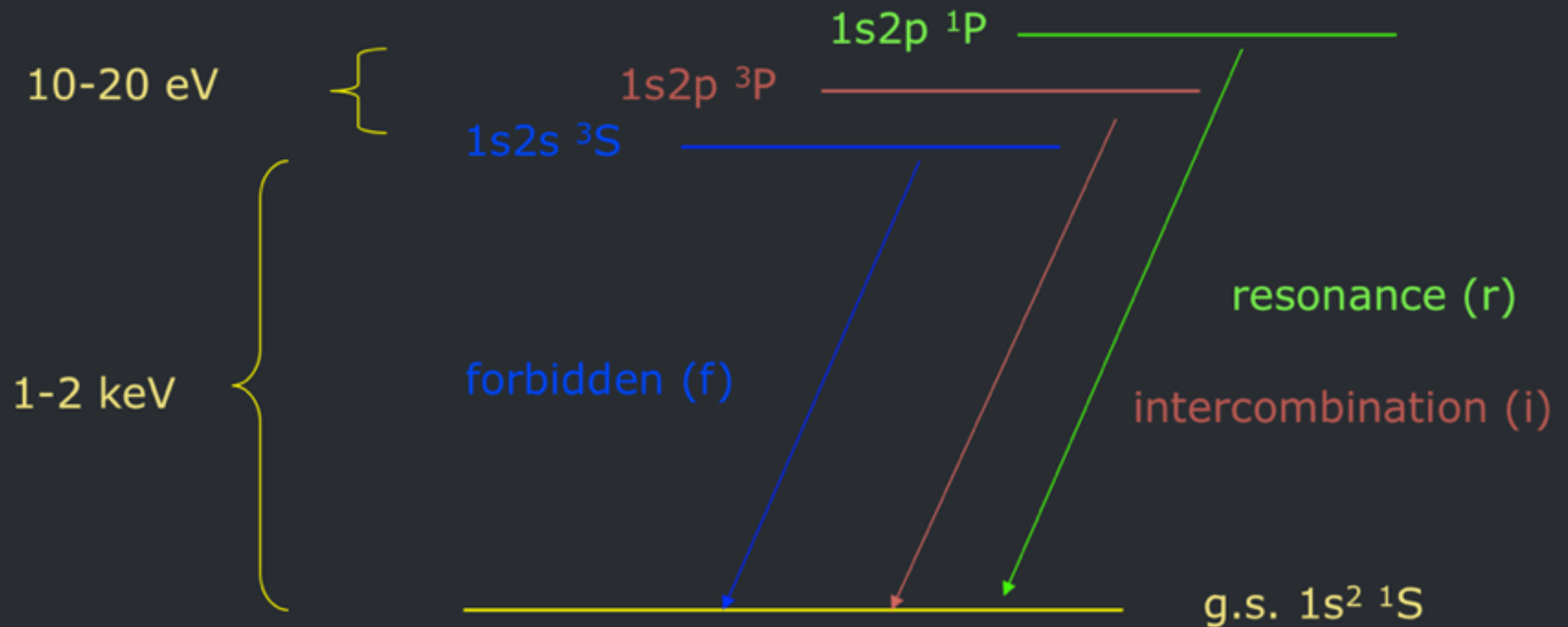
2. X-ray spectroscopy provides diagnostic information about plasma temperatures, velocities, and absorption



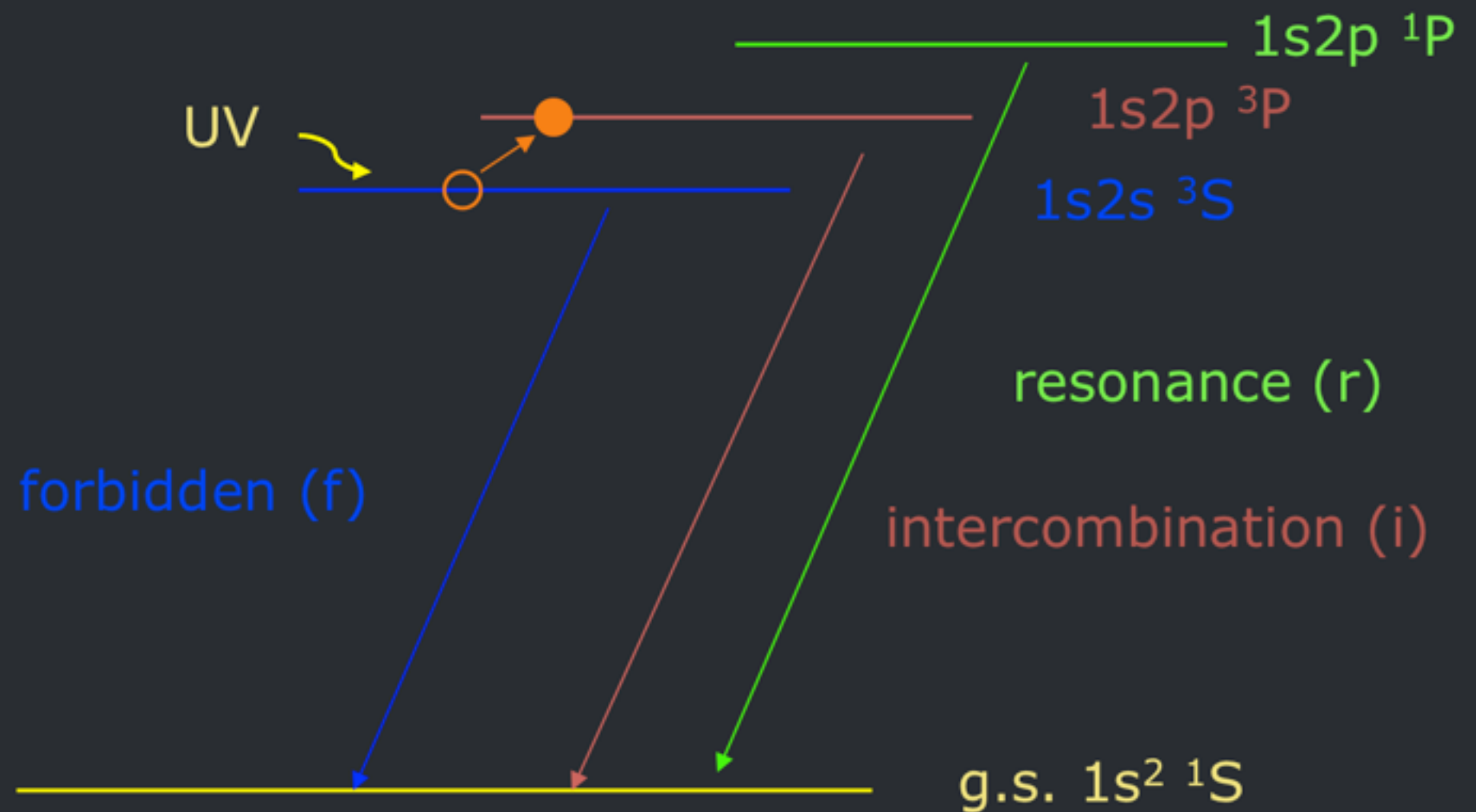
Extra Slides

f/i ratios for diagnosing location of the hot plasma

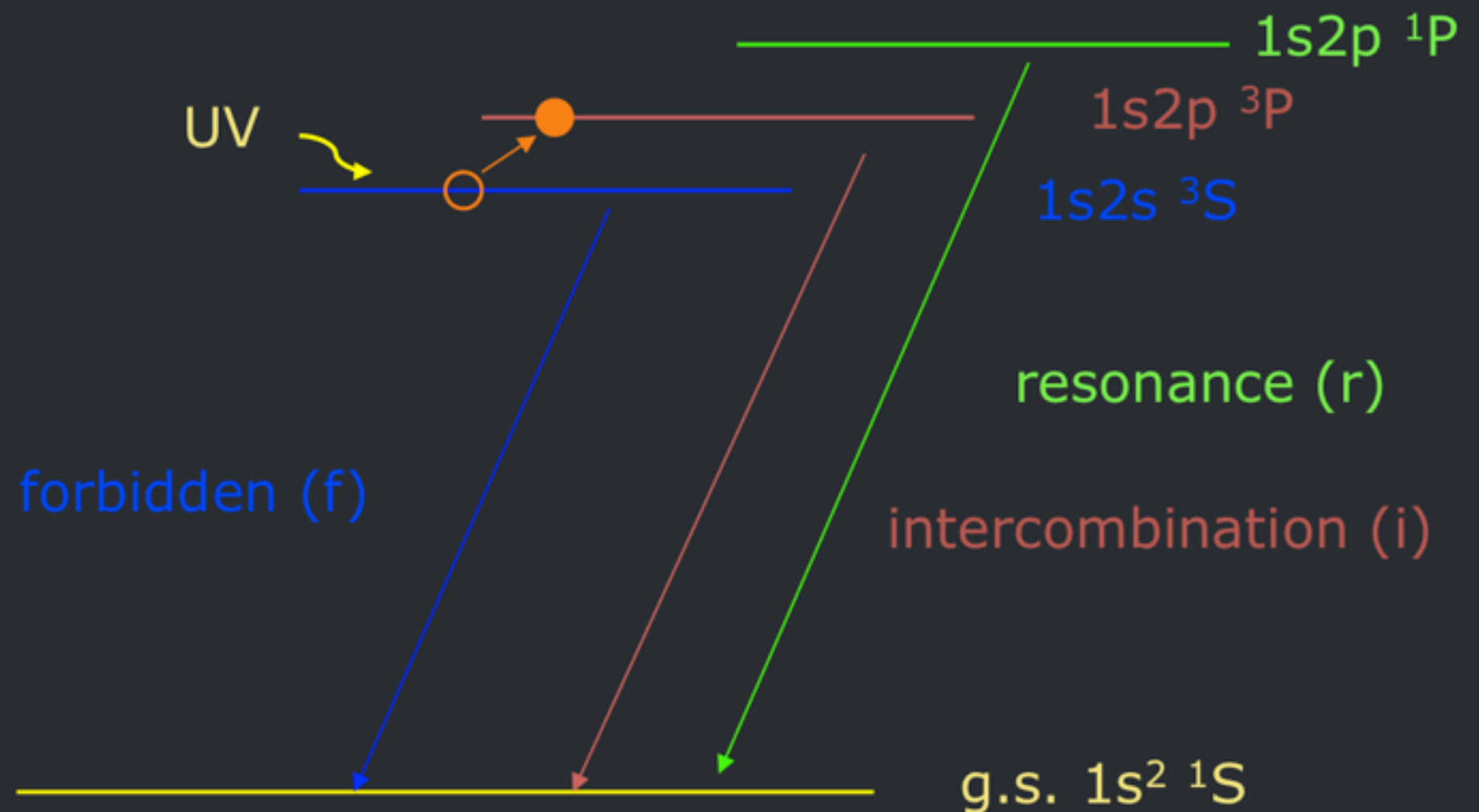
Helium-like ions (e.g. O^{+6} , Ne^{+8} , Mg^{+10} , Si^{+12} , S^{+14}) – schematic energy level diagram



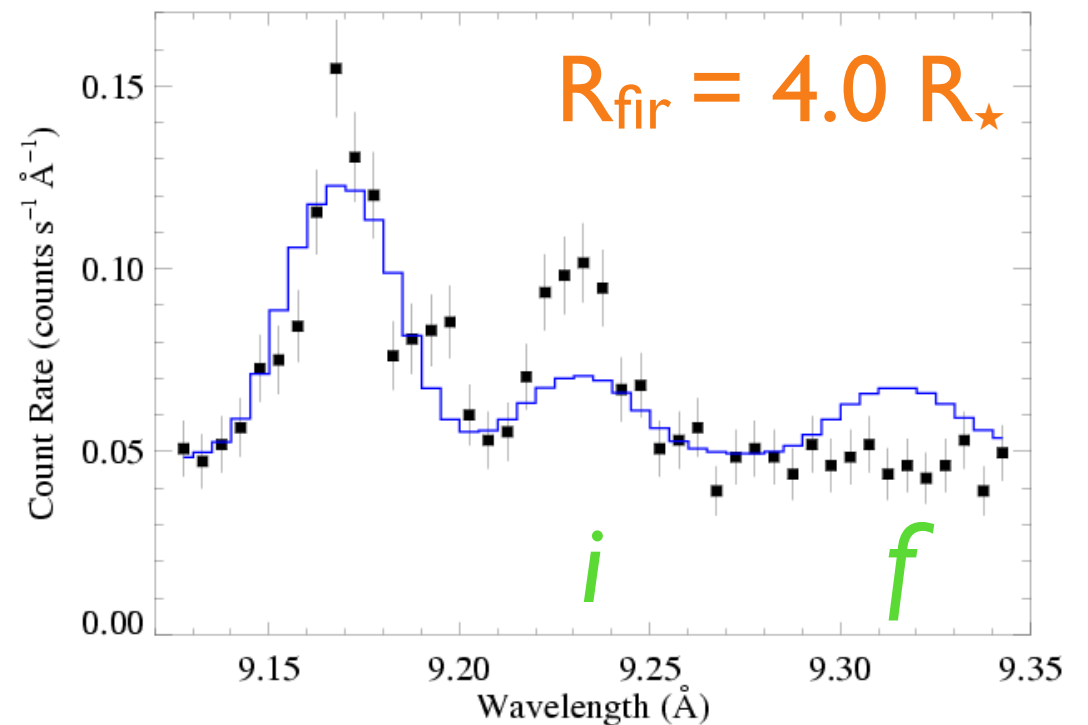
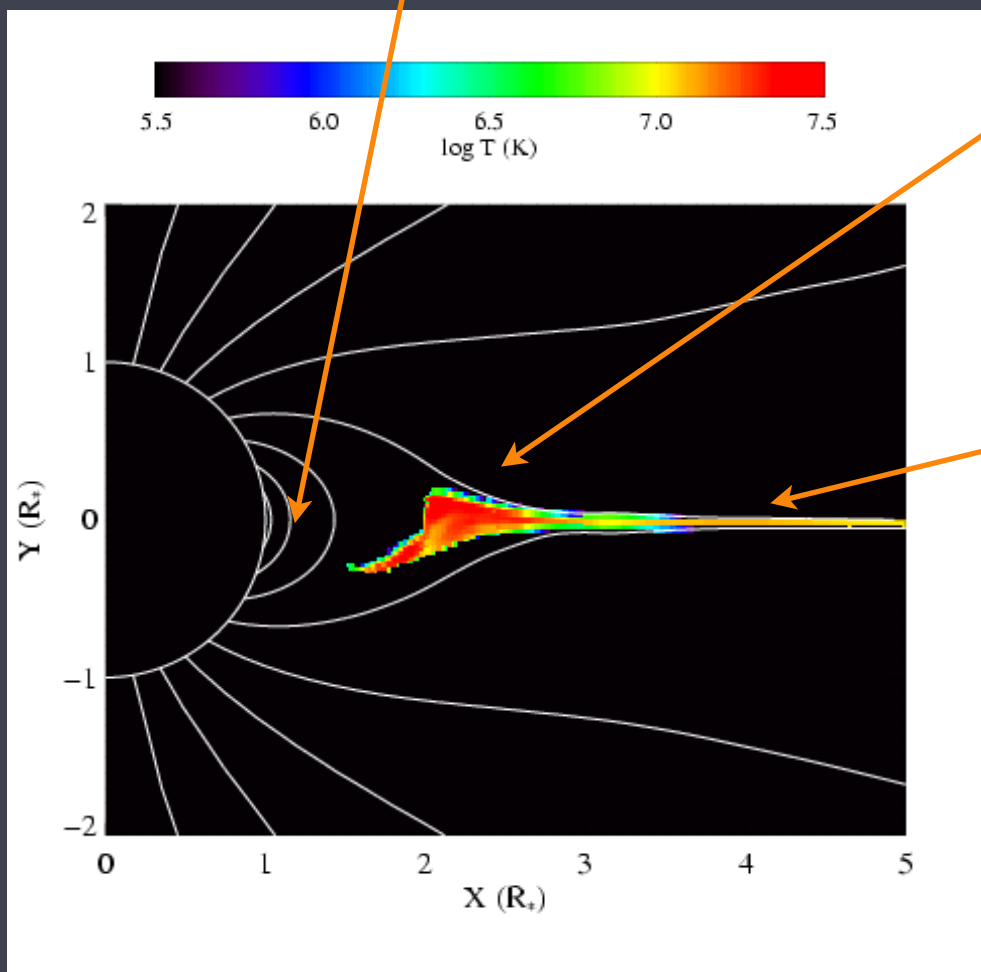
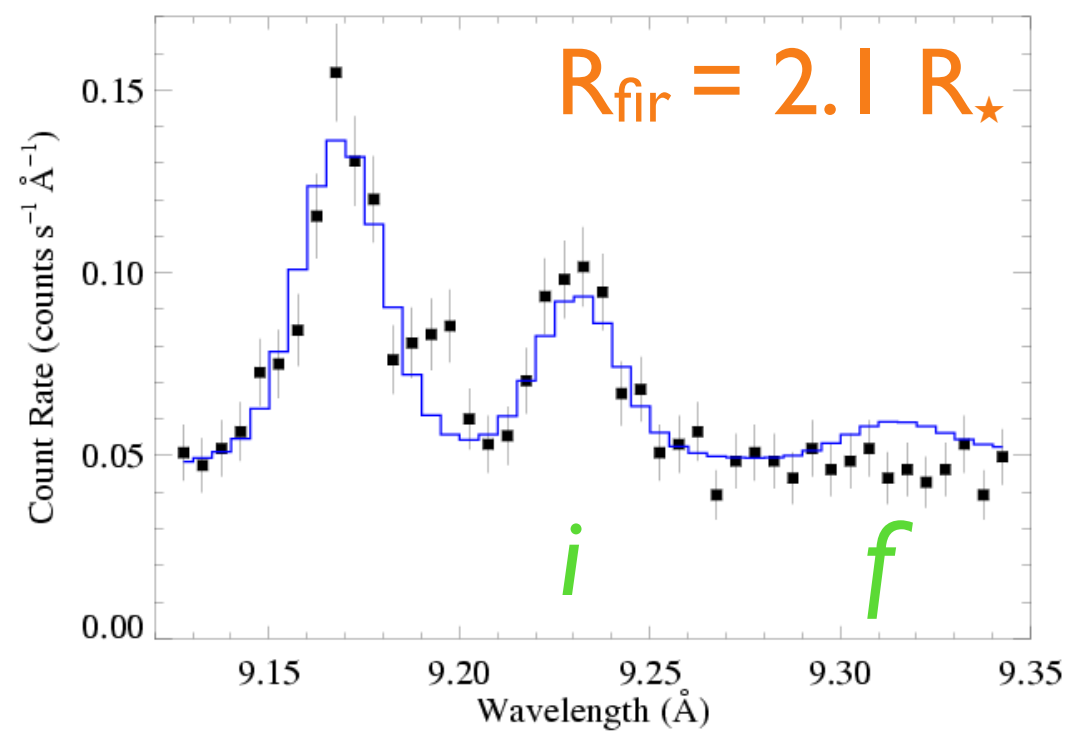
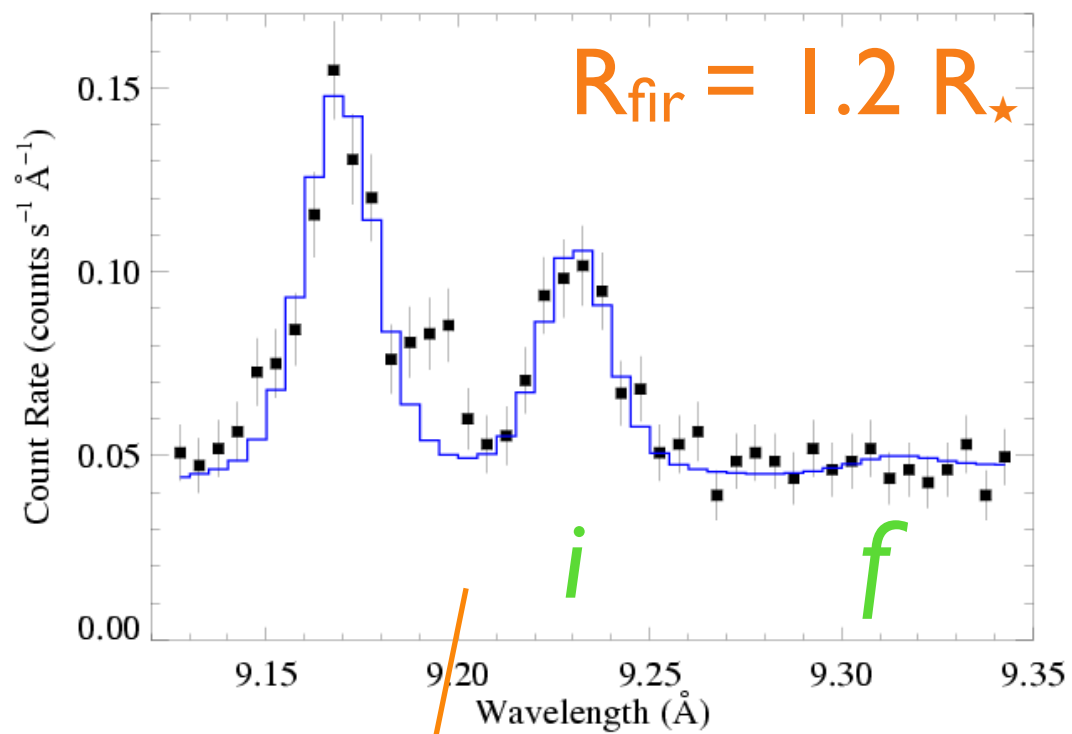
The f/i ratio is thus a diagnostic of the strength of the local UV radiation field.



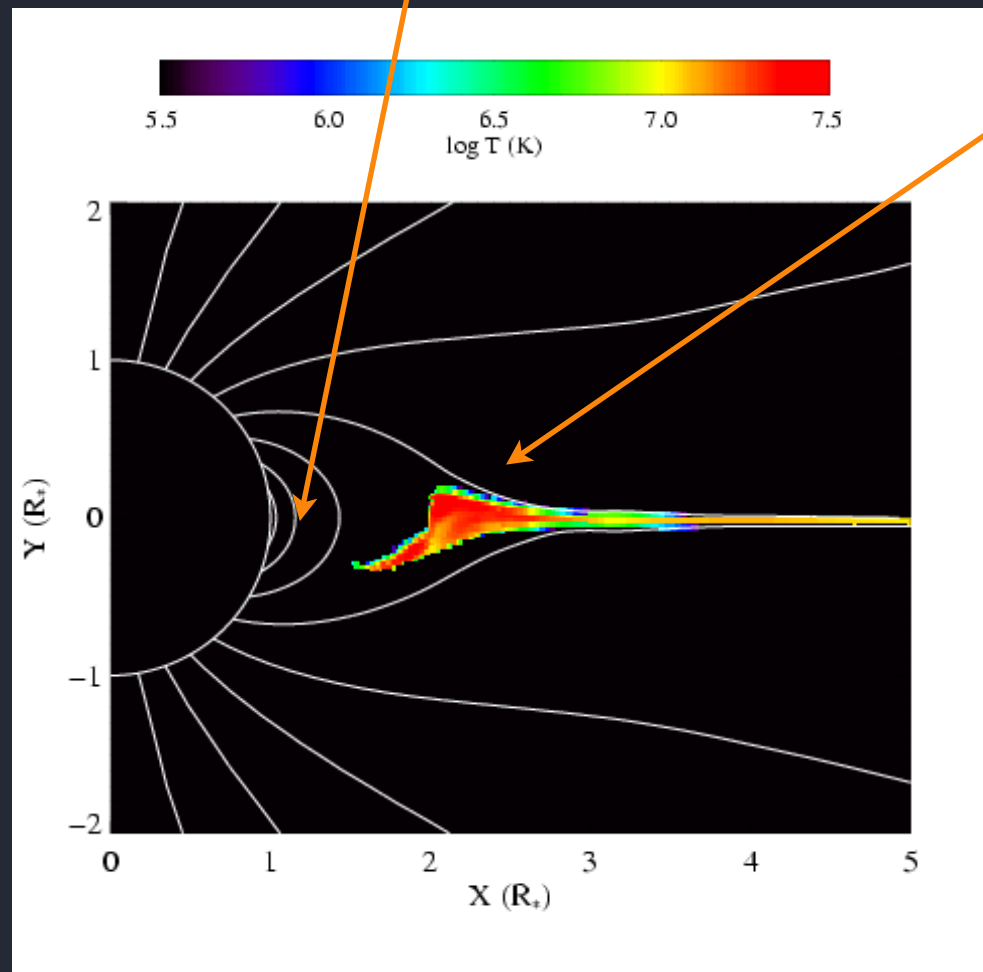
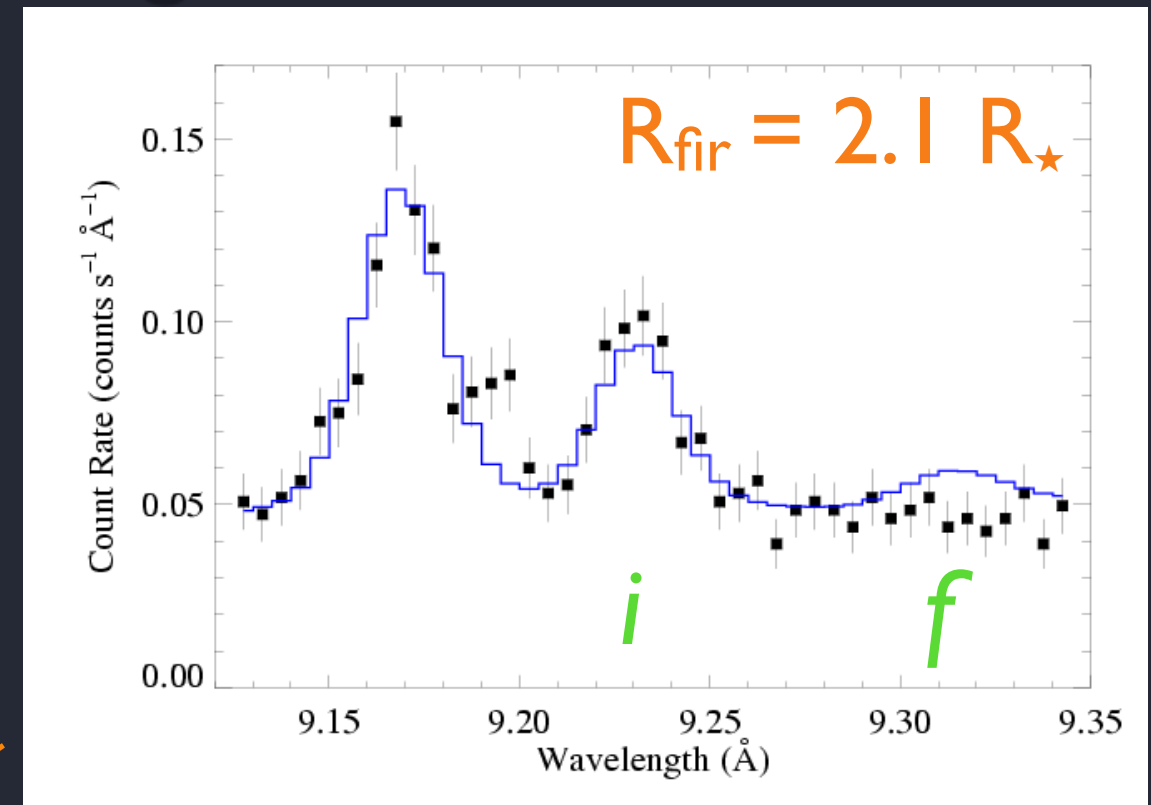
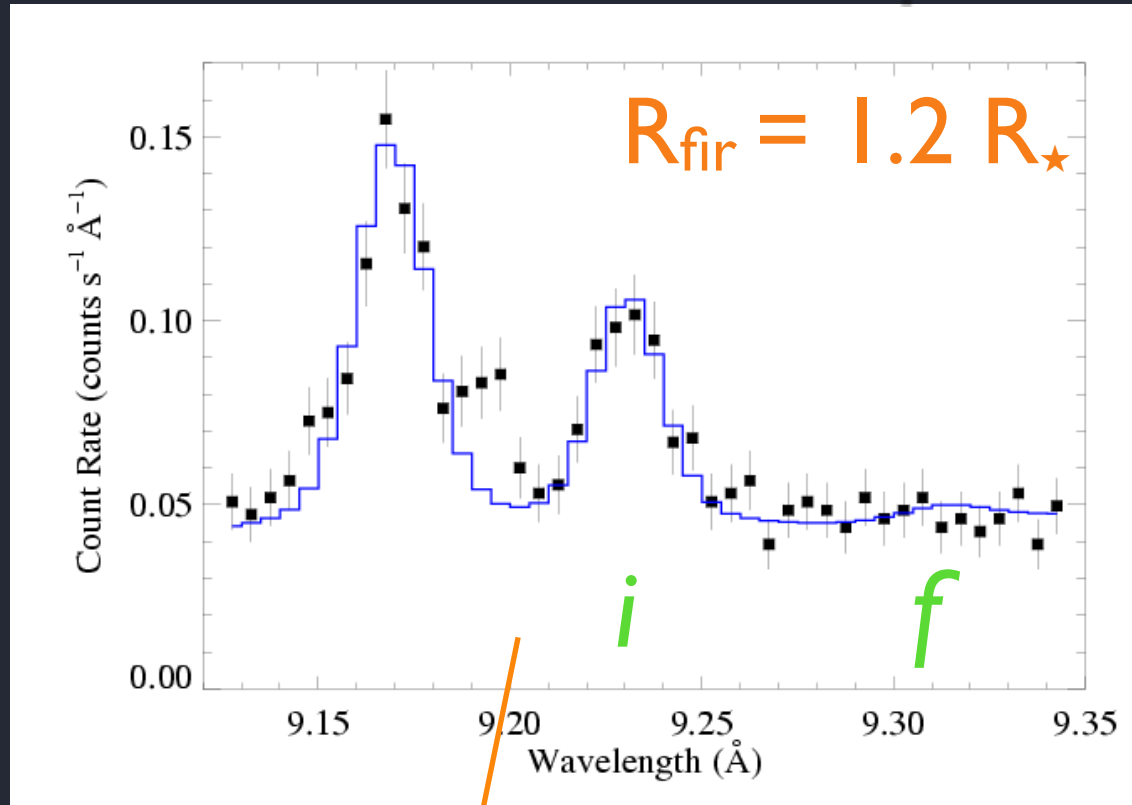
If you know the UV intensity emitted from the star's surface, it thus becomes a diagnostic of the distance that the x-ray emitting plasma is from the star's surface.



θ^1 Ori C: prototype magnetic O star



θ^1 Ori C: prototype magnetic O star



MDH simulations are only marginally consistent with *f/i* constraints

data say hot plasma is closer to the photosphere

What produces the hot, X-ray emitting plasma in massive stars?

plasma with $T > 10^6$ K radiates X-rays ($h\nu > 100$ eV)

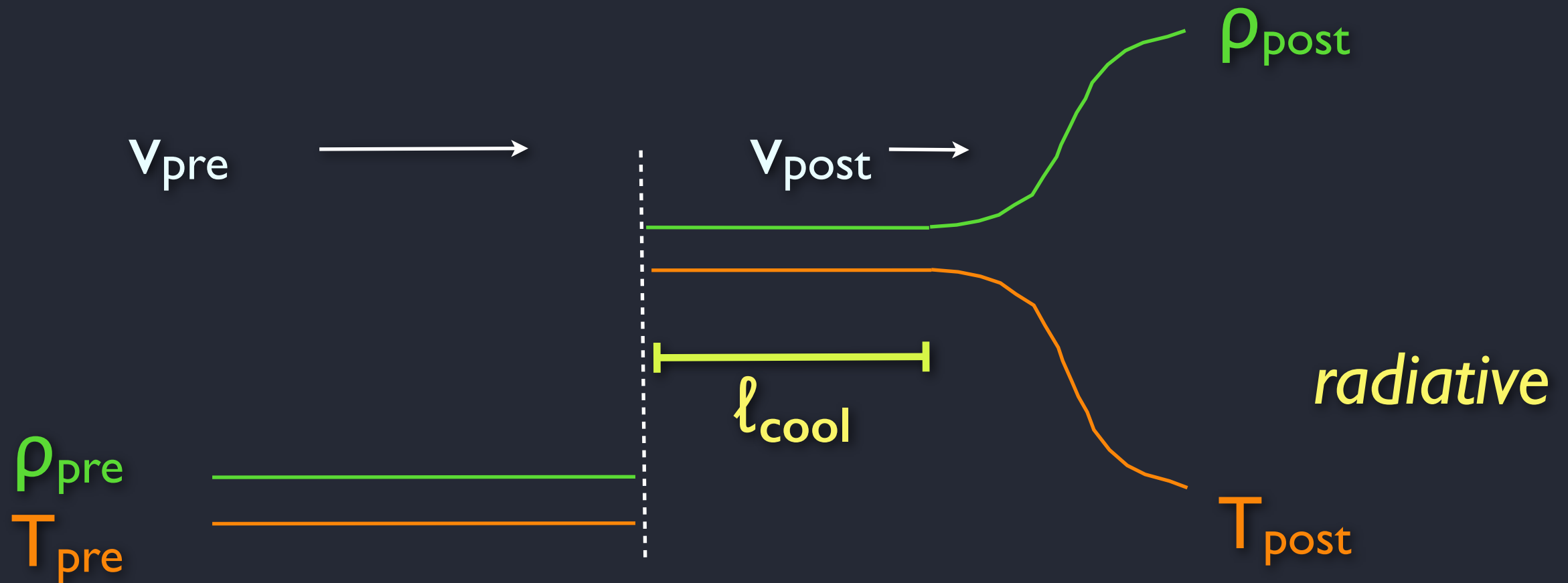
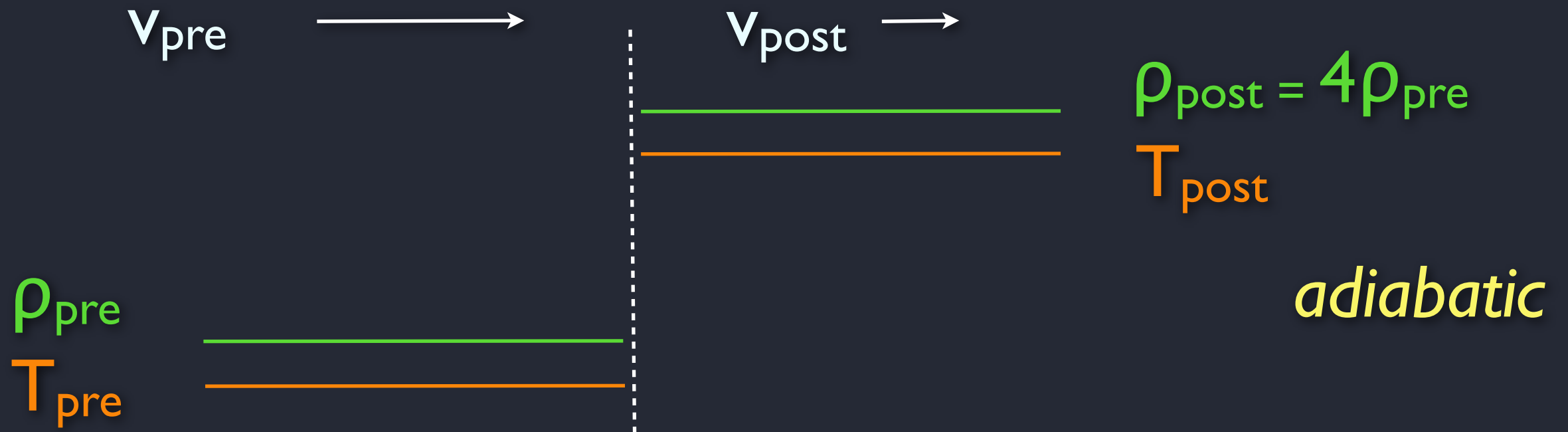
shocks heat plasma to $T \sim 10^6$ K

if $\Delta V_{\text{shock}} \sim 300$ km/s

and $T \sim (\Delta V_{\text{shock}})^2$

shocks are *radiative* in dense O star winds, but *adiabatic* in lower-density early B star winds

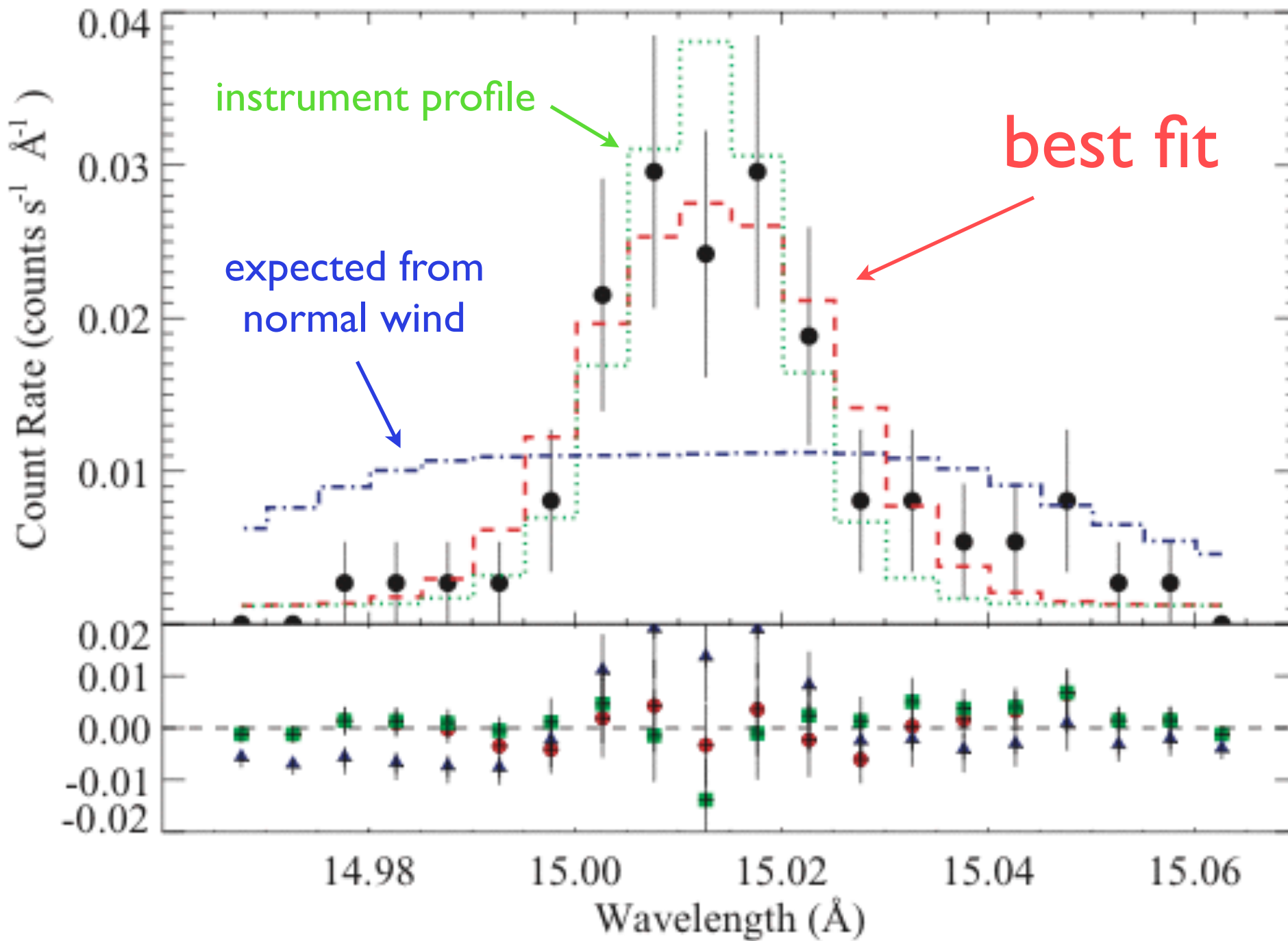
$$\Delta v_{\text{shock}} = v_{\text{pre}} - v_{\text{post}}$$



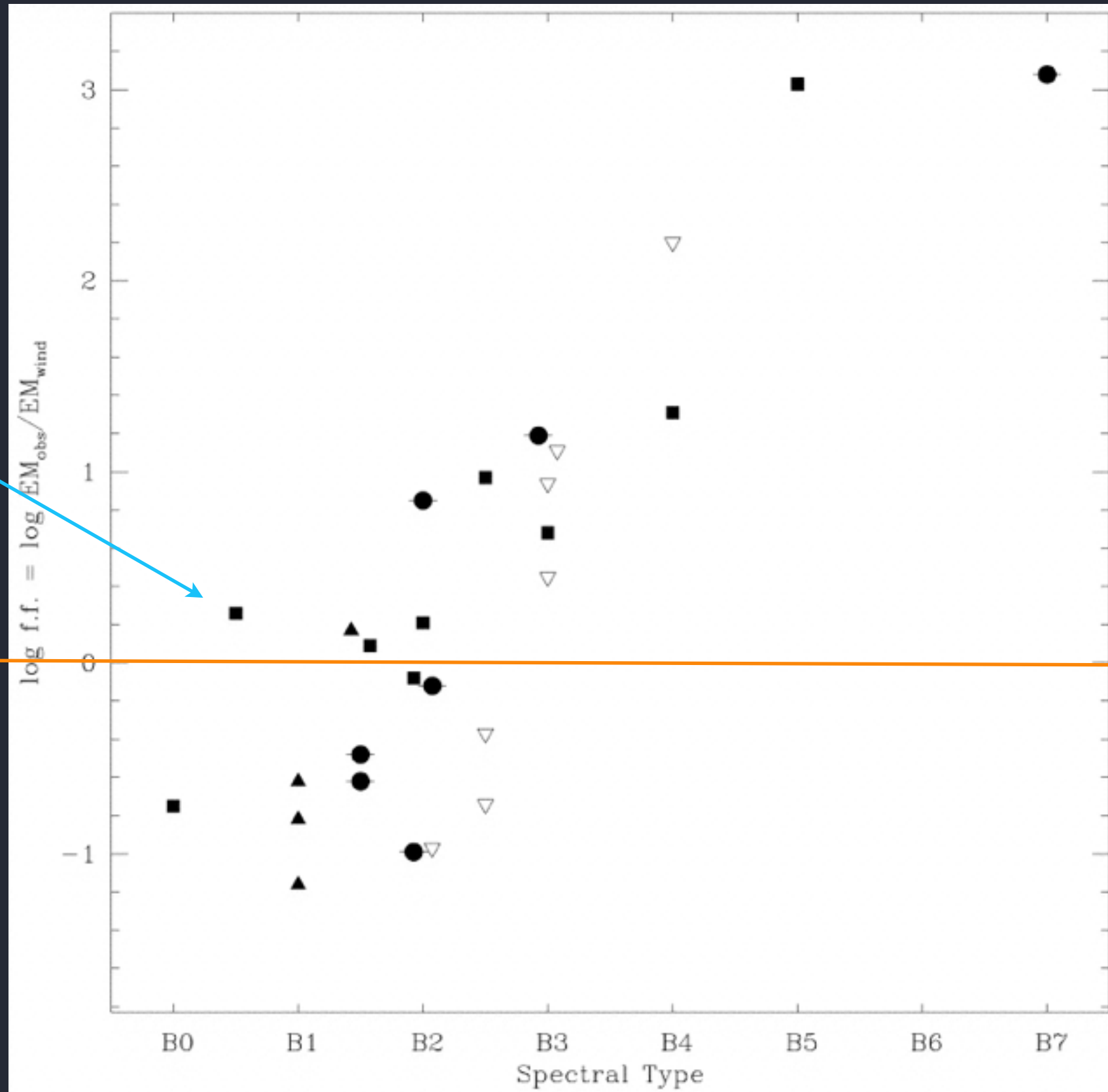
β Cru (B0.5 III)



Fe XVII line in the *Chandra* grating spectrum of β Cru (B0.5 III)



X-ray filling factors of B stars



β Cru



100%

B0 B1 B2 B3

Cohen et al. 1997

B star winds have low density, shocks are *adiabatic*

once the wind is shocked (at $\sim 1.5 R_{\star}$) it essentially *never* cools \Rightarrow outer wind is (nearly completely) filled with hot (few 10^6 K) plasma that is no longer radiatively driven

hence, narrow-ish X-ray lines



